ShadX Presents :

"A Cost-Efficient High-Performance Advanced Pilot Training Aircraft"

AIAA Graduate Team
Aircraft Design Competition
2017-2018

MAY 2018

SIGNATURE SHEET

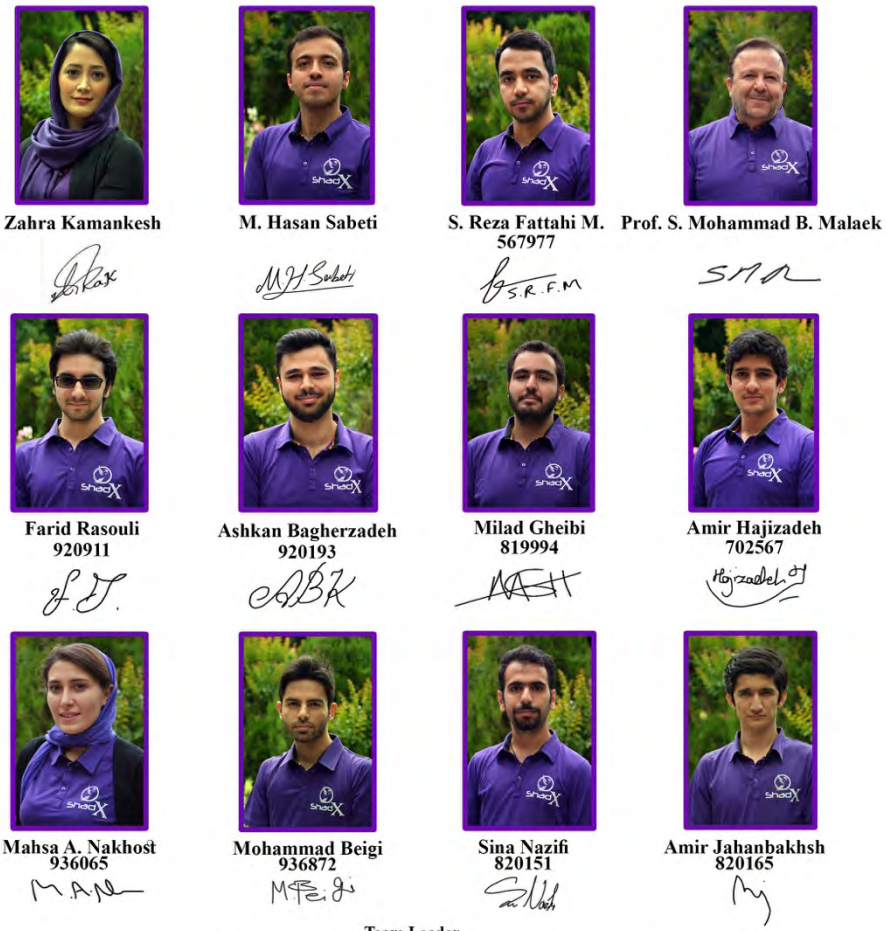

EXECUTIVE SUMMARY

"There's no such thing as a natural-born pilot."

— Chuck Yeager

In response to the 2017-2018 American Institute of Aeronautics and Astronautics (AIAA) Graduate Team Aircraft Design Competition Request for Proposal (RFP) and after spending more than 6500 engineering man-hours, it is a great honor for all of us at ShadX to present the T-68 "Saena[1]"; a cost-efficient, high-performance advanced pilot training aircraft (APTA).

At ShadX, we firmly believe that we have effectively met the RFP Requirements. In addition, we have also been able to devise specific features to cover a broader range of training-target aircraft and other potential markets. Such features have been made possible with the help of a configuration; which externally inspires safety and tradition; while internally, through its efficient systems, is the aircraft of the future and has many features like advanced embedded training system and variable stability. Hence, bringing Saena to a superior training effectiveness level.

Saena is an efficient, cost-effective apparatus that effectively serves future pilots' training programs that is designed to conduct training programs that include formation flight and combat scenarios. This approach definitely helps future pilots understand the criticality of the maneuvers while making training safe and exciting!

Benefiting from a modular-designed engine and cockpit, through proper positioning of different sub-systems and access doors, "Saena" would be an easily-maintainable cost-effective design, revealing itself as a budget-friendly APTA for USAF. On the other hand, with features like cross platform training together with "Variable Stability Augmentation System", Saena is an aircraft of the future, ready to serve 5th gen. fighters.

ShadX has developed a particular design cycle, in which a cost-based optimization method has been implemented. So, a highly iterative process has been performed by the team to arrive at a well-balanced final design.

In comparison with its rivals, Saena has the lowest operating & unit cost, highest maximum turn rate, outstanding roll power, long-lasting platform, and matured technologies. Hence, proving itself as a distinctive feasible response to the RFP.

[1] **Saena** is a benevolent, mythical bird of Persian legend credited with possessing great wisdom.

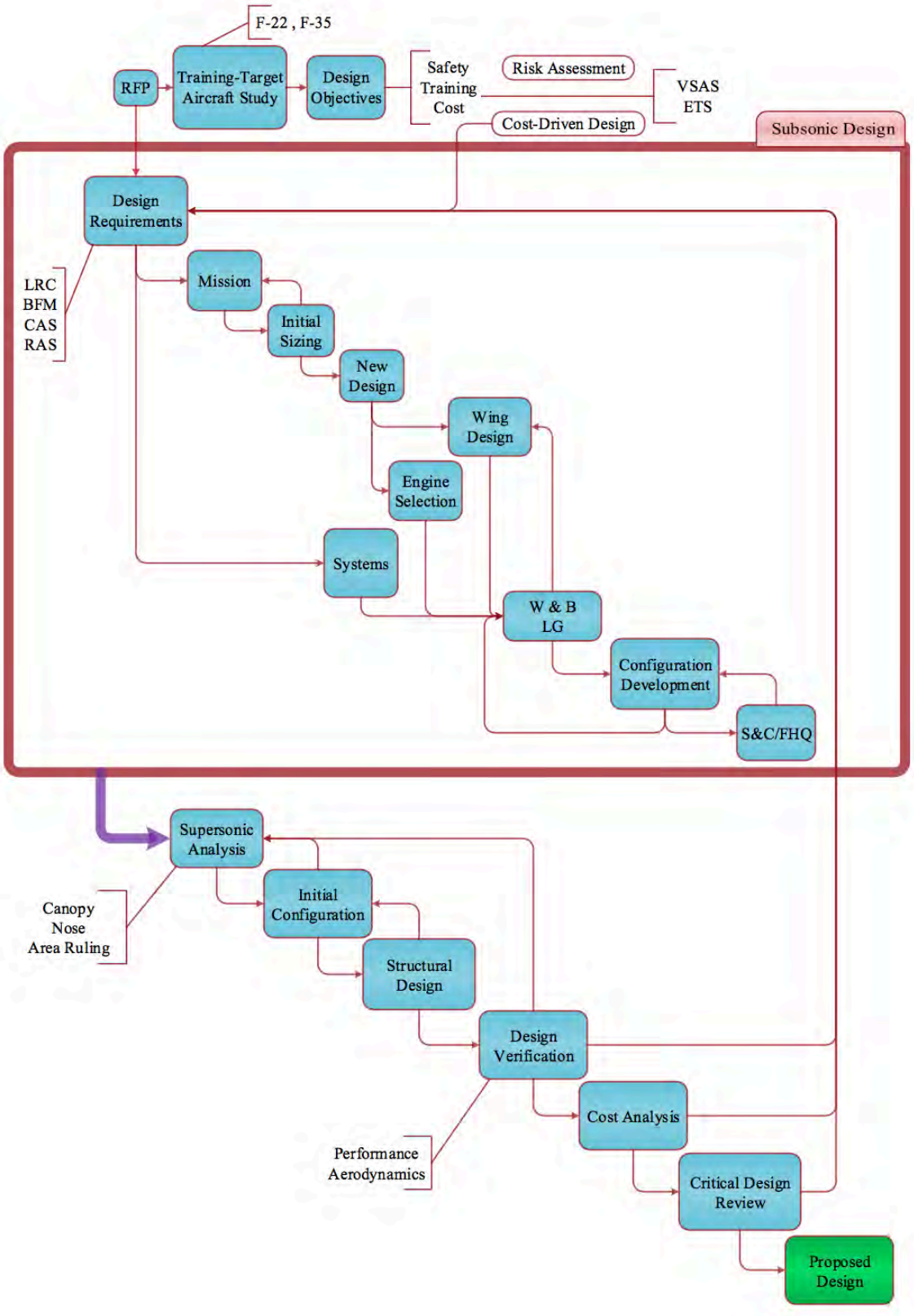

Figure 1-ShadX Waterfall Design Cycle

General Characteristics	T-68 Saena
Crew	2
Length [ft.]	41
Height [ft.]	14.27
Wingspan [ft.]	29.84
Wing Area [ft^2]	222.5
M.A.C. [ft.]	8
Empty Weight [lbs.]	7610
Max. Takeoff Weight [lbs.]	13350
Internal Fuel [lbs.]	4100
Combat Weight [lbs.]	11308
Power Plant	1×Snecma M88
Dry Thrust [lbf]	11200
Thrust with Afterburner [lbf]	16900
Max. R/C @ SL (Dry/Wet) [fpm]	25000/37000
Absolute Ceiling [ft.]	53000/60500
Time to Height (53,000 ft.) [min]	< 2
Wing Loading [lb./ft^2]	60
T/W Takeoff Weight (Dry/Wet)	0.84/1.26
T/W Combat Weight (Dry/Wet)	0.99/1.49
Max. Level Speed [Mach]	1.3
Required Runway Length [ft.]	5610
Max. Turn Rate [deg/s]	25.8
Max. Design g-Load	[+9.0 / -3.0]
Unit Cost [M$]	12.39
Operating Cost [$/hour]	5440

ShadX©

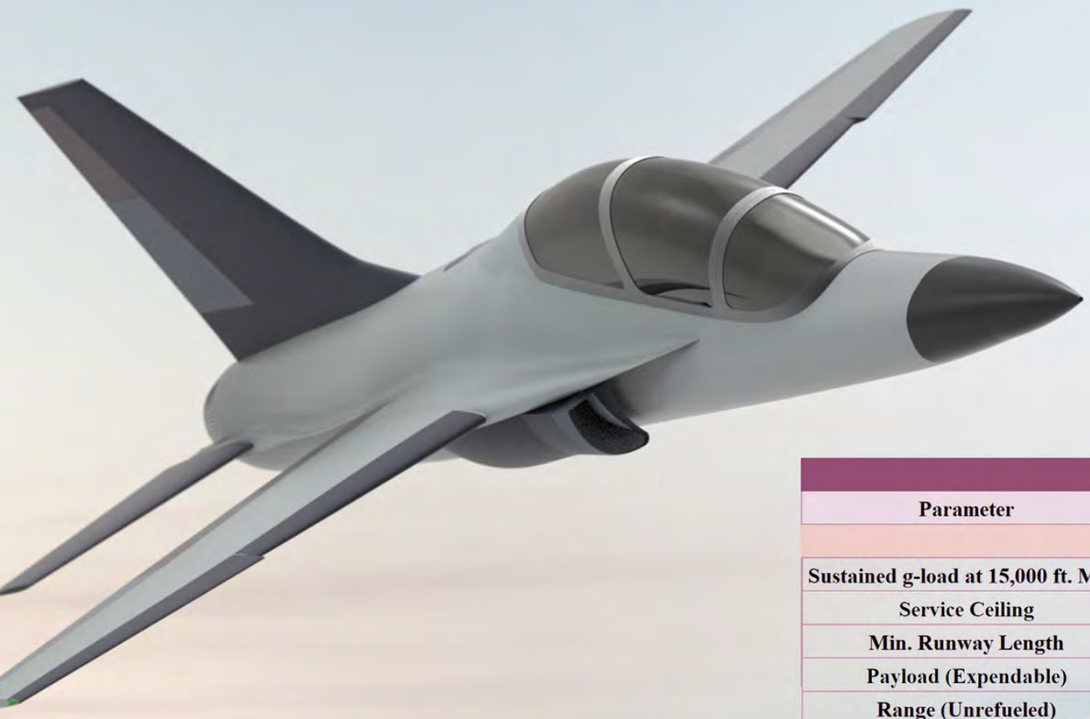

Compliance Matrix		
Parameter	RFP	Saena
Performance		
Sustained g-load at 15,000 ft. MSL	8g to 9g	9g
Service Ceiling	40,000 to 50,000 ft.	53,000 ft.
Min. Runway Length	8,000 to 6,000 ft.	5,610 ft.
Payload (Expendable)	500 to 1,000 lbs.	1,000 lbs.
Range (Unrefueled)	1,000 to 1,500 nm	1,500 nm
Cruise Speed	0.7M to 0.8M	0.77M to 0.82M
Dash Speed	0.95M to 1.2M	1.3M
Structure		
Design Limit Load Factor	+9 and -3 vertical g's	+9 and -3 vertical g's
Structural Limit	2,133 psf (M=1.2 at sea level)	2,133 psf
Safety Factor	1.5	1.5
Design Service Life	30,000 hours	More than 30,000 hours
Stability		
Static Margin (S.M.)	[-5% to 15%]	[4.77% to 15%]
Max CG Excursion	7% M.A.C	6.77% M.A.C
Cost		
Total NRE Cost	500 M$ to 1 B$	753 M$
Per Unit Cost	10 M$ to 20 M$	12.39 M$

Isometric view
Scale: 1:120

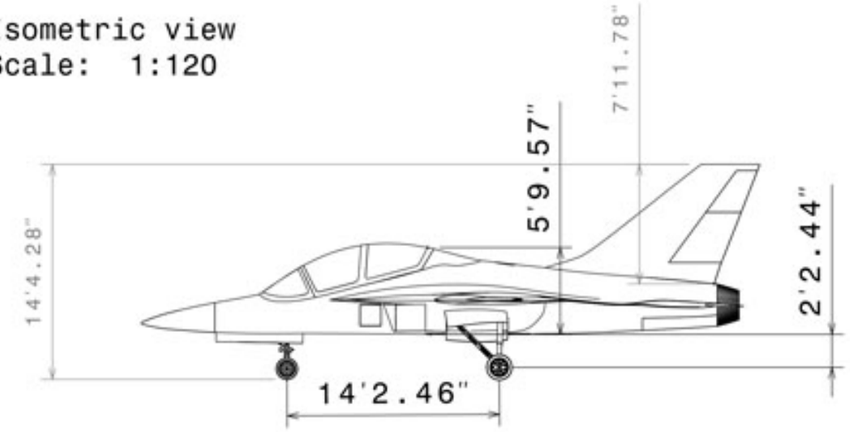

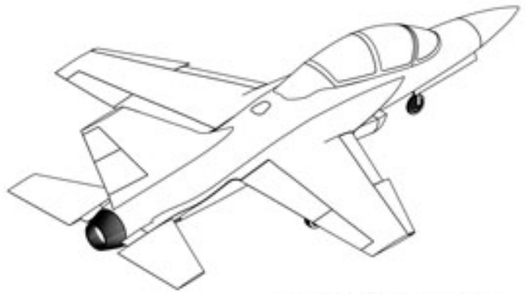

Isometric view
Scale: 1:120

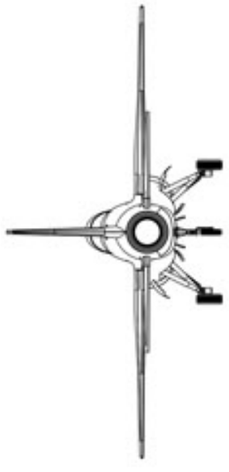

Right view
Scale: 1:120

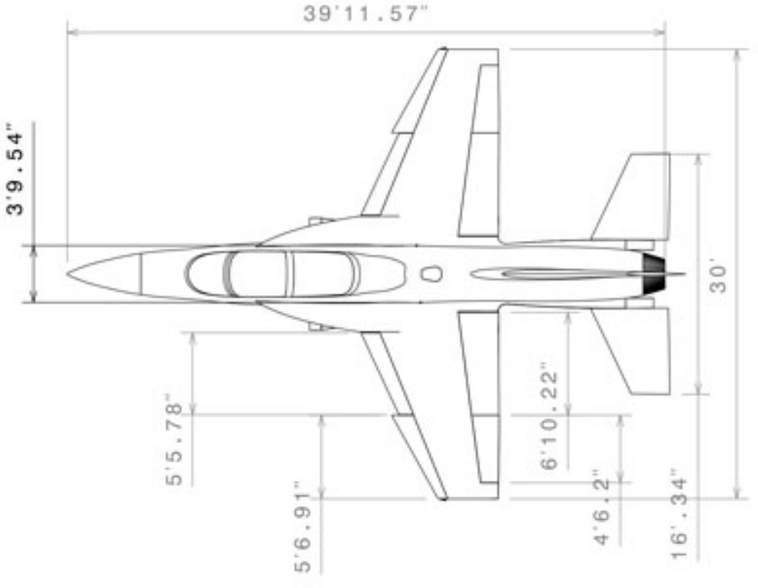

Front view
Scale: 1:120

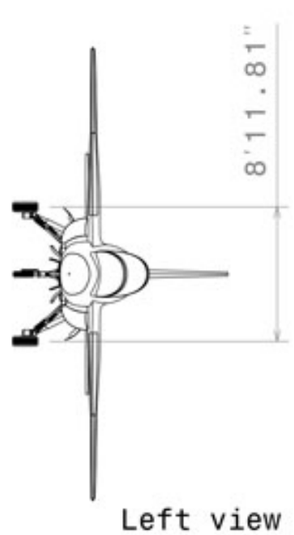

Left view
Scale: 1:120

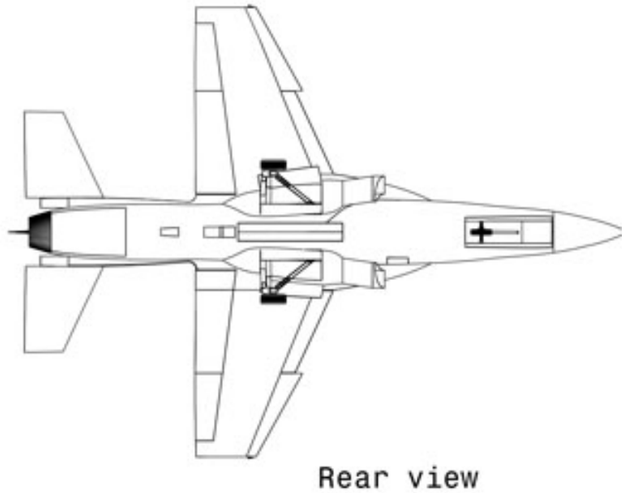

Rear view
Scale: 1:120

Content

Acknowledgment

The ShadX team would like to thank friends and families for providing us with their continuous emotional support and patience as we have been completing this proposal. We also extend our special gratitude to **Mr. Abdolreza Taheri**, **Mahmood Mohammadi and Mr. Mahdi Moradi** for their remarkable inputs to the overall integration and presentation of the design. A very special thanks to **Dr. A.H. Kordkheili** who had helped us with their support on providing the team with facilities.

1 SHADX DESIGN APPROACH

1.1 BIG PICTURE & RFP UNDERSTANDING

The design process of T-68 - Saena starts by extensively studying the RFP [1] and extracting the requirements of the design. Common design concepts from the literature on trainer design [2], [3], [4], and [5] as well as the requirements from the real world domain, mainly from USAF have been highlighted and observed to form The design space as depicted in Figure 1.

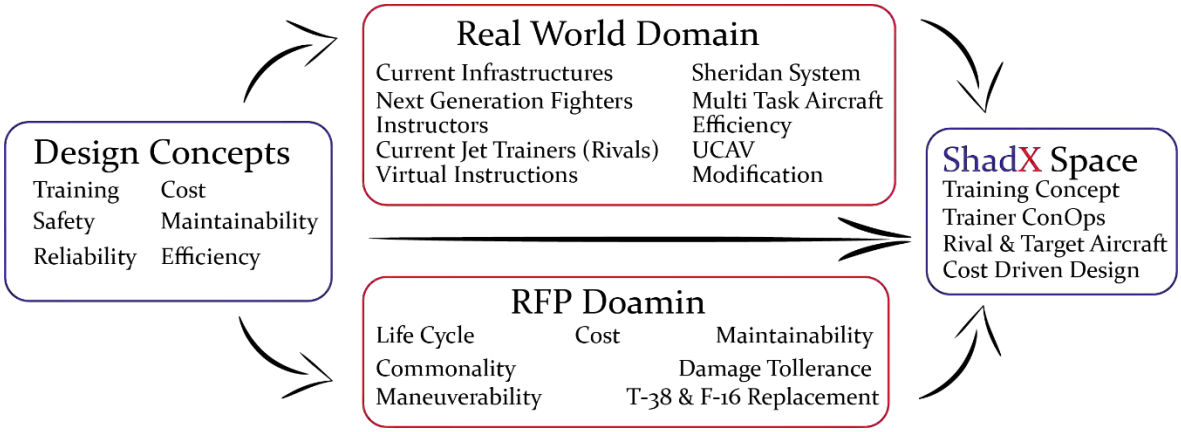

Figure 2 Design Space

In brief, the design space resolves a set of design concepts for Saena that are considered vital for a trainer aircraft. The main concepts promoted by RFP are Training, Cost and Safety. After thoroughly analyzing the real world constraints, we select three main objectives to form the core of the APTA design: effective training, satisfying the safety requirements, and cost-effectiveness.

During literature review, it was discovered that the RFP of the competition is closely related to that of the T-X program [2]. [6].We assume that USAF is the major target market for the T-68. For this goal market, we have thoroughly studied 5th generation fighters *F-22* and *F-35*. Consequently, Saena utilizes a new Variable Stability Augmentation System (V-SAS), to fly as close to the 5th generation fighters as possible, the feasibility of the V-SAS for F-22 has presented. (section 9.4.3).). This feature broadens the potential market of Saena as it can be employed as a trainer for different types of fighter aircraft.

It is well-known that student pilots are prone to make small misjudgments or miscalculations. These faults should not in any way jeopardize the safety of the crew. Therefore, the aircraft safety must be advanced enough to be *forgiving* towards these errors, and yet not too passive to hinder the maneuverability of the aircraft. A compromise between the desired level of maneuverability and safety is made by introducing the VSAS into the training program. More detailed information on the system is given in section 9.4.3.

To keep the overall cost as low as possible while maintaining the desired level of safety and maneuverability, the team took the “Design to Cost” approach wherever justifiable (e.g. in selection of AR or ROC). Such design strategies form the cornerstone of Saena’s design. To reduce the operating cost, training Improvement is achieved using high technology systems and cross platform training is carried out. The cross platform training allows air and ground crew training to be performed in one sortie which makes the training process more efficient. The selected concepts are studied independently in the following sections.

1.2 Design for Safety

In this section, based on available accident database, four hazards have been identified as the most probable accident causes; Bird Strike, Mid-Air Collision, Ejection Failure, and Mechanical Failure. A risk analysis has been done on these hazards and design mitigations are proposed to lower the risk.

In this section, based on available accident database, four hazards have been identified as the most probable causes of accident; Bird Strike, Mid-Air Collision, Ejection and Mechanical Failure. A risk analysis is carried out on these hazards and design mitigations are proposed to lower their risk. The review is carried out on the most common jet trainers used by USAF, the T-38 and F-16. The identified hazards and their likelihood are listed as follows:

1. **Mechanical Failure (12%):** due to errors in inspection, maintenance, or system failures.
2. **Bird Strike/ingestion (10%)**: usually causes a shattered canopy or skin. 73% of these accidents resulted in total loss.
3. **Mid-Air Collision (10%):** involving two or more aircraft. Either due to loss of control, or poor visibility.
4. **Ejection Failure (8%):** The main problem is usually an out of envelop ejection or the sequence of ejection which resulted to death of pilots.

1.2.1 Risk Assessment

In addition to accident hazards, we identified 3 more operational hazards, which may harm the safe operation of the aircraft. The mitigations introduced here, have been implemented into the design in their subsequent chapter.

Table 1-Risk Assessment

Operational Hazards	Severity	Likely hood	Risk Mitigation	Severity	Likely hood
Engine Failure	Low	Low	Engine monitoring	low	Low
Runway excursion	Low	Low	implementing speed brake	Very Low	Very Low
sustain g-force to pilot	low	Moderate	multi-positioning seat to reduce g-force	Very low	Very low
Ejection Sequence	Extreme	High	Inter-seat sequence for ejection seat	Low	Low
ejection out of ejection envelope	High	Low	Ejection seat with zero-zero envelope	Low	Low
Mechanical Failure	High	High	Preventative maintenance for Saena	Low	low
Bird Strike	High	High	Use stretched Acrylic for Canopy	Moderate	Moderate
Mid-Air-Collision	High	High	implement embedded training system and high responsive actuation	Low	Low

1.3 DESIGN FOR TRAINING

ShadX has studied the training program, using SHELL model, to identify the necessary requirements. These requirements are in terms of performance such as high G maneuvers and system such as runway field length. The embedded training system and VSAS concept has also been introduced.

1.3.1 Program overlook

The SHELL model mainly assumes five main components for every system and focuses on the interfaces among them. The program itself is an important interface between the student and the aircraft, so this model would be a fine choice. Since our concern in this proposal is the aircraft, the scope of the analysis is restricted to one-one interfaces; Training course – aircraft, Pilot – aircraft, Environment-Aircraft and Instructor Aircraft

1. Training lessons – aircraft interface (S-H)

   The training lessons is defined as the training skills and maneuvers. This interface had been broken into four main categories; General Mission, Skills and Maneuvers and Availability. The mission requirements for training has been analyzed in section 2.2.

   a. Skills and maneuvers

      The APT is carried out in form of a set of skills and maneuvers. These skills and maneuvers were studied based on the training program of F-22 and F-16. The study led the team to requirements, which

had an effect on different part of the design. The details of requirements are not presented due to limited space. The performance requirements have been analyzed, and the critical condition has been identified as the 9g maneuver which is discussed in section 3.2. System and Cabin requirements are satisfied by cockpit commonality and the utilization of embedded training system. The embedded training system, is an advanced computer based system which simulate a battle environment in HUD and sensor outputs. Further study is presented in section 5.

b. Availability

Study of the program revealed that currently USAF is facing pilot shortage and has requested high level of availability. Saena uses an advanced maintenance system to keep the availability as high as possible. Further determination on availability has presented in section 12.3.

2. Pilot – aircraft interface (L-H)

The main purpose is to give the pilots proper experiences and feel, during the flight. Based on this approach two concepts have been implemented to support it:

a. Cockpit commonality

This concept compares the similarity of cockpit and displays with the target aircraft. In T-68 Saena commonality has been achieved in stick position, displays, and actuations. Further discussion is presented in section 0.

b. Variable stability augmentation system

The VSAS concept changes the dynamic behavior of the aircraft and simulate a fighter dynamic behavior. The detail of VSAS design is presented in section 9.4.3

Another aspect that concerns student pilot experience and training cost is the ground base training systems (GBTS). USAF has requested a 100% increase in GBTS offloaded hours, so Saena is equipped with a communication system that provides connectivity and data sharing between the aircraft and GBTS during the flight. The system allows cross platform training which means in addition to the student pilot in the aircraft another student or non-pilot flight crew can get trained in the GBTS, in the same sortie. The details of this system and type of connections, are presented in section 5.9.

3. Environment-Aircraft (E-H)

To be sure about the safe operation of the aircraft, an analysis of the expected operational airports has been done and used in the section 3.2. Five airports which are specified by USAF to be the home for the new jet trainers, have been considered in this analysis. The results of the study are presented Table 2.

Table 2-USAF AFB Study

Air force Base	Runway Length	Altitude	Min-Max Temp
Vance(Oklahoma)	5,024-9,202	1,297	-23 - 46
Columbus(Mississippi) to Laughlin(Texas) distance			783.86 Miles

4. Instructor-Aircraft (L-H)

To ensure the reliability of the VSAS system, a touch screen has been implemented in cockpit, so he would have full control over the system at all times. (section 4.4)

1.4 DESIGN TO COST

Considering the USAF constraints imposed on the Life Cycle Cost of the new APTA, a sensitivity analysis of the unit cost with respect to the design variables is carried out, the result of which show a high impact levels for variation of these variables on cost. ShadX decided to include the cost analysis from the beginning the design process. After iterations in preliminary design, the best cost-effective solution has been achieved Table 3 summarizes the most sensitive design parameters obtained from the cost model. The sensitivity is used in analyzing and optimizing the performance requirements from RFP.

Table 3-Sensitivity of Design Parameters to Saena Unit Price

Parameter	Value	Change	Effect (K$)
Takeoff Weight (lbs.)	15320	+360	+100
Max design Speed (SLS Knots)	585	+15	+100
Rate of Climb (ft./min)	30,000	+670	+100

Table 4-ShadX Cost Reduction Solutions

Section	Cost of	explanation	Implementation
Labor	Acquisition	Reducing cost sub-contracting some parts to lower developed countries	YES
Airframe	Acquisition	Using some existing parts of other aircraft and existing infrastructure	NO
Manufacturing	Acquisition	New manufacturing methods	YES
Quantity	Acquisition	Increasing the production quantity by expanding market to other countries	YES
Engine	Acquisition/operation	Number of Engines	YES
Trainer	Operation	Refining training programs and reducing flight hours	NO
Maintenance	Operation	Reducing maintenance cost by Digital data collection and managing system	YES
Training	Operation	Reduce need for secondary aircraft for ACM & Formation	YES

2 MISSION ANALYSIS

2.1 DATABASE REVIEW

ShadX database is established based on advanced supersonic and subsonic intermediate jet trainers which are mostly considered as a light attacker aircraft as well. Some of them have been previously a fighter (e.g. T-38 and T-50 which are modified from F-5 and F-16), while others have been a clean sheet design (e.g. Yak-130, M-346, L-15, and JL-9). The gathered information about these jet trainers helps to develop a baseline and compromise Saena with them in weight, shape, and performance directly. On the other hand, after a comparison between the database of these trainers and aircraft design references, a promotion has been discovered in advanced jet trainers which makes them more similar to fighters' database. Thus in specified values, fighters' database was employed to estimate more detailed parameters. Table 5 presents a brief information about the selected database, also provides all of the required information for initial sizing phase. More specific values such as shape parameters or prices are illustrated in relevant sessions.

Table 5-Advanced Jet Trainers' Database

Jet Trainer	MTOW [lb.]	EW [lb.]	Max R/C [fpm]	Service Ceiling [ft.]	Wing Area [sq. ft.]	Thrust [lbf.]
MB339A	9700	6889	6595	48000	208	1 x 4000
IAR 99	9700	7055	6900	42300	201	1 x 4000
Aero Albatros L-39	10139	7617	4130	36000	202	1 x 3792
CASA C-101	10692	7385	4900	41000	215	1 x 3550
MDB Alpha jet	11023	7374	11220	48000	188	2 x 2940
FMA IA 63 Pampa	11464	6525	5950	42325	168	1 x 3500
Northrop T-38	12500	7165	33600	50000	170	2 x 2050
Soko G-4	13955	7165	6100	42160	210	1 x 4000
Kawasaki T-4	16534	8536	10240	50000	226	2 x 3520
Bae Hawk T1W	17000	8040	9300	50000	180	1 x 5650
Aero L-159	17637	9590	12220	43300	202	1 x 6330
Hongdu L-15	18960	9921	40000	52500	270*	2 x 5552
M-346	20945	10165	22000	45000	253	2 x 6250
Guizhou JL-9	21605	10934	51180	52500	355*	1 x 9900
KAI T-50	27300	14285	39000	48000	255	1 x 11925
Yak-130	22686	10141	10000	42660	253	2 x 5512

Note: All gathered information in this table is public information found in the aircraft specification sheet except starred values which estimated using digitizer program based on length and wingspan.

2.2 MISSION & PERFORMANCE SPECIFICATIONS

After deciding on design objectives, ShadX specified the values in attachment 2 of [7] based on observations from the real world. ShadX desires to reach the objectives that mentioned in RFP.

As a RFP requirement to be capable of 8-9g maneuvering, T-68 Saena is designed to perform the 9g maneuver to be sharp, ready, and experienced for high-g maneuvers in operational fighters (5th generation).

To reach the dash speed in practice area, ShadX decided to exceed RFP objective for the following reasons [8];

- Reduced control surface effectiveness due to nonlinear aerodynamic in 0.95-1.2 Mach
- High structural vibration due to shock formation

On the other hand, sensitivity analysis results (section 1.4), every 0.1 Mach (SLS) increase 441 k$ in unit cost, it has been decided to have 1.3 Mach.

In order to compete with APTA like M346 that has a rate of climb of 22,000 fpm. ShadX decided to have a rate of climb of at least 23,000 fpm, which is also above the average (section 2.1) that is 17,000 fpm. Desired range of Service ceiling (Table 6) has been determined according to section 2.1.In order to operate in all USAF training bases the max required runway length needs to be specified according to database. These bases have 6250, 5024 and 6320 ft. runway lengths. The 5024 ft. runway is for Oklahoma AFB which has also a 9000 ft. runway, so the RFP objective is specified to be satisfied.

Team desires to pass the RFP objective for Cruise Mach Number, which would specify after iterations.

Table 6-Saena Performance Specifications

Parameter	ShadX Specifications	RFP Objective
High-g Maneuver	Sustained 9g	✓
Payload Weight (lbs.)	1000	✓
Dash Speed	1.3 Mach (30,000 ft.)	Higher than objective
Rate of Climb (ft./min)	Min 23,000	Not specified
Service Ceiling (ft.)	45,000-50,000	✓
Min Runway Length(ft.)	6000	✓
Cruise Speed	0.8	✓

2.3 MISSION SCENARIOS

As the first strict bound to the training concept, mission scenario is responsible for adaptation of training concepts with aircraft performance. According to [3], two general types of missions are defined:

- Specialized Undergraduate Pilot Training (SUPT) which is based on aircraft transition, training concentrates on navigation, instruments expertise, and aircraft dominance.
- Introduction to Fighter Fundamentals (IFF) which is focused on maneuvering, performance, and fighting scenarios mostly.

Based on these concepts and RFP requirements, four mission profiles have been developed to discover crucial performance of an APTA. These missions are defined to eliminate unnecessary sizing of referred ten different missions belong to SUPT and IFF separately. The rationale behind this definition is to divide different borders of training into weight limiting and performance limiting scenarios.

2.3.1 Mission Profiles

Following Mission Illustrated in Figure 3 and Table 7 are discussed:

I. **Long Range Cruise (LRC):** It's a mission based on [3] (discussed as transition & navigation training). In this scenario aircraft max range is conducted which weight limiting mission that should be attained.

II. **Basic Fighter Maneuvers (BFM):** A mission based on RFP's 1st attachment. Fuel transfer is not planned in this mission. But, refueling training and training maneuvers would be performed. In other words, maneuvering in practice area is allowed independently of the fuel transfer in the refueling area. It is a weight limiting mission as well.

III. **Close Air Support Training (CAS):** IFF 6th profile is demonstrated to meet the ultimate performance of the aircraft. Initial weight sizing stated that performing "dash in/out" in the training area would require additional weight compared to the BFM mission. Dash in segment should be in the same elevation with practice area. Yet, according to the supersonic fighters and jet trainers it is not possible to conduct supersonic flight in such low altitude. In order to keep CAS mission performance limiting, a supersonic dash-out at cruise III altitude. Although it is acceptable to require more fuel for a higher performance, it is not desired. So fuel transfer is anticipated to reduce the take-off weight and supply the required fuel for the rest of the mission in refueling area. In conclusion, CAS is a performance limitation.

IV. **Refueling Abortion Scenario (RAS):** CAS mission is defined for a lighter aircraft take-off than is required. Accordingly, there is a min fuel weight for take-off that is estimated for a refueling abortion mission. So, the aircraft which has been failed to refuel should be able to abort the mission and return to the base.

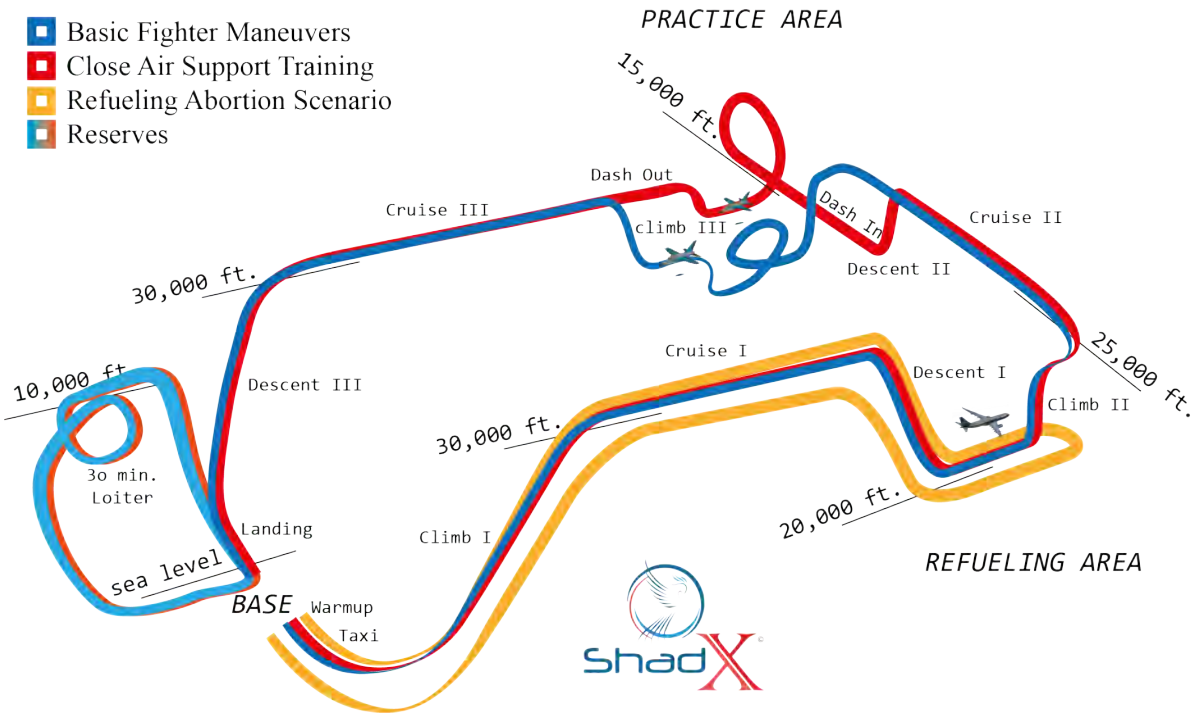

Figure 3-Mission profiles illustration

Table 7-Mission Segments Range

Segment	Long Range Cruise	Cruise I/III	Cruise II	Dash-In/Dash-Out
Range [nm.]	1500	150	100	20

Proposed missions are sizing oriented, in order to overcome the worst-case scenarios. Consequently, other cases are covered by these missions. Formation flight could be performed in LRC, BFM, and CAS as system specifications of [3] proposed these missions in the same profile with SUPT and IFF simple missions.

3 INITIAL SIZING

In this section, weight and performance sizing have been done based on section [2.1]. An iterative method has been developed to calculate the L/D. First, an assumed value for the L/D according to [9] has been taken as an input and then adjusted for the weight fraction and altitude of each flight segment, as the drag polar is updated momentarily. The BCM and BCA have been established, then. As the performance requirements have been decided by ShadX, different demanding and non-demanding constraints have been plotted on the constraint diagram and the optimum design point has been finalized.

3.1 WEIGHT SIZING

Four proposed missions are sized and arranged in a weight limiting order. The max take-off and gross weights are dictated by the mission which requires the highest amount. Consequently, for sizing the CAS mission the take-off

weight has been taken as the determined take-off weight of RAS mission. Moreover, calculated empty weight is used as the final weight for CAS mission and max gross weight as the max refueling limit. Then,the required fuel transfer in CAS mission is calculated with these restrictions. The calculation methods for each parameters are presented in Table 8. LRC and BFM missions are sized as well using this method and results are presented in Figure 4.

Table 8-Weight Sizing Calculations Method

Parameter / Weight Fraction	Method
SFC	Aircraft Engine Design Eq. 3.55 [10] using Altitude, Mach and sea level SFC
Rate of Climb	Linear Rate of Climb reduction into the service ceiling
L/D	Drag polar Class I estimation according to [9] Part I Chapter 3
Warm-up / Taxi	fuel consumption given in [7]
Climb	L/D and SFC are calculated in 500 ft. steps and differential weight calculated through energy method Chapter 3.10 [11]
Cruise / Practice Area	Breguet range equation (using range and speed) [9]
Refueling	Amount of fuel transfer required/conduct as a cruise with no fuel transfer
Payload Drop	Refined weight fraction after payload drop based on [9] Part I Chapter 2.
Loiter	Breguet range equation (using endurance)
Take-off / Descent / Landing	Constant values assumed in [9] Part I for military jet trainers.

Empty and max gross weight are calculated consdifering the BFM mission and utilized to refine the weights of other missions. Calculated mission weights are presented in Table 9.

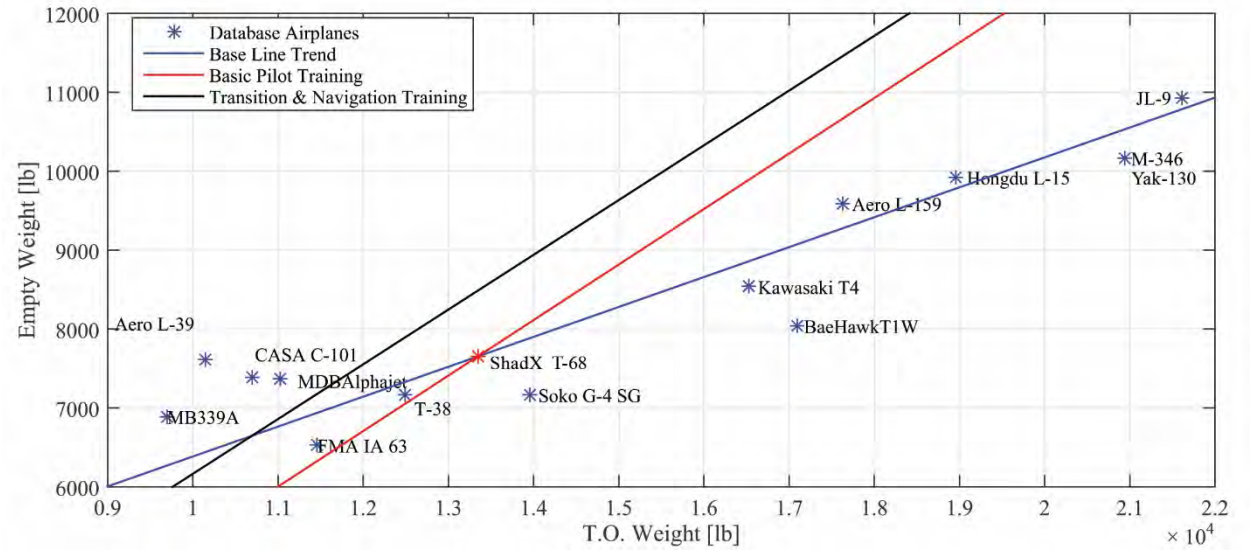

Figure 4- Weight Sizing Results of the Weight Limiting Missions

Table 9-Estimated Weight Breakdown for Missions

Mission	Take-off Weight [lb.]	Empty Weight [lb.]	Fuel Weight [lb.]	Crew [lb.]	Payload [lb.]
BFM	13350	7610	4080	550	1000
LRC	12690	7610	4530	550	0

RAS	11600	7610	2435	550	1000
CAS	11600	7610	2440+2200	550	1000

Table 10-BFM Phase-by-Phase Mission Parameters

Phase	KTAS	Altitude [ft.]	L/D	Endurance [min.]	Weight Fraction	Weight [lb.]
Warmup	N/A	0	N/A	1.0	0.9974	13315
Taxi	N/A	0	N/A	30.0	0.9438	12567
Take-off	N/A	0	N/A	0.5	0.9900	12441
Climb	316	0-30000	5.95	2.1	0.9856	12263
Cruise	461	30000	9.02	19.5	0.9700	11894
Descent	N/A	30000-2000	N/A	1.5	0.9950	11835
Refueling	335	20000	11.60	20.0	0.9668	11442
Climb	269	20000-25000	7.38	0.3	0.9974	11413
Cruise	493	25000	8.04	12.2	0.9704	11075
Descent	N/A	25000-15000	N/A	0.3	0.9950	11020
Practice Area	470	15000	5.23	20.0	0.9413	9373
Climb	269	15000-30000	7.38	0.7	0.9943	9320
Cruise	494	30000	7.72	12.2	0.9475	8831
Descent	N/A	30000-0	N/A	1.2	0.9900	8742
Landing	N/A	0	N/A	0.5	0.9950	8698
Reserve	220	10000	10.82	30.0	0.9611	8360

Table 11-CAS Mission Phase-by-Phase Information

Phase	KTAS	Altitude [ft.]	L/D	Endurance [min.]	Weight Fraction	Weight [lb.]
Warmup	N/A	0	N/A	1.0	0.9970	11565
Taxi	N/A	0	N/A	30.0	0.9353	10817
Take-off	N/A	0	N/A	0.5	0.9900	10709
Climb	316	0-30000	5.77	2.1	0.9768	10460
Cruise	472	35000	8.88	19.1	0.9644	10088
Descent	N/A	30000-20000	N/A	2	0.9950	10038
Refueling	335	20000	9.13	20.0	1.1492	11535
Climb	269	20000-30000	8.62	0.5	0.9959	11487
Cruise	481.5	30000	6.78	12.5	0.9736	11185
Descent	N/A	30000-15000	N/A	05	0.9980	11162
Dash In	532	15000	4.35	1.5	0.9916	11068
Practice Area	470	15000	6.45	20.0	0.9460	9470
Climb	292	15000-30000	7.45	1	0.9845	9322
Dash Out	766	30000	3.02	1.5	0.9891	9221
Cruise	409	30000	5.57	11.1	0.9609	8861
Descent	N/A	30000-0	N/A	2	0.9900	8772
Landing	N/A	0	N/A	0.5	0.9950	8728

Reserve	220	10000	10.82	30.0	0.9611	8389

3.1.1 Assumption Verifications

Mission Time: The total mission time for BFM and CAS missions are calculated to be 2 hours including 30 minutes of ground time, which is also pointed out in as an appropriate training time in almost every mission.

Payload Drop: Drop calculations is carried out according to F-16 drop example in [9] (Eq. 1) and calculating the landing weight from Eq. 2.

Eq. 1

$$wf_{PA_{new}} = 1 - \left((1 - wf_{PA}) \times \left(1 - \frac{W_{PL}}{M_{ff_1} \times W_{TO}}\right)\right)$$

Eq. 2

$$W_L = \left(\left(M_{ff_1} \times W_{TO}\right) - W_{PL}\right) \times M_{ff_2}$$

Reserve Calculation: RFP mandates a 30 minutes loiter which is utilized in the reserved fuel calculation, instead of the 10% of the mission time which is approximately 12 minutes. Max endurance speed occurs at 86.6% of the max lift-to-drag ratio (according to [12] Fig 13.5). Therefore, reserved lift to drag ratio and velocity has been estimated first and corrected after the precise lift to drag ratio calculated in section 7.

Long Range Cruise Mach: Long range cruise Mach is calculated utilizing LRC mission cruise phase drag polar (Figure 5). Max cruise Mach is 0.77 at 35,000 ft., so long-range cruise Mach is 0.79 with 1% decrease in fuel mileage.

Practice Area Average Velocity: According to [9] Part V, cruising speed must be less than 0.9 of the max cruising speed and maneuver speed must not exceed the cruising speed, so an average value of 480 knots has been taken for calculation of consumed fuel in the practice area.

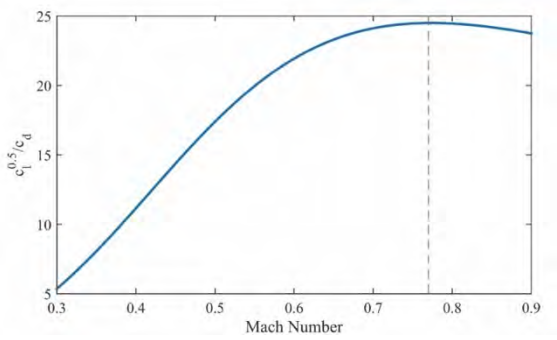

Figure 5-Long Range Cruise Mach Number

3.1.2 Sensitivity Analysis

In this section a numerical method is developed to analyze the fuel burn versus RoC, cruise Mach, and Altitude. The sensitivity analysis is carried out based on these results and the best design point has been selected.

Rate of Climb: Results highlight the effect of R/C on the mission fuel burn. As it increases, sensitivity decreases and when it is approximately higher than 25,000 fpm, it faces an slight weight reduction. Constraint lines for different Maximum R/C's have been plotted in the constraint diagram, in order to have flexibility in the design point

selection process. The decision on whether to meet this requirement with the use of A/B or not, has been made and justified in (section 3.2).

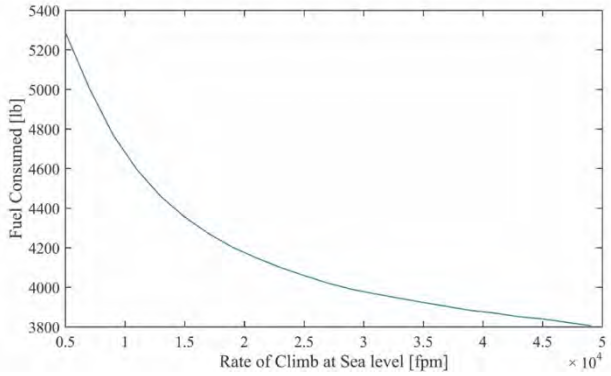

Figure 7-Fuel Weight Sensitivity vs. R/C Without Afterburner

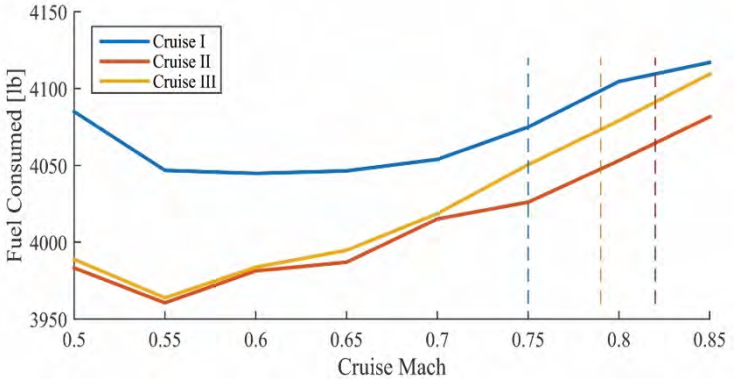

Figure 7-Fuel Weight Sensitivity vs. Cruise Mach

Cruise Mach: Cruise speed almost has no effect on mission fuel burn and aircraft unit cost. Calculations have revealed that this effect is less than 150lb for fuel burn and less than 100 k$ for unit cost, if the cruise speed is 200knots. Decreasing the cruise time has the benefit of more efficient training and less life cycle cost. Then the average max cruise Mach is selected with respect to the critical Mach and gross weight.(Figure 7)

Best Cruise Altitude: Although increasing cruise altitude lessens the drag and structural loads, it burns more fuel for climb segment. As a result, an optimum zone forms for cruising altitude. Noting that, cruising altitude does not have significant effect on weight. So the weight optimized design point is selected.(Figure 8.)

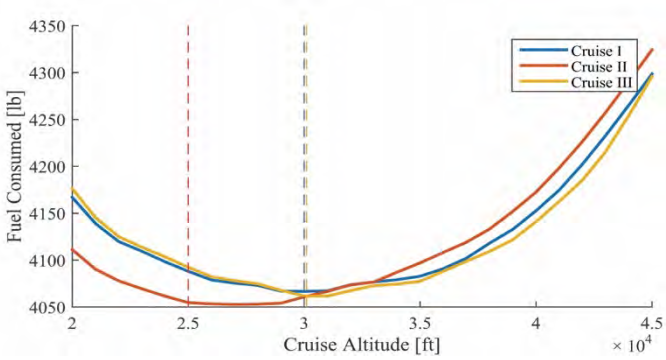

Figure 8-Fuel Weight Sensitivity vs. Cruise Altitude

3.1.3 Cost Sensitivity

Cost sensitivity analysis highlights that the max take-off weight has a major effect on the unit cost. As a result, the decision has been made to reduce the weight. Based on section 3.1.2, optimizing max sea-level R/C and cruise altitude causes 2,000 lbs. weight reduction (MTOW reduced from 15,650 lbs. to 13,350 lbs.) and approximately 1 M$ unit cost reduction (section 12.3). Based on these optimizations T-68 Saena has less weight than almost all of the APTA in the T-X program database. (section2.1, Figure 4)

3.2 PERFORMANCE SIZING

Performance sizing has been carried out primarily based on [9] and [13] First, the performance requirements demanded by the RFP and translated by ShadX are laid out in the constraint diagram. Then the design space has been studied and the design point selected.

3.2.1 Performance Requirements

A set of challenging point performance requirements as well as the ones mentioned in the RFP have been demanded in section 2.2. Here, details of the said requirements have been determined by ShadX mainly based on [3] and [14].

1. It has been decided to consider a 360-degree turn pulling 9gs, followed by a 9g pull-up/push-over. A total of 6 maneuvers have been decided to be executed in practice area, sequentially.
2. a 1000 lb. air-to-surface dummy bomb is dropped during an aggressive 6g 180-degree turn maneuver.
3. Dash in at M = 0.85 at 15000 ft. and dash out at 30000 ft. and M = 1.3 in CAS mission. Cruise at Mach 0.79 at 35000 ft.
4. 25000 fpm rate of climb at sea level (section 3.1).
5. 50000 ft. service ceiling, 6000 ft. min runway length.

According to [3] 9g maneuvers mentioned above can be met with or without the use of A/B; a decision that has been made later in this chapter. In order to size the aircraft to meet these requirements, an initial drag study has been carried out and the results are presented in the following section.

3.2.2 Drag Polar Estimation

Drag Polar used for initial sizing was estimated based on flight conditions specified in section 2.3 using [AAA]. The skin friction coefficient (C_F) is estimated to be 0.003 based on [11] equation 2.22 and [9] provided database.

Based on the equation 4 of [15], Oswald Efficiency Factor (e) in clean configuration has been calculated to be 0.87 in initial sizing, with an AR of 4.

Eq. 3

$$e = \frac{1}{1.05 + 0.007\pi AR}$$

The above estimation was verified with the help of figure 3 in [15], with a value of CD_0 to be 0.0153. Also [13] suggests an empirical equation for calculating e for the proposed design. Equation below have been used and a value

of 0.92 was obtained. It was decided to continue with the value of 0.87 to have a more conservative initial sizing. In takeoff and landing condition, e was estimated to be 0.82 and 0.77, respectively.

$$e = 4.61(1 - 0.045AR^{0.68})(Cos\varphi_{LE})^{015} - 3.1$$

The initial Drag Polar used for performance sizing is presented in Table 12. The verified Drag Polar can be found in section 7.3. The induced drag parameter (K) has been held constant in this step of the design. The compressibility effect emerges when Mach numbers are higher than 0.5 [9] and has been estimated using figure 12.7 from [9] and is added to the subsonic CD_0 in different regions.

Table 12-Drag Polar for Different Flight Conditions

Flight Condition	Drag Polar
Clean, $M < 0.5$	$0.0153 + 0.0915C_L^2$
Clean, $0.5 < M < 0.9$	$0.0203 + 0.0915C_L^2$
Clean, $M > 1.2$	$0.0393 + 0.0915C_L^2$
Takeoff Flaps, Gear Up	$0.0363 + 0.0970C_L^2$
Takeoff Flaps, Gear Down	$0.0563 + 0.0970C_L^2$
Landing Flaps, Gear Up	$0.0803 + 0.1033C_L^2$
Landing Flaps, Gear Down	$0.1003 + 0.1033C_L^2$

Increment in zero-lift drag coefficient due to takeoff and landing flaps has been estimated to be 0.024 and 0.065, respectively.

3.2.3 Method of Sizing

With the use of estimated drag polar, each requirement has been sized and the corresponding T/W & W/S has been plotted on the constraint diagram [figure…]. All performance calculations have been based on standard day conditions with no wind.

3.2.3.1 Stall Speeds

Stall speeds have been estimated using [16]and [17] have been verified in section 11.1 later. The estimated values are presented in Table 13.

Table 13-Stall Speed in different Flight Conditions

Flight Condition	Stall Speed [kts]
Takeoff, sea level	115
Landing, sea level	90
Clean, Practice Area	144
Clean, Cruise Ⅰ 30000 ft.	206

3.2.3.2 Dash Speed

As requested by ShadX, the aircraft has been sized to be able to dash out at Mach 1.3 at 30,000 ft. as well as cruise at its long-range cruise speed at Mach 0.79 at 35000 ft. It has been noted that Mach 0.79 is not a demanding requirement. Weight at the start of the dash speed (Mach 1.3, CAS mission) and long-range cruise have been determined to be 11162 and 11467 lbs., respectively.

3.2.3.3 Required Runway Length

The take-off and landing distance calculation has been done based on [9] and [13]. The aircraft has to be designed to takeoff on a 6000 to 8000 ft. runway on dry and icy conditions at sea level. Takeoff and landing distance has been

initially guesstimated to be 2500 and 2900 ft., respectively, based on the available database [17]. [13] presents a quick estimation $S_L = 0.3V_A^2$ which has been calculated to be 3500 ft^2, assuming $V_A = 1.2V_{S_L} = 108\,kts$. As studied, every 100ft increase in estimated landing distance with constant $C_{Lmax,\,LA,}$ would increase wing loading only by 1 unit, so landing distance requirement has been plotted on the constraint diagram with a 300-ft difference between each line.

Initial sizing has been done using the approximation given by the RFP; sum of takeoff and landing distances is set equal to the required runway length, so an optimization method has been used to find the shortest takeoff and landing distance, hence lines of constant runway length have been generated and plotted on constraint diagram. It is required to move along these lines, which would result in a runway-length-optimized design point. These values have been verified later in section 11.1. Figure 9 shows one of the iterations done, for $C_{Lmax,\,TO}$ =1.6 & $C_{Lmax,\,LA}$ =1.9.

Takeoff from Hot & High air force bases, like Vance, Oklahoma (1300 ft. AMSL and 46^0c) has not been an aggressive constraint, as it is seen on Figure 13 For calculations of required landing distance in icy runway conditions, a factor of 1.6 has been used to ensure adequate landing distance. Balked TO scenario has been accounted for, with the assumption of $\frac{W_L}{W_{TO}} = 1.1$ [9] for military trainers.

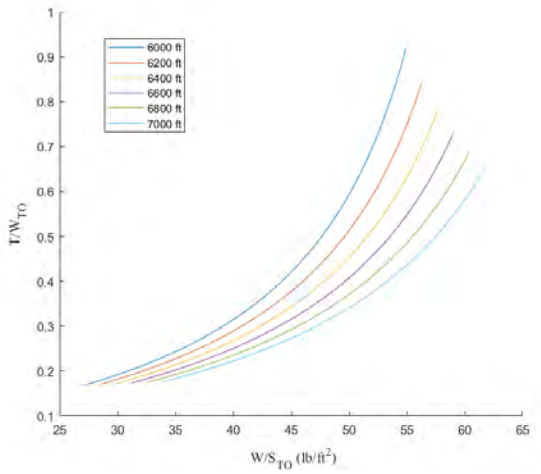

Figure 9-Required Runway Length Optimization for CLmax, TO =1.6 & CLmax, LA =1.9

3.2.3.4 Climb Performance

To assess the rate of climb ability of the aircraft, a range of different specific excess powers as well as the desired sea level RoC, have been plotted on constraint diagram to give a better handle to decide on the design point. The sizing has been done using energy-method; general equation of constraint analysis [18]. Service Ceiling requirement was also calculated. Other requirements for CGR of 0.05 and 0.025 (Balked Landing) have also been sized.

3.2.3.5 9g Maneuvers & Payload Drop

9g maneuvers requirements have been calculated for BFM and CAS mission with the use of [AAA]. The decision on execution of high-g maneuvers with or without use of A/B's made at the end of this chapter.

Sizing for the payload-drop maneuver was done with the use of the equation 4-1 [19] and the constraint has been plotted on Figure 13 As seen in the constraint diagram, the payload-drop constraint line falls well below the design space.

3.2.3.6 Cost-Based Decision on Aspect Ratio

In order to arrive at an optimum aspect ratio for the design, a study has been done on aspect ratios ranging from 2 to 6; a range, extensive enough to cover all the existing jet trainers' database (average AR of 4.5). Using [Raymer], the effect of AR on TOGW has been studied and the results are presented in Figure 10 .

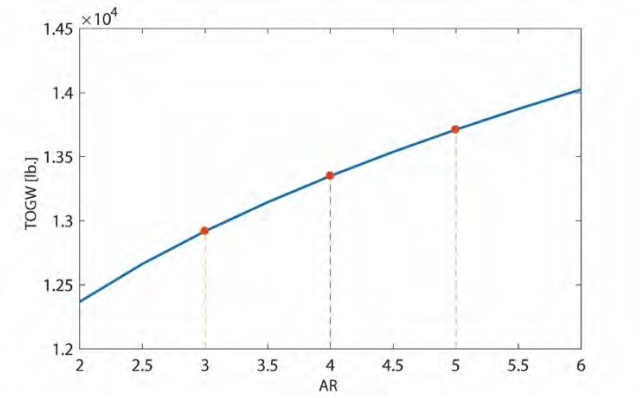

Figure 10-TOGW vs. AR

With increase in aspect ratio, the takeoff gross weight also increases which means a higher unit cost at the end. It is seen that an increment of 1 unit in aspect ratio, makes the design 390 lb. heavier which leads to a more expensive aircraft (+110k$), based on the sensitivity analysis done in section 1.4.

In order to find the optimum AR, it is required to plot an AR-independent constraint line on carpet plots and find the corresponding desired design point, which meets a certain performance requirement. Runway length requirement has been chosen to be plotted on carpet plots and 9g turn maneuver has been selected to be studied, as it is a controlling requirement. Figure 12shows the different design points for different AR's. One of the design points is shown on the plot.

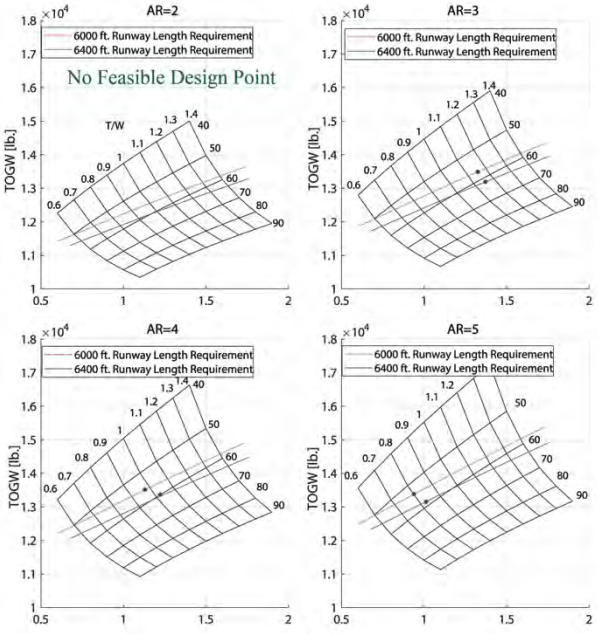

Figure 11-Carpet Plots for Different AR

Carpet plots containing lines of constant runway length for four values of AR has been drawn in Figure 11. For each AR, design point has been selected in a way so that it meets the 9g maneuver constraint. Figure 12 presents the corresponding design points on the constraint diagram. It so appears that aspect ratios of 2 or lower could not meet the 9g turn and runway length requirement at the

same time, hence no feasible design point is available for AR of 2. the aspect ratio values of 3, 4, and 5 are able to meet the 9g turn maneuver requirement. As TOGW increases with AR, it is rational to choose the min value, so AR of 5 is also not desirable to be selected. Figure 11 also shows the increase in takeoff weight with increase in AR. A lower AR results in a better pitch attitude at approach, which helps the pilot in his/her landing training.

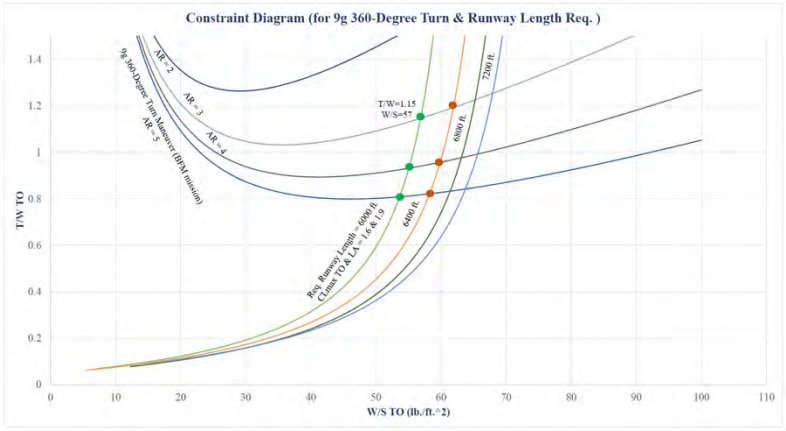

Figure 12-Constraint Diagram (9g Turn and Runway Length)

This argument has led to selecting the lowest AR, capable of meeting the desired requirement while keeping the TOGW as low as possible. Selecting AR of 3 results in a higher T/W and lower W/S on 6000-ft. runway, on the other hand choosing AR of 4 results in a lower T/W and higher W/S on 6400-ft. runway, so a value of 4 has been selected for AR to arrive at an optimum point.

3.2.3.7 Decision on Max Lift Coefficients

A $C_{Lmax,\ clean}$ range of 0.8 to 1.5 according to [11]and [20] has been selected to be studied in order to select the best value corresponding to highest W/S and lowest T/W. A range of values between 1.5 to 1.9 and 1.8 to 2.1 has also been studied for takeoff and landing max lift coefficients, respectively. A constant difference of 0.8-0.9 has been considered between $C_{Lmax,\ clean}$ and $C_{Lmax,\ LA}$ to decide on different values of $C_{Lmax,\ TO}$ and $C_{Lmax,\ LA}$ to be study, based on the technology available today [11]. The effect of different max. lift coefficients on takeoff and landing distance requirements are shown on constraint diagram. According to [11], landing distance establishes the $C_{Lmax,\ LA}$.

Selecting higher $C_{Lmax,\ clean}$ would increase the required thickness of the wing and hence a more sweep angle would be needed to achieve the same critical Mach number. Higher sweep angle then results in more wing weight, drag, and more AC shift which is not desirable due to stability concerns addressed by the RFP. So, the final values for maximum lift coefficients are shown in Table 14.

Table 14Max. Lift Coefficients for Different Technology Levels

Flight Condition	High-Tech Value	Med-Tech Value	Low-Tech Value	Final Selected Value
$C_{Lmax,\ LA}$	2.1	2	1.8	1.9
$C_{Lmax,\ TO}$	1.9	1.7	1.5	1.6
$C_{Lmax,\ Clean}$	1.5	1	0.8	1.1

3.2.4 Constraint Diagram & Design Point Selection

The constraint diagram of Saena has been presented in Figure 13In order to arrive at the optimum design point, the feasible design space has been thoroughly studied (green area in constraint diagram) and the design point selected.

3.2.4.1 Design Space Study

To have a general idea about the location of the design point of the existing aircraft and the way they are constrained, At first, jet trainers' and fighters' data has been extracted according to [9] and [18] with the exception of F-35A, and the design point of the two T-X contenders, Boeing T-X and Lockheed Martin T50A has been estimated with the assumed wing area of about 250 ft^2 (as T50A is a modification of T50) and a weight given in [21]. The corresponding design points have been plotted on the constraint diagram, then.

As seen in Figure 13 ,the design-space-controlling constraints (demanding constraints) are the Mach 1.3 dash speed, the 9g maneuver and the lines of constant required runway length, hence other constraints act relatively inconsequential. Non-demanding constraints are plotted in dashed grey lines at the background The severity of demanding constraints may result in an unviable design, but in order to stay competitive, it has been decided to go on with the requirement of Mach 1.3. The 9g maneuvers is necessary to be executed due to the need of training 5th gen. fighter pilots.

3.2.4.2 Decision on Design Point

Well-balanced design is achieved when the point of intersection of the constraint lines is selected as the design point, accordingly two optimum design points are shown on the constraint diagram; One for a 6000-ft. (point A) and the other for a 6400-ft. runway length (point B). The 400-ft. difference has been selected to allow flexibility in selection of the design point, as it is possible to reduce the req. runway length by the means of speed brakes/drag chute, if a longer runway is yielded. The corresponding T/W and W/S of these points are presented in table 2 .

Table 15Feasible Design Points

Performance Metric	Point A	Point B
W/S_{TO} [lb./ft^2]	55	60
T/W_{TO}	0.92	1.02

It is not desired to compete with 5th generation fighters like F-22 in performance metrics, as it would be pointless for a trainer to become a raptor, but in order to show that Saena is of course a platform capable of training future pilots for said fighters, these two design points have been selected to be in the vicinity of the design point of the raptor. F-35 was far away from the selected design space because of its high wing loading.

According to [13], a low wing loading will always increase the aircraft weight and cost, hence a tradeoff study has been carried out to select the final design point. According to [RAND-IV Cost Model], every 0.01 increment in thrust loading, increases the unit cost up to 30k$, but a 10 ft^2 increase in wetted area, makes the final aircraft 190k$ more expensive. With that in mind, selecting the point with lower T/W and lower W/S (point A) tends to increase the final unit cost, because the lower wing loading has more effect on the unit cost. This acts against selecting the point A. Although this point shortens the runway length, but it makes the design heavier and draggier, and causes poor ride quality in turbulence and is prone to structural vibrations.

The off-the-shelf engine mandate by the RFP, as a non-performance constraint, acts actively in the decision-making process and the design penalty should be assessed and accepted, which in our case, may result in an excess thrust. At this point, a quick study has been done on available engines which lie inside the design space, in order to assess the feasibility of each design point. A thorough discussion can be found in [available engines study section].

Selection of point B results in a required thrust of 14960 lbs. (9% installation loss has been assumed) which is closer to the available engines, independent of number of engines.

In conclusion and after consultation with the team supervisor, suggesting that a justifiable excess thrust is always appreciated, the point B has been selected as final design point.

3.2.4.3 Decision on Afterburning Capability

As the study suggests section 6.4, only one of the candidate engines does not benefit from an A/B (F125). It can be concluded then, in order to keep the design low-weight (low-cost) and viable, the offending requirements can be relaxed if an afterburning engine is selected. In that way, 9g turn maneuvers and dash speed requirements could be met with the use of A/B; allowing the engine to be effectively used through the dominant subsonic flight envelope. With that in mind, point B is considered to be the Max-power T/W_{TO}, so the MIL-power T/W_{TO} lies below the design space, at the point of intersection of the 25000 ft./min RoC and 6400 ft. runway length constraint line.

3.2.5 Conclusion

The final values of W/S_{TO} and T/W_{TO} (dry/wet) are presented in table 4 and are compared with the existing database. The corresponding installed & uninstalled thrust and wing area (with 13350 lbs. as MTOW) is reported in table 5.

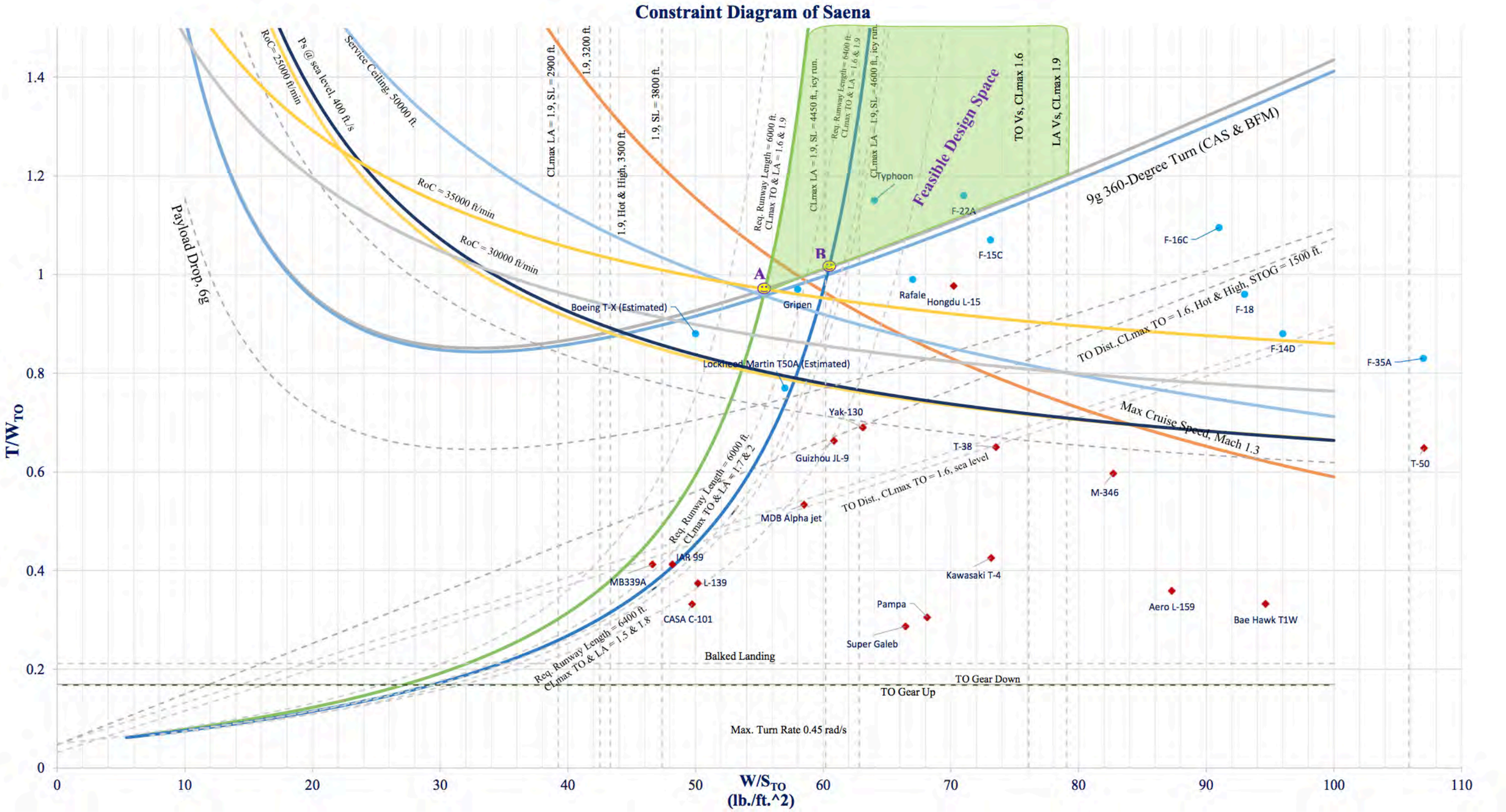

Figure 13-Constraint Diagram

Table 16The Selected Design Point in Comparison with Rivals

Performance Metric	Saena	Existing Jet Trainers	Advanced Jet Trainers	Database [Roskam]
W/S_{TO} [lb./ft^2]	60	68	79	40-80 (average of 57)
T/W_{TO} (dry/wet)	(0.78/1.02)	0.49	0.63	0.38

Table 17-Required Thrust & Wing Area

Req. Installed Thrust [lb.]	Req. Uninstalled Thrust [lb.]	Required Wing Area [lb./ft^2]
13620	14960	222.5

The selected design point is plotted on the carpet plot containing the demanding requirements presented in Figure 13. Figure 14verifies that the desired point is of course able to meet all the requirements.

As the selected design point is also in the vicinity of F-15, JAS 39 Gripen, Dassault Rafale, Eurofighter Typhoon, and T-X contenders; theoretically speaking, Saena is able to perform a set of maneuvers which are common between these fighters, making it a possible training platform for other fighters.

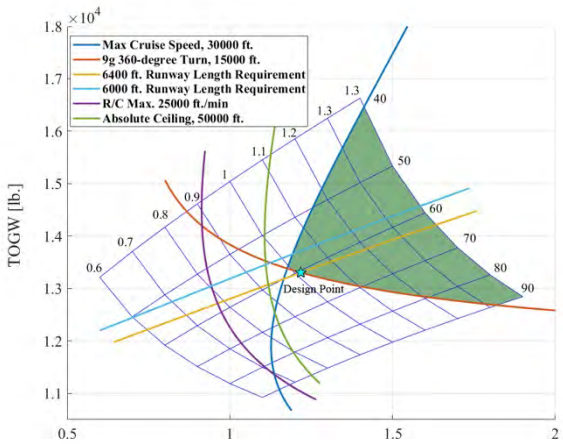

Figure 14-Carpet Plot for Demanding Constraints

4 CONFIGURATION STUDY & DEVELOPMENT

In this section, in order to choose the best possible configuration for T-68 Saena important requirements have been considered. After first comparison between 8 configurations, 3 of them have been chosen for further analysis. Contemplating the pros and cons conventional configuration is selected for Saena. The cockpit dimensions and instruments layout is calculated and formed according to RFP requirements. Also, the fuselage sizing has been carried out by estimating the dimensions of components.

4.1 NEW DESIGN VS. MODIFICATION

Looking at the history of jet trainers, ShadX realized that most of the previous trainers has been modified versions of fighters or existing aircrafts. The finding brought forth the option of modifying an existing aircraft instead of the new design. Using an analysis on modification and existing aircraft, ShadX found that the best answer to the RFP would be a new design with focus on training.

Study on history shows a changing path, caused by the lack of sound knowledge about training and wartime constraints. At first the simple economic constraints justified the use of modified fighters instead of new designs. Studies on training programs revealed that the training effectiveness affect the overall performance of USAF more than expected, and trainer aircraft plays an important role. Based on this study, ShadX decided to go with the new design or redesign of an existing aircraft. ShadX analyzed the maneuverability of existing aircraft and select the ones in 20% domain of the determined design point. The T-38 and F-16 has also been added to comparison, since they are the current trainers and using them would reduce the NRE and crew training cost very much. some candidates may have similar maneuverability, but they have very different performance, which needs modification. The type and level of modification determines the cost of the modification. The comparison is mainly between fighters, F-22, F-15, Gripen, Rafale, Typhoon and the two previous trainers T-38 and F-16.

The case for fighters is almost similar, since they all have very high takeoff weights and therefore high engine thrusts. The redesign of these fighters involves severe reduction in weight and reduction in thrust, which means change of the engine. The off the shelf engine constraint would limit the available engine sizes which brings forth the need for changing the structure. Changing the structure is the last option in redesigning an aircraft because it would affect the structural integrity, and decrease the effectiveness of redesign. It is noted that this problem happened because there were little existing light weight fighters.

The T-38 was studied. The platform of T-38 has low G-tolerance and would require a redesign on structural limit. Also the old avionics and actuation system, needs serious modification to flight control system. Also the T-38 has two old engines which has low efficiency and insufficient thrust for 9G maneuvers. The replacement of this engines with two new engines would needs resizing of the aft body. Also the refueling system is one of the mandated capabilities requested by RFP, and the integration of this system into the aircraft would cause serious structural and stability modifications. These modifications in overall would increase the cost of redesign to the point where it would not be profitable anymore.

In case of F-16, ShadX studied the aircraft. Besides the heavy structure which is still there, the F-16 has good characteristics which makes it a good option for redesign. The complete cockpit set systems and sufficient maneuverability makes the F-16 a good option for redesigning. The team took an analysis over the F-16 and encountered insufficient design data, specially about the location of CG and the corresponding static margin. Since a

rather strong constraint on CG excursion has been set by RFP, estimating the CG characteristics would cause illogical results which affect the design deeply. In email communication with The Lockheed Martin Supplier Communications Team on March 3,2018, regarding this problem, the company stated that due to personal privacy and security issues divulging any information is not possible.

So the team found that a new aircraft, with focus on the training, would better meet the RFP requirements.

4.2 SAENA CONFIGURATION SELECTION

In brief, the process of configuration selection consists of ranking eight general candidate configurations by scoring them in the decision matrix shown in Table 18. The performance and cost characteristics of configurations are the columns of the matrix that are chosen based on the main design objectives. The scores are decided relatively between configurations. The safety parameters in the comparison are based on the accident history (section 1.1).

Table 18- Configuration Decision Matrix

	Maneuverability	Familiarity	Safety	Reliability	RDTE Cost	Estimated EIS	Weight	Total Score (higher better)
Impact factor	3	3	3	2	3	3	1	
Conventional	2	3	3	3	3	3	1	49
3 Surface	3	2	1	2	2	1	1	32
Joined-Wing	3	2	1	3	2	1	3	36
Blended Wing-Body	1	2	1	2	1	1	3	25
Control Configuration Vehicle	3	2	1	3	2	1	1	34
Tail-less Delta wing	2	2	2	2	3	2	1	38
Tandem Wing	1	1	1	1	2	1	3	23

Based on In brief, the process of configuration selection consists of ranking eight general candidate configurations by scoring them in the decision matrix shown in Table 18. The performance and cost characteristics of configurations are the columns of the matrix that are chosen based on the main design objectives. The scores are decided relatively between configurations. The safety parameters in the comparison are based on the accident history (section 1.1).

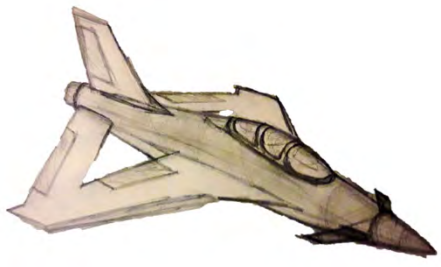

Figure 15-Joined-Wing Initial Sketch

Table 18, the top three configurations chosen for more detailed analysis and development of the preliminary sketches are conventional, Joined-Wing, and CCV.

1. Joined-Wing

The main advantage of Joined wing is the reduced induced drag. A rough comparison between the joined-wing and the conventional configuration has resulted following points:

- 5% reduction in weight
- 40% increase in lift production
- 3.5% lower total drag
- Possibility of the CG Control (It is noted that, such capability is an important feature for a small military aircraft)

Besides good features, an important disadvantage is the lack of built models, which results in less known lift, structural behavior, and safety record. This lack of the database affects RDTE, flight test, certification, and maintenance cost. These problems would increase the RDTE time and postpone the EIS date.

Figure 16-Initial Conventional sketch

2. Conventional

The best feature of conventional configuration is the known dynamic behavior and mature database. This maturity gives very flexible and vast space to design the aircraft. Based on the safety records, the conventional configuration would be the best choice.

3. Control Configuration Vehicle (CCV)

The CCV configuration increases the number of control surfaces, develop an advanced flight control system in order to decrease the coupling effect of surfaces, and increase the maneuver precision of the aircraft. The lack of database and knowledge about different control surfaces, along with very complicated control system makes the configuration costly and unsafe.

Figure 17-Initial CCV sketch

4.2.1 Conclusion

To choose an adequate configuration, ShadX has analyzed the current financial state of USAF, which revealed that the cost efficiency and EIS date constraints are very important. ShadX has performed a cost analysis on USAF Training operation. That is, USAF spends 1.22 B$/year more, operating T-38 instead of SAENA. Evaluated TRL of CCV and Joined-wing are estimated to be less than 5, which postpones the EIS for 3 years more. Therefore, we decided to go with the conventional configuration and avoid any increased cost or delay in EIS date.

4.3 COCKPIT DESIGN

RFP mandates the Cockpit commonality with 5th generation fighters. The most important issues are the location, configuration, and actuation of controls and displays between Saena and 5th generation fighters Cockpits. To have better training effectiveness cockpits of F-22, F-35 and T-38 were compared. (Table 19)

One of the most important problems with the T-38 cockpit is lack of fly-by-wire control system to transfer the actuation feel to student pilot. Furthermore, according to RFP, on-board sensors must not be required. So, Embedded Training System (ETS) is used in Saena cockpit for simulation of; on-board sensors, data link capability, and training environment in practice area (section 5).

Table 19-Comparison of Old APTA and New APTA with Fighter Targets Cockpits

Aircraft	F-22 Raptor	F-35	T-38	Saena
Flight Control	FBW	FBW	Mechanical	FBW
Stick force	Right-side stick	Right-side stick	Centered-stick	Right-side stick
Throttle position	Left	left	left	left
Displays	Glass-cockpit	Glass-cockpit	Glass-cockpit	Glass-cockpit
On-board sensors	Has on-board sensors and data link capability	Has on-board sensors and data link capability	No sensors and data link capability	Simulated on-board sensors and data link

4.4 COCKPIT INSTRUMENT LAYOUT

As RFP mandates, the cockpit of Saena is designed for two pilots with tandem configuration. The glass-cockpit design provides aircraft control for both pilots. Furthermore, the instructor is in command of ejection mode and has the ETS presentation of student pilot in aft cockpit multifunction displays (MFD). Two up-front displays are located for both cockpits, up the MFDs for standby flight instrument, warning, and caution. Due to higher reliability, lower weight, and readability; displays are decided to be LCD [22]. Both pilots control the aircraft with the Hands-on Throttle and Stick (HOTAS) concept. In order to adjust the variable SAS during the flight, a touch panel is located in the aft cockpit, for the instructor to load and control the settings on the display. The location and type of displays,

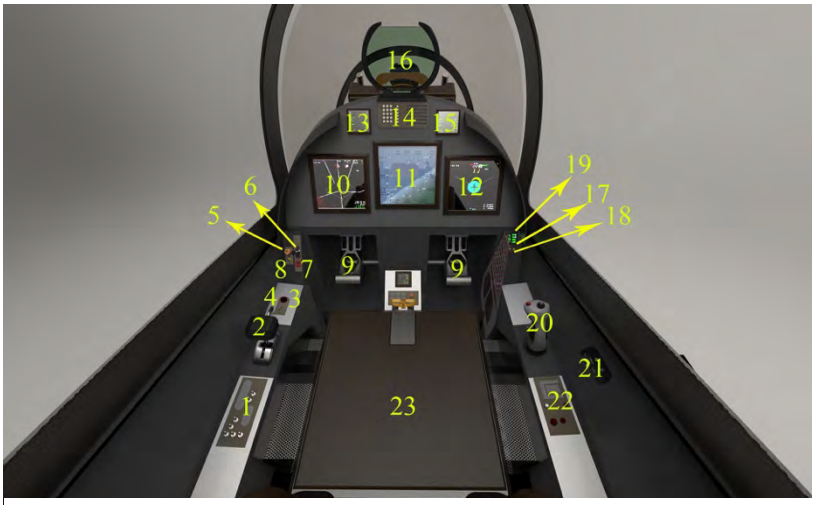

Figure 18-Cockpit Instrument Layout

Controls, and other instruments is selected in a way to achieve the

highest commonality. Figure 18

Cockpit Dimensions & Pilot Visibility

RFP mandates to meet 95th percentile anthropometric accommodation [23] for student pilot and instructor. Cockpit dimensions were determined according to [9] assuming ejection angle of 15 degrees, and clearance of helmet and canopy. As RFP mandates for both pilot visibility, the cockpits are designed to achieve high visibility during different phases of mission. The side visibility of both pilots is more than 300 degrees. Figure 20 & Figure 19

1 Communication Control
2 Throttle
3 Engine Start
4 Defog Control
5 Emergency Landing
6 Landing Gear Control
7 Landing & NVG lights
8 Parking Brake
9 Pedals
10 Multifunction Display 1
11 Multifunction Display 2
12 multifunction Display 3
13 Up-Front Display
14 Integrated Control Panel
15 Up-Front Display
16 Heads Up Display
17 Auto Recovery Switch
18 Ejection Mode Selector (aft cockpit)
19 Touch panel (aft cockpit)
20 Side Stick
21 Canopy Control
22 Arm Rest
23 Ejection Seat

4.5 On-board Ladder

An on-board ladder has been placed in front of the fuselage for both pilots. Telescopic ladder has been selected to occupy less space in the fuselage. Nonetheless, the instructor pilot should use LERX to get into position.

Integration of ladder into fuselage has been shown in Figure 21

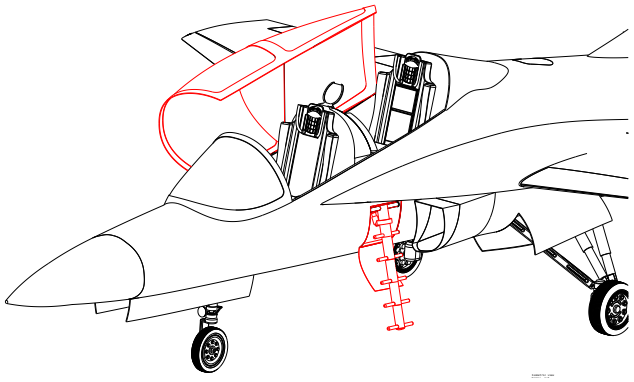

Figure 19-Canopy Opening & Ladder Integration into

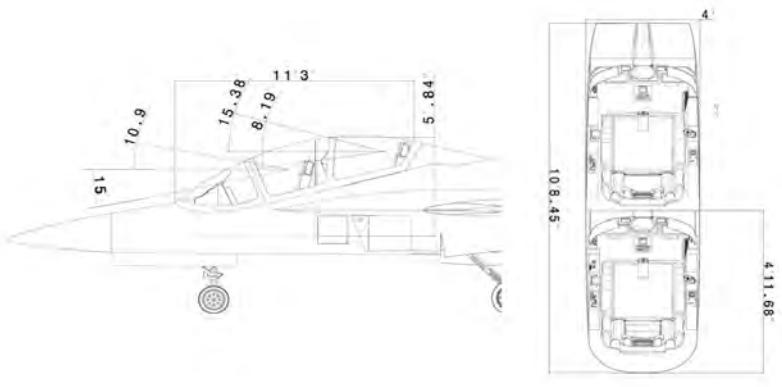

Figure 20-Pilot Visibility & Cockpit Dimensions

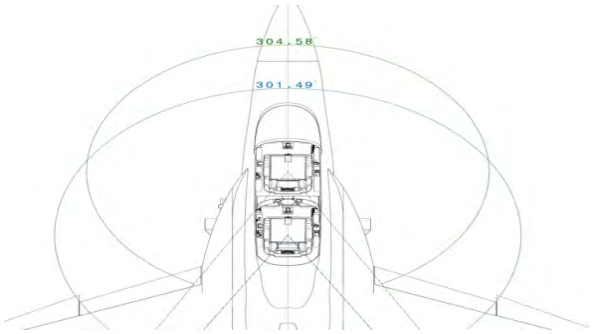

Figure 21- Pilots Max Side Visibility

4.6 CANOPY

The canopy is decided to be stretched acrylic to lower the bird strike risk. Furthermore, to reduce the complexity of the aircraft and low-maintenance of the avionics and cockpit, ShadX has decided to open the canopy to the side and in one part instead of top 2-part opening. The canopy is also equipped with explosive card to ensure safe ejection.

4.7 FUSELAGE DESIGN

According to [11] Chapter 8 initial fuselage sizing is carried out with volume estimation for each component also the volume of each section in the fuselage. ShadX decided to engage the dimensions of the component instead of volumes to calculate the fuselage dimension. Fuselage divided to four sections and relevant components have been assigned. Dimensions in Table 20 are "length * width * height".

Table 20 Fuselage Required Volume

	Dimensions	Volume [ft^3]		Dimensions	Volume [ft^3]
Nose	7*3.8*3	20.9	**Mid-Section**	6.9*4*5	108.3
Avionics	2*1*3	3	**Intake (inner section**	9*(1.88 ft^2)	15.7
Radar	1*1*1.5	4.7	**Receptacle**	1.6*1.6*0.5	1.3
Cockpit Electronic Compartment	2*1*0.5	1	**Power Generator**	3*1*1	2.6
Nose Gear	5*3.7*1.5	27.75	**ECS**	1*3.2*2	6.4
Vehicle Man. Sys.	2*0.5*1	1	**Main Gear (each')**	4.2*2.8*1	11.8
Hydraulic Sys.	2*1.5*1	3	**APU**	2.33*1.46*1.58	4.11
Cockpit	12.5*4*6.5	153.5	**Payload**	7*0.7*0.7	3.4
Multi-Function Displays	0.66*0.66*1	0.5	**Aftbody**	11.6*3.5*3.5	111.5
Heads Up Displays	0.7*0.7*1	1.6	**Engine**	11.6*2.8*3	56.19
OBOGS & OBIGGS	1*1*2	2	**Ballast**	-	negligible
Ejection Seats	2.3*2*2.75	8	Fuselage	38*6.5*4	394.2

Nose shape and cross sectional area has been optimized for supersonic. (section 7.3) Also, limited CG excursion and desired static margin refined fuselage dimensions. (Table 21.) Implementation of these restrictions form a short-coupled aircraft. This feature causes non-linear aerodynamics behavior thus CFD analysis employed to verify the results.

Table 21 Fuselage Final Dimensions

	Nose	Cockpit	Mid-Section	Aftbody	Fuselage
Length [ft.]	8	11.3	7	13.6	40
Max. Height [ft.]	3	7.1	5	4	6.5
Max. Width [ft.]	3.8	4	4	3.5	4
Volume [ft^3]	25.3	152.9	109.9	126.9	415.0

In conclusion fineness ratio of Saena is compared with APTA and database of [9] in order to verify designed dimensions. Results demonstrate that these dimensions are competitive and in the acceptable zone.

Table 22 Fineness Ratio Comparison

Parameter	l_f / d_f	l_{fc} / d_f	θ_{fc}
Reference	5.4 - 7.5	3 - 5	0° - 8° (for fighters)
Database	5 - 8.5	-	-

Saena	6.15	1.84	7.125°

5 SYSTEMS

In this section the systems implemented in Saena are explained, and it has been illustrated in Figure 24.

5.1 ELECTRICAL SYSTEM

A 150 kW generator with 145 lbs. weight is decided to be used in Saena to supply the power needed for the electrical and hydraulic system. Also, Rubi 3 Auxiliary Power Unit is used to generate the power needed for avionics and electrical systems in case of generator failure and in-flight engine start with a pilot reaction.

5.2 AIRCRAFT LIGHTING

Exterior lighting is needed for night landing, navigation, formation flight in day or night, and Night Vision Imaging System. The interior lighting is needed for the display readability and controls for NVIS training. So, nose gear lights, wingtip lights, and inlet lights have been considered respectively for night landing, formation in day or night & navigation. Also, lights have been considered for the stick, throttle, and displays for NVIS.

5.3 ENVIRONMENTAL CONTROL SYSTEM

An environmental control system (ECS), is used for cockpit pressurization, crew station, avionics cooling, and pilot g-suite. Also, OBOGS has been used to supply fresh air for the pilots. The system uses 2 percent of the engine inlet airflow, which has been considered in the inlet sizing (section 6.6).

5.4 HYDRAULIC SYSTEM

Two independent hydraulic systems have been used for Saena to increase redundancy, which is used for extending and retracting the landing gears and wheel brakes. For actuating aerodynamic and Control Surfaces Electrical system is used, so hydraulic pumps are not needed.

5.5 PAYLOAD

Payload weight has been specified in section 2.2. External payload increases aircraft drag about 40 counts and structural weight, while internal payload requires a payload bay door that causes a slight increase in drag. Therefore, following the placement of armaments in F-22 & F-35, Saena carries 1000 lbs. of internal payload. X-location is decided to be near the aircraft CG due to W&B considerations.

5.6 FUEL SYSTEM & DE-ICING

De-icing sensors are set in wing leading edge and inlets to prevent icing. The position of the sensors is illustrated in Figure 22. Fuel tanks that carry JP-8, are self-sealing to get protected from damage during the mission. Three compartments have been considered for fuel tanks to minimize the longitudinal C.G changes during the flight. Boom receptacle has been located top of the fuselage and aft cockpit of Sana. Since, the targets F-22 Raptor and F-35 use flying boom method for refueling. Total wing volume is calculated according to [9] Part 2 Chapter 6, sizing the wing structure revealed that only *58%* of this value is available for fuel tanks. So the remaining fuel needs to locate in central fuel tank inside the fuselage.

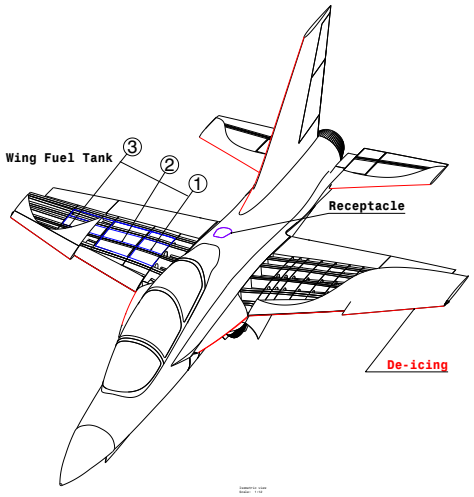

Figure 22-Wing Fuel Tanks & De-icing Sys. Locations

5.7 FLIGHT CONTROL SYSTEM (FCS)

As it has been mentioned in section 4.3, FBW type of control has been selected for Saena. Comparison between three types of FCS is represented in Table 23. The main reasons are the commonality, high maneuverability, safety, and reliability [24].

Table 23 ShadX Comparison of FCS Types

	FBW	FBL	Mechanical
System Weight	Decreased	Decreased	Increased
Maintenance	Easy	Easy	Difficult
Maintenance Cost	Low	Low	High
Reliability & Safety	High	High	Lower than Others
Maneuverability	High	High	Low
Dependency to Electrical System	High	High	Low
Influence of Temperature	Low	Low	High
Commonality with Targets	Yes	No	No
Technology Readiness Level	High	Lower than others	High
Production Cost Level (high grade means more expensive)	2	3	1

Maintainability, safety, weight, high response in formation flight, and maneuverability of the aircraft have been considered for type selection of control surface actuators. Three types of actuators which had been used in civil or military aircraft and are compatible with FBW have been compared. That are hydraulic, electromechanical, and electro-hydrostatic. Table 24 represents the summary of this comparison [25].

According to [26], EHA has a better dynamic response in comparison with EMA. Also Table 24 represents that EHA has a better level of safety with no Backlash, so EHA has been selected for Saena.

Table 24 Comparison of Actuation Technologies

Type of Actuation	Electro-Mechanical	Electro-Hydrostatic	Hydraulic
Pros	High efficiency Easy maintenance Less maintenance cost Low noise emission	High efficiency No backlash High response in comparison to others Less production cost High level of safety Low noise emission	High forces No backlash High reliability Parallel movement
Cons	Backlash Single movement only Not good for high forces	Limited stiffness Single or serial movement	Low energy efficiency Higher weight

5.8 ETS (EMBEDDED TRAINING SYSTEM)

As RFP mandates no need of on-board sensors and external stores, ETS has been implemented in Saena to reduce operating cost of training and improve the crew safety. Also, with ETS, training task effectiveness is improved by 30%. [27] Training tasks which have been considered for student pilots on ETS are mentioned as in the following:

- Air to Air intercepts
- Air Combat Maneuvering
- Air to Ground
- Tactical Data link Operations & Night Vision Imaging System (cockpit environment)
- Formation Flight

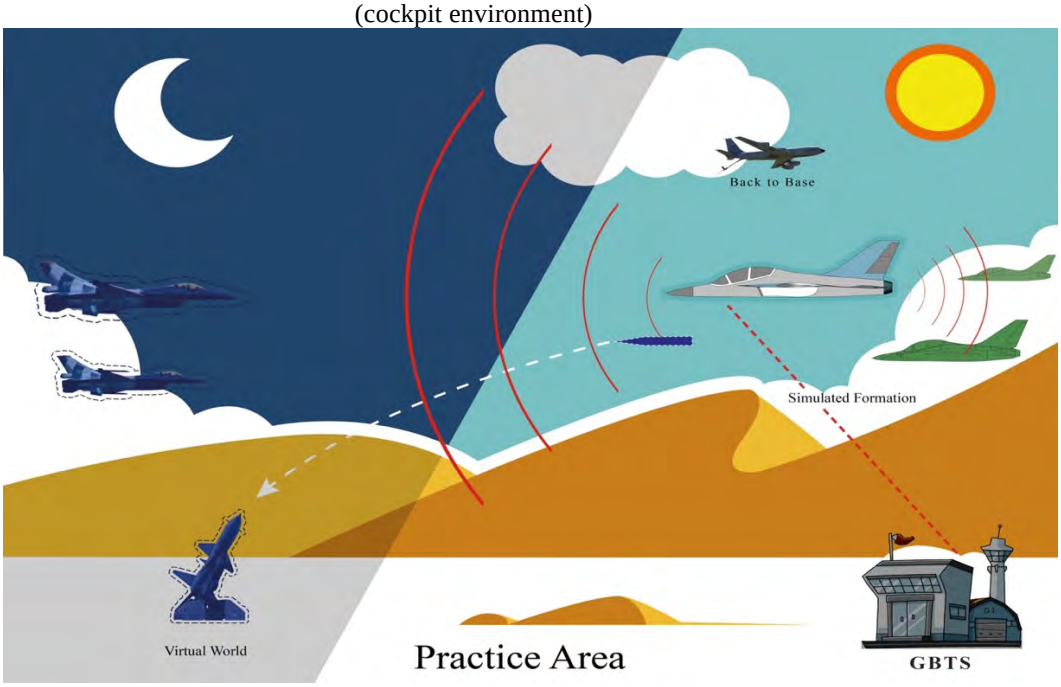

Figure 23- Training simulation in Practice Area (Operational Concept of ShadX)

5.9 SAENA-GBTS CONNECTIVITY

The connectivity between Saena and GBTS is implemented with data link to connect Saena with GBTS within 100 NM Line-of-Sight from local flying base. UHF/VHF antennas has been used for communication of Saena to Saena, and Saena with air traffic controls, and Saena-GBTS.

5.10 EJECTION SEAT

According to RFP a zero-zero ejection seat with anthropometric accommodation of 95th percentile of USAF weight and size requirements is required. Ejection seats are compared for their pilot weight requirement, seat dimensions, Max speed, and seat altitudes. Although Martin-Baker Mk18 is a T-X program design ejection seat, it has not been considered in the decision-making process due to lack of data. To reduce the sustained g-force to the pilot, automatic positioning of seat is implemented in the cockpit. Also, based on accidents review in section 1.2, Inter-seat sequence is considered in seat selection.

Table 25 Comparison of Ejection Seats Based on Flight Envelope

Ejection seat model	Manufacturer	Ejection speed(knots)	Ejection altitude(ft)	Crew weight range(lbs)	Disadvantage
K36-D	Zvezda	0-2.5 Mach	0-55,000	-	
K37-800M	Zvezda	48-136	0-16,400	125.66-201.44	lack of zero-zero capability
UTC ACES 5	UTC aerospace	0-600	0-60,000	103-245	-
Mk-17	Martin-Baker	60-250	0-25,000	103-245	lack of zero-zero capability
Mk15	Martin-Baker	60-300	0-40,000	152-216	lack of zero-zero capability
Mk16-T-38	Martin-Baker	0-600	0-50,000	140-237	Not in crew range requirement
Mk16-F-35	Martin-Baker	0-625	0-65,000	126-273	Not in crew range requirement

UTC ACES 5 seat has a modular structure and Inter-seat sequence for crew safety, so it is selected for Saena. Modular structure of seat leads to easy maintenance [28].

5.10.1 Ejection Seat Sequence for Pilot & Instructor

According to T-38 accidents due to ejection, Inter-seat sequence cockpit is implemented for two-seat to Saena for improving the safety. Three modes are considered Solo, Both, and CMD FWD which could be selected by the instructor. In all the three modes, the canopy would jettison prior to the ejection. Also, GR700 recovery parachute is selected to reduce the descent rate.

Table 26 Inter-Seat Sequencing Modes

Mode of Sequence	Solo	Both	CMD FWD
Student Pilot ejection	Both seats will be ejected at the same time	Instructor pilot will be ejected first followed by Student.	Instructor pilot will be ejected first followed by Student.
Instructor Pilot ejection	Both seats will be ejected at the same time	Instructor pilot will be ejected first followed by Student.	Both seats will be ejected at the same time

6 PROPULSION SYSTEM

According to [9] and RFP's service ceiling and speed requirements, turbofan and turbojet types of engines are suitable for Saena. Yet, engine market study reveals that there is no turbojet engine available for military aircraft. So, low bypass turbofan has been selected.

6.1 ENGINE

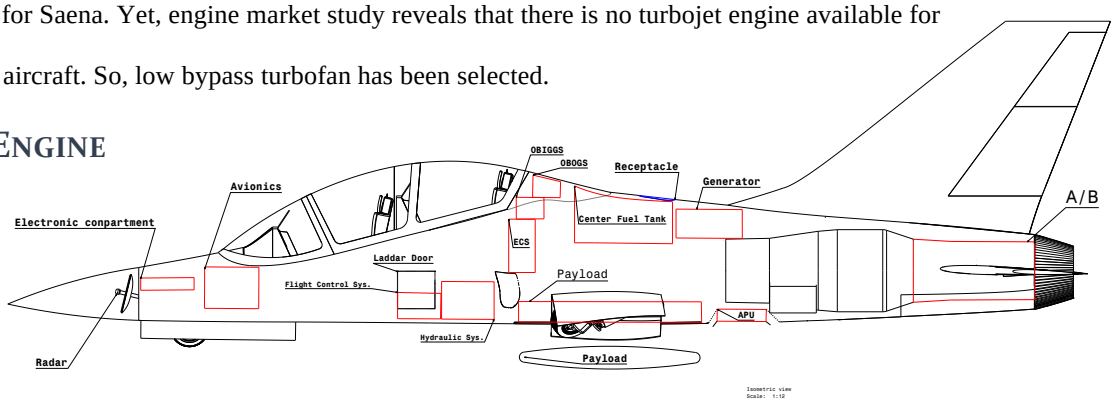

Figure 24-Saena Systems Integration

RELIABILITY & OEI

Engine reliability also aircraft safety requires an automatic relight system in case of flameout to initiate an automatic engine recovery [3]. This feature especially for single-engine case causes reducing the probability of in-flight engine failure. Although, for the single-engine configuration, in-flight shutdown rate should be considered in the decision-making process, due to lack of data it is not considered. MTBO of engines are also compared to increase the reliability and availability of Saena.

6.2 NUMBER OF ENGINES

According to database, both single and twin engine types of APTA are available. This critical decision requires some important measure of merits as below:

- Flight safety (accidents history and review)
- Weight
- Mission Thrust requirements
- Production and operating cost

Advantages and disadvantages of single-engine & twin-engine configurations are explained in Table 27 [29].

Table 27 Advantages and Disadvantages of Tingle-Tngine & Twin-Angine Aircraft

Cases	Advantages	Disadvantages
Single engine	Lower cost Ease of maintenance Better air to air performance	Redundancy of single engine, Smaller cockpit

	Smaller, lower weight Simplicity	
Twin engine	Better redundancy Better space for cockpit	Increase drag Increase maintenance cost More complex

According to decided design philosophies in chapter 1 of the proposal, safety and cost should be considered in propulsion system selection. Also, maintainability is an important factor in engine selection [30]. Single-engine is cost-efficient, low- maintenance, and has better air to air performance. Furthermore, it increases the simplicity of the aircraft while lowering the weight and size which causes lower thrust to drag ratio improving the maneuverability. However, single engine configuration heightens the risk of engine failure. Yet, to increase the safety features an engine which is suitable for single engine aircraft (section 6.4) is selected.

6.2.1 Effect of Number of Engines on Saena Unit cost

According to design philosophies discussed in section 1, considered with a comparison between two types of engines suitable for either of single-engine or twin-engine configurations. M88 and F404 are selected for single-engine and F124 and F125 for twin-engine configuration. Selecting M88 or F404 in a single-engine configuration would lower the aircraft unit cost about 3 M$.

6.3 Cost of Engine Rubberizing

RFP mandates reduction of acquisition and production cost. Therefore, off-the-shelf engines are considered in the engine selection process of Saena instead of production and rubberizing an engine to reduce Saena unit cost and RDTE cost. The published dimensions of the manufacturers are used to draw the CAD of aircraft, no rubberized dimensions is used [13].

6.4 Available Engines Study

In this part, the military engines which are available and suitable for Saena is studied. Market study leaded to engines in Table 28. For T/W of 0.78 for dry and 1.02 Wet and W_{TO} of 13350 lbs.

Table 28 Available off-the-shelf Engines Suitable for Both cases of Single-Engine & Twin-Engine Saena

Engine Model	Manufacturer	OPR	BPR	Takeoff Thrust [lbf]	Wet Thrust [lbf]	Modular Components	MTBO
F404-102	GE	26	0.34	11000	17700	6	4000
F404-RM12	GE	28	0.31	12100	18100	6	4000
F414	GE	30	0.4	12500	22000	6	4000
M88-4E	Safran	24.5	0.3	11200	16900	21	6000
EJ	Rolls-Royce	26	0.4	13500	20000	15	6000
F125	Honeywell	19.4	0.49	6280	9080	-	-
F125(dry)	Honeywell	19.2	0.49	6280	-	-	-

6.5 Engine Comparative Study & Selection

For engine selection, considered measures of merits are:

- Thrust to weight ratio of engine
- Thrust to weight ratio of aircraft
- Fuel consumption
- Maintainability
- MTBO
- Dimensions
- High-speed performance of engine
- Safety

Afterburner usage is also an important decision in propulsion system design. Both F-22 and F-35, are targets for training with afterburner. Although, afterburner is not used before IFF level of training, ShadX decided to implement it, so student pilots could experience it. Also, afterburner is used to achieve dash speed and pass transition speeds because of the drag rise in the transonic regime in practice area. So, according to dash speed of 1.3 in section2.2 afterburner is required. First engines are selected based on T/W= 0.78 dry and 1.02 Wet and W_{TO}= 13350lbs.

According to the data presented in Table 28, M88 and F404 engines are selected for further analysis. M88 has more modular components and easy access to engine parts. So, the maintenance cost of aircraft would be reduced by choosing M88 for Saena.(Table 29)

Table 29-Comparison Between Selected Engines

Merits	SFC(dry)	Weight	Modularity	MTBO	T/W (dry)	High speed	Diameter	Safety	Decision
M88	0.78	1978	21 components	6000	5.66	✓	27.4	✓	✓
F404	0.84	2282	6 components	4000	4.73	✗	28	✓	✗

6.6 Intake Location, Geometry & Design

The goal for intake design is reaching the max intake pressure recovery compatible with mission Mach number, in tradeoff with weight and production cost of intake to reach the Mach number of 0.45 in compressor face [11]. Normal shock and external compression intakes are suitable for Saena based on max Mach number of mission 1.3. Although normal shock intake has lower weight and production cost, it has lower pressure recovery [11]. So it has been selected in the design process. Two types of subsonic and supersonic diffuser designs are considered. Supersonic diffuser generates more entropy (loss), while flying sub-sonically, in comparison with a subsonic diffuser flying super-sonically. Also, less than 1% of the Saena missions is in the supersonic regime. Therefore, subsonic design is decided to implement. A boundary layer diverter is considered for improving aerodynamic stability in supersonic flight by isolating intake shock from boundary. For intake area sizing, eq.10.3 of [31] has been used with a 4% safety margin. For improving sideslip performance of Saena, the area of ramps is considered 25 percent bigger in case of a blocked ramp. The intake area is calculated to be 3.8 ft^2. Also, for calculation of diverter thickness, the eq. 16.19 of [11] below

with 1.3 safety margin is used [11].Where x is the distance between nose and diverter. The diverter intake from fuselage has been calculated 0.4 ft. So, required intake area with considering 4% of safety margin [31] is 1.88 ft. square.

There are some important criteria for location and type selection of the intake; like droppable systems, radar location, maneuvering capability, drag, and pilot-duct interference. Therefore, different intake locations were compared. Nose intake configuration has been rejected because of high-pressure loss and increasing drag due to the location of engine that is aft-fuselage buried. Also, Nose intake limits us in radar location.

Dorsal intake like F107-D fighter was another option. Which has been rejected because of pilot visibility and aerial refueling problems which takes place above the aircraft [32]. So, the number of ramps, under-wing or up-wing mounted has been decided. The goal in intake location selection is to minimize the impact of intake on producing

moment. Up-wing intake reduces wing area which has a negative impact on maneuverability and produces a moment in AOA. In under-wing intakes, wing turns the airflow to the intake and there is no intake moment [11]. Also, with using 2-ramp divided intake, the duct length would be reduced with a small pressure drop [33]. So, ShadX decided to use divided 2-ramp under-wing intake configuration. (Figure 25)

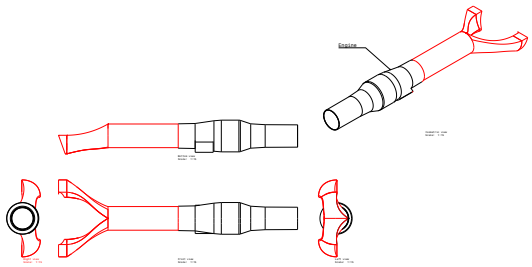

Parameter	Value
Intake Area	1.90 ft^2
Diffuser Length	10.7 ft.
Diverter Thickness	0.4 ft.
L/H	5.95

Figure 25-Intake Parameter for Each Ramp

6.7 EXHAUST GEOMETRY

Throat Area of Exhaust must be changed caused by two conditions of afterburner operative and inoperative. According to [33], C-D nozzle has better performance and lower installation loss in comparison with a convergent nozzle. Therefore, Throat area A_t would be sized for C-D nozzle in different phases of mission. The area ratio of exit & throat of the nozzle has been calculated on the authority of [31] relations which results are summarized in Table 30. NPR of Saena has been estimated for different flight conditions by engine cycle analysis and has not been $NPR < 6$. The nozzle throat Mach number has been taken 1 [34].

Table 30 Exhaust Area Change in different Flight Conditions

Flight Condition	$\dot{m}_8$ (lb./s)	P_{t8} (lb./ft2)	M_8	M_9	$A_t(ft^2)$	A_e (ft^2)	A_e/A_t
Dash	66.56	8204.93	1	2.97	0.67	4.48	6.68
Long-Range Cruise	66.89	4537.61	1	2.84	1.05	3.91	3.72
Cruise	107.45	4713.59	1	2.68	1.54	3.31	2.13
Takeoff	99.10	5014.47	1	2.59	1.63	3.01	1.84

After determining the throat and exit area of the nozzle, nozzle wedge angles are determined. (Table 31)(Figure 26)

Table 31 Geometric Parameters of Nozzle in different Flight Conditions

Flight Condition	R_9	R_8	θ	α
Dash	1.2	0.46	55.6	32.5
Long-Range Cruise	1.15	0.58	49.4	25.1
Cruise	1.03	0.7	43.9	15.7
Takeoff	0.98	0.72	43.1	12.7

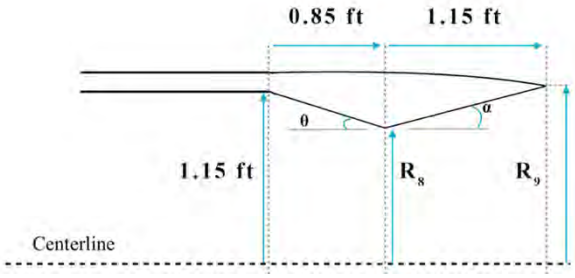

Figure 26-Nozzle Geometry

6.8 Installation Loss

To determine the installation thrust loss of the aircraft, inlet pressure loss, power extraction, and Boat Tail drag have been considered in different flight conditions [31]. The Boat Tail drag coefficient is estimated from [11] which is considered variable in various flight conditions. Takeoff requires the most careful consideration. Results of installation loss in flight conditions have been represented in Table 32.

Table 32 Installation losses in various flight conditions

Flight Condition	Percent Reduction in Thrust	Flight Condition	Percent Reduction in Thrust
Climb	5.39	Dash Speed (Wet Thrust)	6.83
Long Range Cruise	5.11	Cruise 2	4.8
Practice Area	4.43	Takeoff	9.15
Refueling	5.86		

6.9 Selected Engine Analysis

Selected engine performance is analyzed in different altitudes by AAA software and represented in Figure 27. This chart is used to analyze aircraft performance in section (performance analysis). This chart has been plotted until Mach 1 for dry thrust and Mach 1.6 for wet thrust.

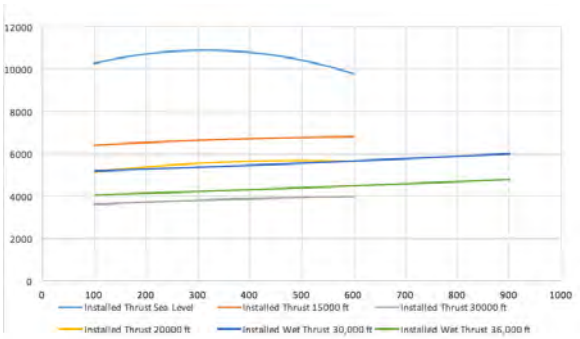

Figure 27-M88 Engine Performance

6.10 Engine Maintenance

For removing easily of the engine from aft fuselage, two mechanisms were compared for easy removal of the aft fuselage engine. If the engine removes from under the

fuselage, frames should get cut down increasing the removal time and complexity of aircraft Resulting in longitudinal engine removal. With this method, the engine will be removed an hour with 4 crew. Engine removal mechanism has been shown in Figure 28.

Figure 28-Saena Engine Removal

7 AERODYNAMICS

Saena is determined to be an advanced jet trainer and its flight time is mostly in subsonic regime. Also it must be capable of demonstrating high maneuverability and supersonic flight. In order to offer the best answer to these requirements, the main considerations for aerodynamic design is determined to be the subsonic cruise region of Mach 0.8. The supersonic flight and high maneuverability is achieved by modifications to nose and utilizing leading edge root extensions (LERX) and high lift L.E slats. The drag determination of the aircraft is also presented to corroborate the performance. The fuselage has been delicately tailored by the area ruling method so the wave drag in transonic region is min. The final planform of the wing is a trapezoidal wing with plain trailing edge and slatted leading edge flaps.(Figure 29)

7.1 WING PLANFORM

Wing planform design is started by selecting the overall configuration. Then sizing for the configuration is presented followed by the airfoil selection. At last a lift distribution for the wing is presented.

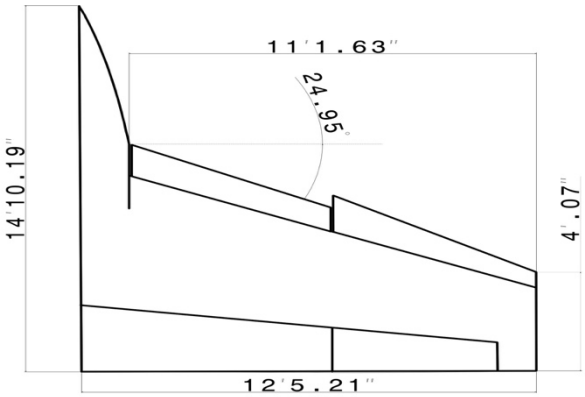

Figure 29-Overall Wing Planform

7.1.1 Overall Configuration

To choose the wing configuration with the lowest manufacturing cost, an analysis is carried out. This analysis revealed that unusual configurations are not suitable for jet trainers and there are 3 most used configurations; trapezoidal shape, Swept back wings, and delta wings.

The trapezoidal configuration is the best choice mostly because of its low weight, ease of manufacturing and high control surface effectiveness. In the other two configuration control surfaces would either cause lift loss or response weaker due to the high sweep angle. On the other hand, the aircraft is expected to fly mostly in high subsonic and low supersonic regions, so the transonic drag behavior is considered as an important factor. Another important factor is the AC shift in subsonic and supersonic flights. The acceptable static margin range, mandated RFP, must be -5 to15. In order to keep the static margin in control, the AC shift is tried to be kept min. Despite the high scores, the trapezoidal wings have low stall angles due to medium taper ratios, this problem is solved, adding leading edge root extensions and high lift LE devices. (Table 33)

Table 33- Pros and Cons for Wing Planforms

	Stall Behavior	Maneuverability	AC shift	C.S. Effectiveness	Manufacturing Cost	Weight	Score higher-better
Impact Factor	1	2	2	3	2	3	
Trapezoidal	Bad(1)	Bad(1)	Good(3)	Good(3)	Good(3)	Good(3)	33
Swept	Mid(2)	Mid(2)	Mid(2)	Mid(2)	Mid(2)	Mid(2)	26
Delta	Good(3)	Mid(2)	Bad(1)	Bad(1)	Bad(1)	Bad(1)	17

7.1.2 Wing Sizing

With the determined values of wing area and AR, the wing span is calculated to be 29.8 ft. The sweep angle is taken 25 deg. in LE with considerations of subsonic cruise Mach and the thickness ratio of the wing. The angle is set to be the min required amount, to keep the drag rise in supersonic flight to min. Although this decision increases the drag coefficient rise in sonic region larger, it is not important since the aircraft total drag is larger in M=1.3.

The taper ratio has been selected according to database and optimization for AC shift to be 0.4. The dihedral angle is decided to be zero since the aircraft stability must be around neutral due to the wide range of stability behaviors that it should cover. The incidence angle is also 0 deg. The AOA of the wing in cruise lift coefficient is zero. Yet, due to the drooped L.E. slats the effective angle of attack is reduced and needs to be adjusted to the incidence angle.

7.1.3 Wing Airfoil

To select the airfoil for the wing, the main design parameter is decided to be thickness ratio to minimize the required sweep in cruise also minimize the drag rise. NASA 64 series was selected for analysis due to their C_L/C_D and zero AOA in

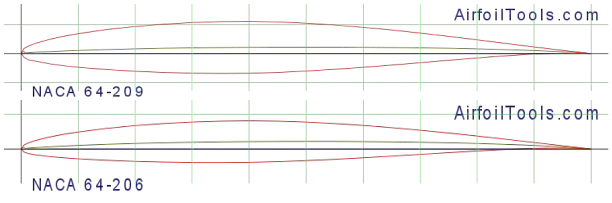

Figure 30-Wing Airfoils [airfoiltools.com]

Cruise Lift Coefficient. the analysis was carried out on 6-10% thickness ratio airfoils of this family and then based on max C_L of them. The candidate airfoils were “NASA 64-206, NASA 64-006, NASA 65-206 and NASA 65-006. eventually two airfoils, which satisfied the constraint of 33 ft^3 fuel volume were selected. The airfoils are “NASA 64-209” for root and NASA 64-206” for tip with no geometric twist on local AOA. Two profiles of the airfoils and their characteristics are presented in Figure 30.

7.1.4 Lift Distribution and lift curve slope

The span wise lift distribution and wing lift curve slope is in Figure 31. Since the wing has two different L.E. slats with a discontinuity in the wing loading is expected. The discontinuity lowers the lift on the inboard section, but increases the outboard section lift which is very useful. The lift distribution and the lift curve slope has been evaluated using Open VSP. Wing lift curve slope, was determined to be 5/rad.

7.2 HIGH LIFT SYSTEMS

The main requirements in sizing the high lift systems have been the stall angle and meeting C_{Lmax} in takeoff and landing configurations.

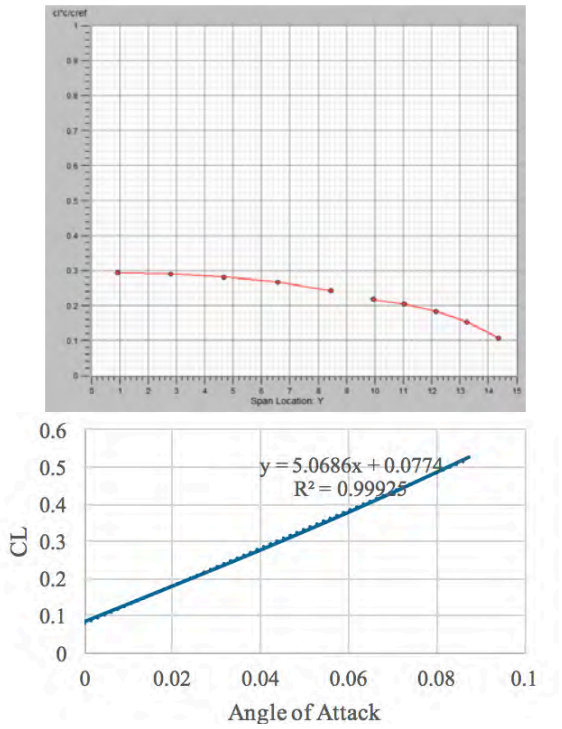

Figure 31-Lift Distribution, AOA=2, and Wing Lift Curve Slope

7.2.1 High AOA

Since high AOA is one of the characteristics of high maneuverability, Saena uses a LERX and a leading edge slat to increase the inherent stall angle of the wing. The area ratio of the LERX is decided to be 0.08 so the max angle of attack increases to 13 deg.[Whitford], the sweep of the LERX are chosen to be 60 deg. to reduce the drag rise in transonic region. 15% of the wing local chord is turned to an automated leading edge slats with dogtooth in the middle, to delay the stall angle. The location of the dogtooth was selected so the responses of each section would be similar. The outboard section of the LE slat has 10 deg. downward droop. The overall of the slat has

increased the stall angle 9 deg. which makes the wing stall angle 22 deg. [roskam VI]. Since, these methods are not accurate, verification is necessary.(Figure 32)

7.2.2 Trailing edge flaps

Saena uses flaperons to both produce the required lift on takeoff and landing and to have control in high speed flight. The flaperons were selected to be plain flaps since the manufacturing is easy. The actuators were upgraded so they can work as the ailerons, too. With considering the wing fuel volume, the flaps are placed at 25% of the chord, and have 25 deg. deflection in takeoff and 35 deg. deflection in landing. (Figure 32)

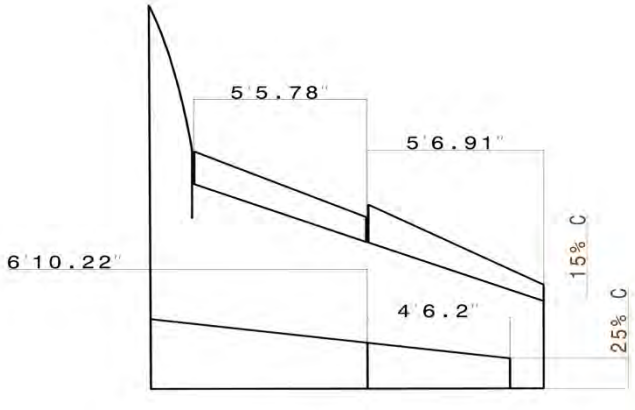

Figure 32-High Lift Systems

7.3 DRAG DETERMINATION

A more precise analysis of Saena drag behavior has been carried out using more accurate methods. The total drag force is calculated by splitting drag into 4 main components, parasite, wave, lift induced drag, and trim drag. To form the total drag determination of the aircraft, these four components have been treated both separately and integrated.

7.3.1 Parasite Drag

The determination of parasite drag has been done using VSP. The total wetted area has been determined to be 1175 ft^2, which has 5.2% difference with the initial estimation and considers within the acceptable range. The contribution of each component to the zero lift drag and the wetted area has been presented in Figure 33.

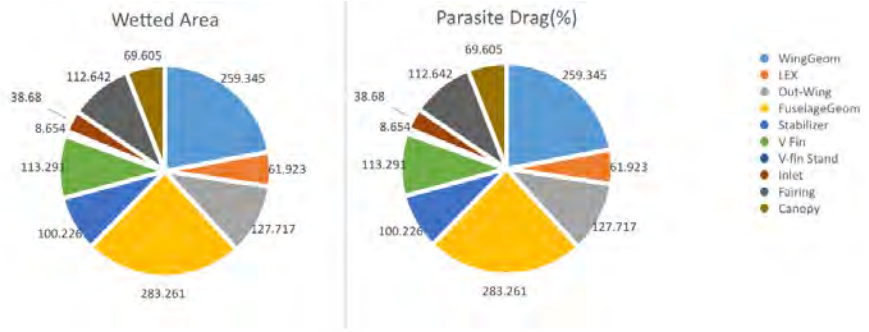

Figure 33-Drag Build-up

7.3.2 Wave Drag

The wave drag is mainly caused by formation of shock waves on the body near transonic regimes. Since most of the aircraft flight time is near transonic speeds, the analysis of wave drag is very critical. the first estimation for wave drag was determined using Open VSP.

The initial evaluation of aircraft area distribution, showed a 0.0487 drag rise in M=1, the critical condition due to thrust pinch effect. The comparison of this distribution with sears-Haack proposed area distribution has been presented in Figure 34. As can be seen the drag rise was due to the sharp risings in distribution.

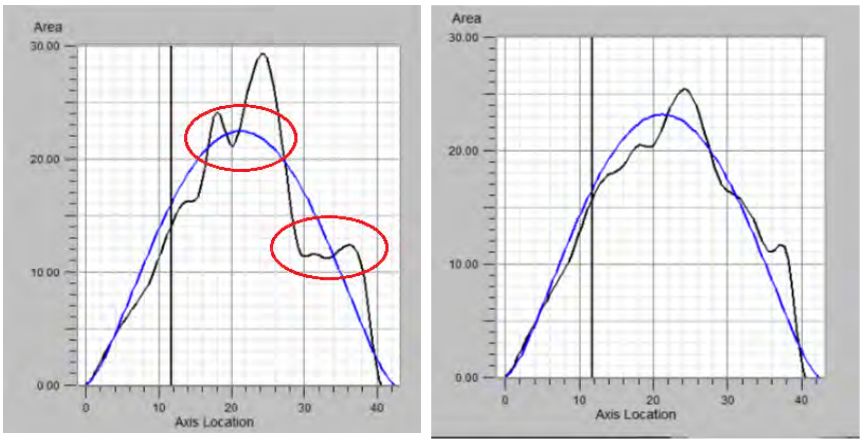

Figure 34- Cross Sectional Area Distribution of Saena

To reduce the drag rise, modifications to the nose and fuselage has been done. For the nose section profile, Von-Karman curve is selected due to good drag characteristics in transonic and low supersonic region (Figure 35). The fuselage width is made skinnier, as much as possible, near the wing to reduce the aggressive cross sectional rise. The curvature of the canopy has also been modified base on the distribution. Although the LERX were originally used for stall delay, it also served as a source of shock, ahead of

the wing, and made the flow subsonic over the wing. The LERX thickness is also modified from area distribution. Using these mitigations, the drag rise reduced to 0.0325.(Figure 34)

7.3.3 Induced Drag

The induced drag is a drag contributing factor of lift. Since the lift induced drag factor, K, changes with velocity a more precise method of determination is used. In this method [Raymer] the calculation is done for two regimes; subsonic and supersonic. The subsonic region has a rather constant value of 0.0915 up to M = 1, but for supersonic region the changes is more notable, so eq. 12.52 from [13] was used. value of K for different flight conditions is presented in

.

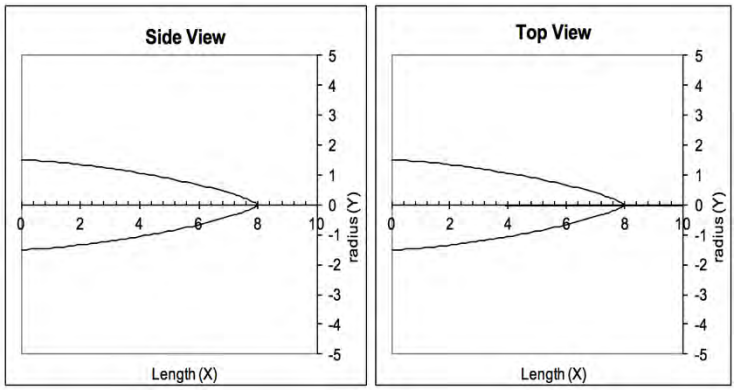

Figure 35-Nose Section Profiles

Table 34-Lift Induced Drag Factor

Flight Condition	Value of K
M = 0.82, Cruise II	0.0915
M = 0.77, Practice Area	0.0915
M = 1.3, Dash Speed	0.223

7.3.4 Trim Drags

Flight Condition	Value of K
M = 0.82, Cruise II	0.0915
M = 0.77, Practice Area	0.0915
M = 1.3, Dash Speed	0.223

This drag has no significant effect on normal conditions, but during the maneuvers, as the deflections are high, its effect must be noted. Saena [7] [23] benefits from an all moving horizontal tail, which resulted to low trim drag. The value of trim drag coefficient for sustained part of the 9g turn is about 0.0004.

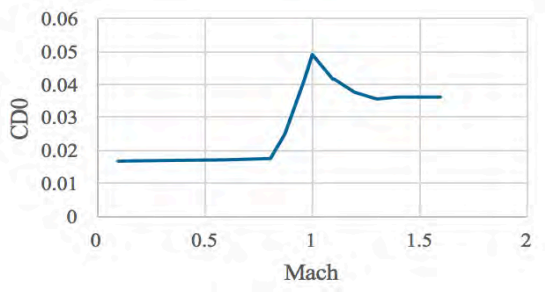

Figure 36-Saena zero lift drag coefficient VS Mach

7.3.5 Zero lift drag Coefficient

According to [35]

the total drag coefficient does not change significantly with altitude below 75000 ft., so the drag polar diagrams has been analyzed with this assumption. The drag diagrams of Saena in clean and dirty configurations, is presented in Figure 36. The drag rise near the sonic speed is around 30 drag count. The drag vs Mach relation is extracted from AAA.

Since the aircraft has rather small wing sweep angle, the reduction of C_{D0} in supersonic region is quite large. In order to validate the design, Saena is compared with other aircraft. The comparison has been carried out with supersonic fighter, since the performance requirements are similar to fighters. The comparison is presented in Figure 37. The data used to generate the plots is extracted from Figure G.4 of [11]. Due to data scarcity, the comparison with existing jet trainers, could not be done. The overall trend lies well compared to others and have no unusual picks. The subsonic drag coefficient is lower than others but the drag divergence Mach starts earlier, which means the drag in divergence region is higher than others. This was the result of smaller dimensions and smaller wetted area and smaller sweep angle. The small value of zero lift drag coefficient of F-22 is interesting compared to others. This unusual drag behavior, is not surprising considering the design. The use of very thin airfoils (6-10% thickness) and inside-body weapon storing, has claimed to reduce the drag considerably. The drag rise is almost similar to the one on F-18 which is the closest fighter to the Saena, considering their 5 deg. sweep angle difference.

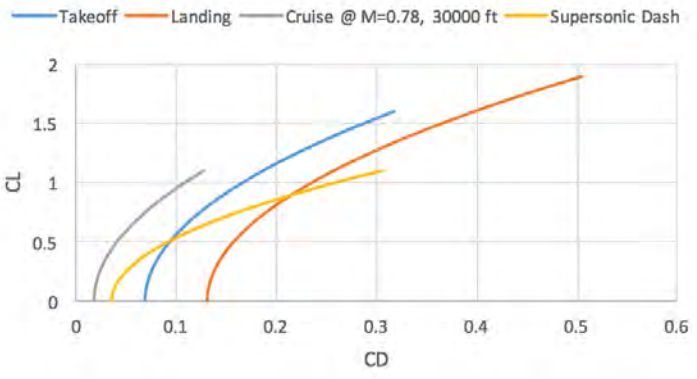

Figure 38-Saena Drag Polar

7.3.5.1 Drag Polar

Figure 38 presents drag polar for 4 main configurations. The overall behaviors are good considering the flap and landing gear conditions. The 30 deg. open flaps and deployed landing gears in takeoff, produce 600 drag counts, and

in landing configuration; the 44 deg. flap and deployed speed breaks causes 534 more drag count. The effect of corrected value of K, in supersonic flight and takeoff and landing configurations is in Figure 38 The details of drag polar conditions is in Table 35. There exists an average of 14% difference between initial and final calculated drags, with the max of 20.6% in landing flaps and gear down condition. It is well noted that this difference might cause a variation in sized and verified performance of the aircraft. Despite this error, it is shown in section 11.1, that all of the requirements are met and in some cases exceeded, due to the higher T/W achieved by selecting an off-the-shelf engine. As it has been discussed in section 3.2, the affected requirements, which are takeoff and landing distances, had not been the controlling legs of the design space, hence no alteration in the selected design point is required.

Table 35- Drag Polar detail calculation

	Takeoff	**Landing (speed brakes deployed)**	**Landing (speed brakes retracted)**	**Cruise II**	**Dash (Supersonic)**
Clean C_{D0}	0.0167	0.0167	0.0167	0.0174	0.0357
additional C_{D0}	0.0512	0.1146	0.953	0	0
Total C_{D0}	0.0679	0.1313	0.1120	0.0174	0.0357
K	0.097	0.1033	0.1033	0.0915	0.223
C_{Lmax}	1.6	1.9	1.9	1.1	1.1

A comparison of drag polar for different aircraft has presented in Figure 39. The figure shows that Saena has more zero lift drag coefficient in M=0.9 than others which is compatible with the Figure 37. The figure shows rather 50% difference in calculated K and the average. This difference in value was due to the assumption of constant K, in subsonic region. This assumption has no significant changes, since the subsonic region is not the critical design condition.

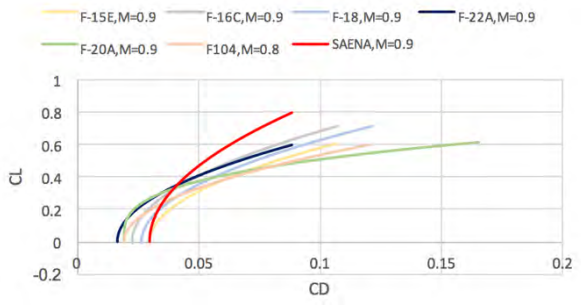

Figure 39-Drag Polar Comparison

.

8 WEIGHT & BALANCE

8.1 WEIGHT BREAKDOWN & DISTRIBUTION

Empty weight breakdown is carried out with different methods for three groups of compartments of the aircraft Table 36. Weight estimation of general structure parts *Structure Group 1* by the [9] Part V chapter 5 USAF method for military jet trainers, Specific minor parts *Structure Group 2* by utilizing their shape, dimension, and material, and systems weight were specified exactly in subsystems selection with respect to the [7] Table 37 illustrates the integrated aircraft weight division including payload and fuel weight contribution.

Table 36 Aircraft Weight Breakdown & C.G. Location

Component	Weight Fraction	Weight (lb.)	Xc.g. (ft.)	Zc.g. (ft.)
Structure Group 1				
Fuselage	10.4%	1816	18.0	2.6
Wing	7.5%	1045	24.5	2.6
Horizontal Tail	1.3%	150	37.5	1.9
Vertical Tail	2.7%	269	34.6	6.7
NLG	0.8%	110	6.7	0.5
MLG	4.6%	645	22.8	1.0
Structure Group 2				
Strake	0.5%	70	15.9	2.0
Speed Brakes	0.2%	20	39.3	2.0
Intake	0.4%	55	23.0	1.8
Ballast	0.0%	30	36.0	0.6
Propulsion Systems				
Engine	14.8%	1978	30.7	2.4
APU	0.7%	123	27.4	0.8
Electricity Generator	1.1%	145	26.5	4.5
Central Fuel Pump	0.4%	50	20.0	3.0
Oil System	0.4%	50	18.0	0.8
Flight Management Systems				
Avionics & Data Bus	0.8%	110	6.5	1.8
Radar	2.2%	300	2.8	1.3
Vehicle Management System	0.4%	50	14.3	0.5
Hydraulic System	0.5%	70	16.3	0.8
ECS	0.7%	100	18.5	3.0
Cockpit Subsystems				
Multi-Function Displays (x3) (Student)	0.1%	20	8.5	2.5
Multi-Function Displays (x3) (Instructor)	0.1%	20	14.0	3.5
Heads Up Display (Student)	0.3%	35	9.5	3.3
Heads Up Display (Instructor)	0.3%	35	14.5	4.3
Cockpit Electronic Compartment	0.7%	100	4.0	1.5
OBOGS & OBIGGS	0.5%	70	19.0	5.0
Ejection Seat for Student	0.6%	80	12.2	1.0
Ejection Seat for Instructor	0.6%	80	17.1	2.0

Table 37 Integrated Weight Division

Empty Weight	55.3%	7678		
Student	2.1%	275	11.8	2.0
Instructor	2.1%	275	16.8	3.0
Payload	7.5%	1000	23.5	0.4
OEM	66.9%	9228		
Central Fuel Tank	16.2%	2165	22.5	4.0
Wing Fuel Tank Capacity	14.4%	1919	22.9	2.3
Fuel Weight	30.6%	4080		
Calculated W_TO	97.5%	13017		
Takeoff Weight		13312		
Weight Error	-0.3%			

Table 38 Mission Segment Static Margin

#	Phase	S.M.	#	Phase	S.M.
1	W_E	N/A	9	Start of Cruise 2	4.07%

2	W_OE	N/A	10	End of Cruise 2	4.07%
3	W_TO	12.57%	11	Start of Practice Area	5.38%
4	End of Taxi	5.39%	12	End of Practice Area	7.03%
5	Start of Cruise 1	5.39%	13	Start of Cruise 3	5.76%
6	End of Cruise 1	5.48%	14	End of Cruise 3	5.92%
7	Start of Refueling	8.71%	15	Start of Landing	14.97%
8	End of Refueling	8.90%			

Fuel consumption in the BFM mission is illustrated in Table 36 and employed to calculated C.G. excursion. Figure 40 represents the results of mission. The mission segment values and static margin of the mission is demonstrated in Table 38. The CG excursion for all loading condition is 6.77%.

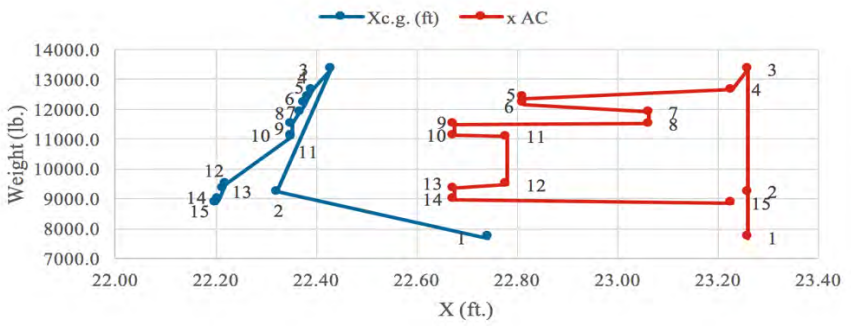

Figure 40- $X_{C.G.}$ & $X_{A.C.}$ Excursion along mission

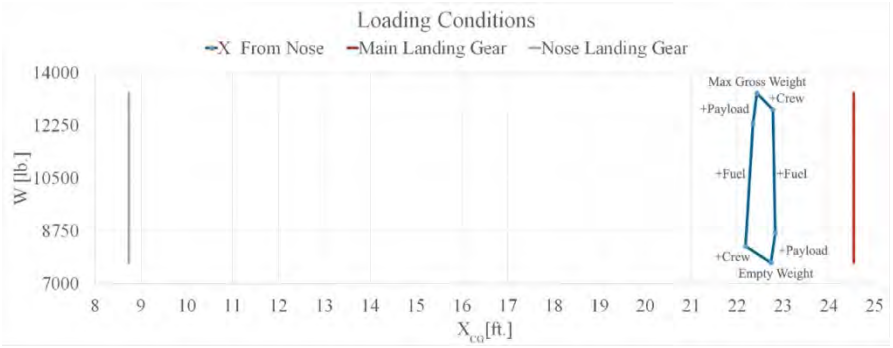

Table 39-C.G Potato for All Loading Condition

8.2 LANDING GEAR

Landing gear sizing is one of critical parts of design process. The goal is to present gear location criteria, retraction type, placing in the body, strut sizing, and tire sizing.

8.2.1 Gear Placement

The method for obtaining gear locations was primarily based on tip-over and ground clearance criteria of [9] Part II; and iteration with W&B moreover, in order to reduce landing gear weight, aircraft distance from ground has been selected as low as possible. This causes to better access to wing for maintenance. These criteria and distances are shown in Figure 41 and Table 40.

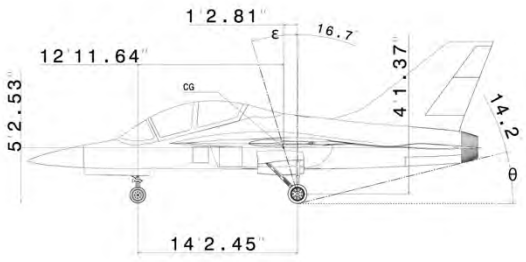

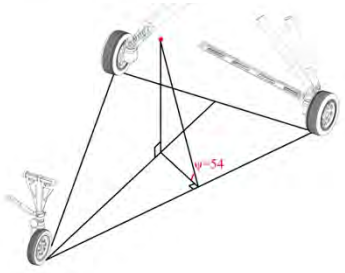

Figure 41- Geometric angle criteria for positioning of gears

Table 40: Geometric Angle Criteria for Positioning of Gears

	Criteria	Selected
ψ	≤ 55	54
θ	≥ 15	14.2
Φ	> 5	15
ε	≈ 15	16.7

8.2.2 strut and tire sizing

Calculations to determine max static load per strut, strut diameter and tire sizes were based on [9] Part II and IV. Due to unconventional main landing gear type which was selected, further loading analysis may be needed. For both main and nose gears single tire per strut and type VII due to its high pressure was selected. Oleo- pneumatic struts were chosen for nose and main landing gear for high absorption efficiency. Table 41 shows the results of strut and tire sizes.

Table 41: Strut and Tire Parameters

Landing Gear	Max Load Per Strut [lbs.]	Weight [lbs.]	Main Strut Diameter [inch]	Tire Outside Diameter [inch]	Tire Thickness [inch]	Tire Pressure [psi]
Main	5900	640	3.2	20.3	6.5	135
Nose	1500	110	2	17	3.25	82

8.2.3 Landing Gear Layout

For main landing gear in the case of attaching to wing there will be some major problems. The strut length would be too long and the wing must be strengthened to bear landing loads. On the other hand required space for retraction needs extra space under the wing and this causes to decrease wing lift. So the decision is to attach main landing gear to the fuselage and to retract into the fuselage. Compering to database, for having less weight and less changes in the aerodynamic body Saena's landing gear has been designed similar to F-16. The main strut has been decided to get attached to main bulkhead and longeron to transfer loadings to the fuselage. The secondary strut was attached to the same bulkhead behind the inlet. For nose landing gear of Saena straight-leg is selected. In comparison to trailing-link

landing gears, straight- legs are lighter, having less moving parts and easier to retract. Forward retraction was chosen for nose landing gear due to safety which in case of failure in opening, airflow would assist.

Figure 43- Nose & Main Landing Gear in Open State

Figure 42-Nose & Main Landing Gear in Close State

9 STABILITY & CONTROL ANALYSIS

This section, describes stability & control features of Saena. As mentioned earlier, Saena enjoys a VSAS which is designed to change its dynamic behavior as needed. This specific feature allows Saena to imitate and behave similar to the target fighter-aircraft for which it has been employed to train pilots. Having that in mind, Saena, has been designed to have different control surfaces at different members; in addition to the classical empennage control surfaces. Stability & control derivatives have been calculated for different important flight-phases; such as Cruising

flight; Take-off as well as Landing conditions. Saena reveals Level-I flying qualities in most flight phases. Moreover, without SAS, Saena is designed to be inherently stable to provide safety for a typical trainee while a malfunction occurs in the SAS. Such feature comes with acceptable maneuvering power to deliver a safe trainer aircraft even during emergencies. Following sub-section describes further details.

9.1 SAENA EMPENNAGE DESIGN

The horizontal and vertical tail areas are assessed using the methods described in [9]. First, an initial estimate is made based on available military jet trainers' geometric data, using volume coefficient and horizontal/vertical tail moment arm. The selected values are shown in Table 42 and the areas are calculated by the definition of tail volume coefficient.

Table 42 estimated horizontal/vertical tail area based on database

$\bar{V}_H$	$\bar{V}_V$	$X_H\ [ft]$	$X_V\ [ft]$	$S_H[ft^2]$	$S_V\ [ft^2]$
0.536	0.07	14.78	11	66	43

Next, directional and lateral X-plots have been drawn to refine the horizontal and vertical tail areas. For longitudinal X-plot (Figure 44), static margin of 5% is recommended for military trainers in [9] This value is chosen in the design to ensure longitudinal static stability, while maintaining an acceptable level of maneuverability at "practice area" flight condition. So the chosen horizontal area is $66ft^2$.

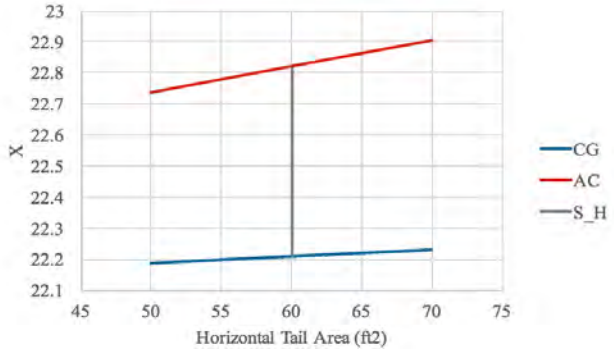

Figure 44-Longitudinal X-plot

In addition, this amount of horizontal tail is sufficient for take-off rotation. The required horizontal tail area for take-off rotation was calculated by equation 4.244 in [36].

The input values for this equation is shown in Table 43 and the value of $S_{H_{req}}$ is estimated to be $58.54ft^2$ assuming -14° horizontal tail deflection and 12 $^{deg}/_{S^2}$ angular acceleration.

Table 43 Required data to calculate required horizontal tail area for take-off rotation

W	12567	S	222.5	$C_{L_{wf}}$	1.7145	$C_{L_{max,H}}$	0.827	η_H	1
X_{cg}	22.39	Z_{cg}	5.52	$X_{ac_{wf}}$	22.31	$C_{m_{ac_{wf}}}$	-0.2961	I_{yy}	18822
X_{mg}	24.54	Z_{mg}	0	Z_{D_g}	5.3	Z_T	5.39	T	10191
μ_g	0.025	C_D	0.1379	ρ	0.002377	$\bar{c}$	7.99	X_{ac_h}	35.61

To size the vertical tail, yawing moment coefficient due to sideslip (C_{n_β}) of 0.0573 rad^{-1} is recommended in [9] for military trainers and the vertical tail area must be 41.51ft^2 at least. However, it was perceived that this amount of area is insufficient for damping the Dutch-roll mode due to short-coupled. So the vertical tail area is raised to 55 ft^2 to ensure at least level 2 handling quality in all flight conditions. The final iteration of directional X-plot is presented in Figure 45.

In every aircraft, there are some design issues that, dictate the positioning, location, and configuration of the aircraft. The flight regimes that Saena flies in impose an all-moving horizontal tail instead of a fixed stabilizer plus a flap-type control surface. The differential tail retains its effectiveness and has a major contribution in roll control, even at high AOA and Mach numbers. Lift center of the aircraft has a rearward shift due to compressibility effects. This phenomenon produces excessive longitudinal stability which makes maneuvering difficult by increasing the required aerodynamic moment of the tail. Besides, the all moving tail reduces trim drag and avoids the shocks that would occur at high Mach numbers [32]. The horizontal tail panels could operate either symmetrically for pitch control or differentially for roll control.

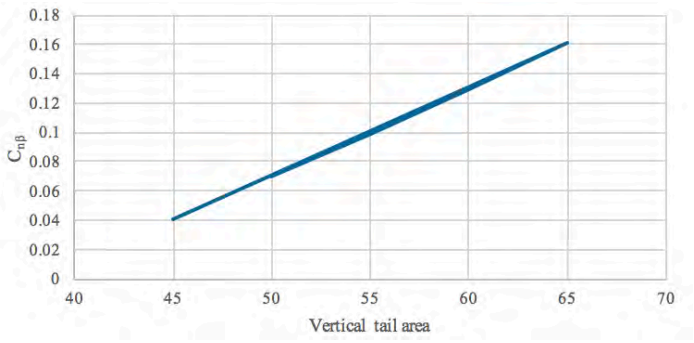

Figure 45-Directional X-plot

The vertical tail platform could be either single or twin fin. The twin fin option is mostly used, for redundancy in case of losing one fin (like in a fight) and to handle OEI situation in a twin-engine aircraft [32]. Saena is going through none of these scenarios, thus a single vertical fin is used in the design. The horizontal and vertical tail locations are checked according to section 21.7 and 11.7 of [11] to justify that there would not be problems during pitch-up and spin recovery since most of the vertical tail and rudder area would remain effective (Figure 46).

9.2 CONTROL SURFACE DESIGN

Control surfaces are sized to trim the aircraft in all flight conditions and perform maneuvers properly. Extensive case-studies is of course necessary to properly allocate sufficient number of control surfaces based on the mission requirements. Nonetheless, initial investigations reveal that having sufficient total number of control-surfaces located on different members would be very helpful. In fact, such approach clearly provides enough redundancies to keep the aircraft controllable even during emergencies.

Figure 46-Side view of horizontal and vertical tail

The variable stability concept is implemented to design by adding control surfaces to the ordinary ones. So two flaperons are used in both left and right wings. Although combining aileron and flap increases complexity and production cost, the performance benefits would prevail this increment where there's an acceptable trade-off. In addition, the rudder has been divided, into two parts and the horizontal tail panels could deflect asymmetrically to provide roll control. Other control surfaces could be sized properly in wind tunnel or flight tests and applied to the Saena Figure 47 is a dimensioned view of the Saena's empennage and control surfaces.

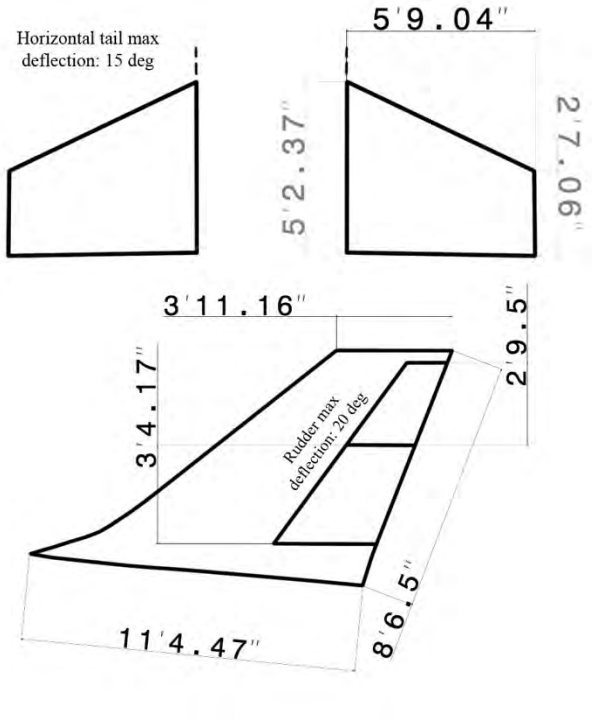

Figure 47-Empennage and Control Surface Dimensions

9.3 TRAINING-TARGET ESTIMATION

The targets are estimated using their geometric data and an approximation of CG location. Since F-35's geometric data was not available, only the F-22 is analyzed. The geometric data was extracted from the appendix of [37] and the aircraft was modeled in AAA software. Then, the approximation of CG location was used from [38]; the F-22's transfer function was calculated in 15000ft with 50% internal fuel at 353 KTAS. It is notable that this is only an approximation and the exact transfer function could be calculated using the exact data. The poles are shown in Figure 51 and Figure 50.

9.4 STABILITY AND CONTROL ANALYSIS

Stability & control derivatives have been calculated using AAA software. These derivatives plus the general data of flight conditions are presented in Table 44 and Table 45.

Table 44-Flight Conditions and Weight Data

Phase	1	2	3	4
Description	Take-off	Cruise I	Practice Area	Landing
Altitude [ft.]	50	30000	150000	50
Mach Number	0.2	0.78	0.77	0.18
Weight [lbs.]	12567	12263	11020	8742
I_{XX}	3096.0	3003.4	2738.5	2186.3
I_{YY}	18654.0	18095.5	16499.7	13173.0
I_{ZZ}	21215.9	20396.9	18576.8	14826.9
I_{XZ}	732.9	692.9	690.2	711.3

Table 45-Stability and control derivatives of Saena in Practice Area condition

longitudinal Derivatives (Stability Axes Dimensions)					lateral-directional Derivatives Stability Axes Dimensions)				
Phase	1	2	3	4	Phase	1	2	3	4
C_{D_0}	0.0167	0.0174	0.0174	0.0167	C_{l_β}	-0.1291	-0.1212	-0.1198	-0.1881
C_{D_u}	0	0	0	0	C_{l_p}	-0.3460	-0.3751	-0.3708	-0.3616
C_{D_α}	0.4277	0.174	0.0864	0.5675	C_{y_β}	-0.6463	-0.7375	-0.7333	-0.6457
$C_{T_{X_u}}$	-1.4544	-0.272	-0.1259	-0.2718	C_{l_r}	0.2156	0.1694	0.1445	0.1459
$C_{D_{\dot{\alpha}}}$	0	0	0	0	C_{y_p}	0.0705	0.0135	0.0013	0.0229
C_{L_0}	0.0676	0.0814	0.0818	0.7148	C_{y_r}	0.5407	0.6060	0.5980	0.5327
C_{L_u}	0.0218	0.2414	0.1120	0.0236	C_{n_β}	0.0821	0.1055	0.0918	0.0820
C_{L_α}	4.1682	4.9771	4.9398	4.1616	C_{n_p}	-0.0898	-0.0225	-0.0098	-0.0353
$C_{L_{\dot{\alpha}}}$	2.7142	3.9767	3.8013	2.7427	C_{n_r}	-0.2465	-0.2629	-.02572	-0.2340
C_{L_q}	6.2592	7.5450	7.3647	6.4841	$C_{l_{\delta r}}$	0.0365	0.0388	0.0439	0.0510
C_{m_0}	0.0072	0.0143	0.0125	-0.1661	$C_{l_{\delta a}}$	0.0658	0.0797	0.0789	0.0657
C_{m_u}	0.0055	0.0488	0.0233	0.0060	$C_{y_{\delta a}}$	0	0	0	0
C_{m_α}	-0.5226	-0.2022	-0.2230	-0.6232	$C_{y_{\delta r}}$	0.2982	0.2179	0.2220	0.2990
$C_{m_{\dot{\alpha}}}$	-4.4897	-6.5883	-6.3026	-4.6019	$C_{n_{\delta r}}$	-0.1712	-0.1214	-0.1230	-0.1695
C_{m_q}	-7.1252	-8.4666	-8.1946	-7.3487	$C_{l_{\delta f}}$	0.1535	0.1638	0.1636	0.1533
$C_{m_{T_u}}$	-0.0097	0.0090	0	-0.0026	$C_{y_{\delta f}}$	0	0	0	0
$C_{m_{T_\alpha}}$	0	0	0	0	$C_{n_{\delta f}}$	-0.0221	-0.0086	-0.0047	-0.0093
$C_{m_{DS}}$	-1.9195	-2.2278	-2.1483	-1.9435	$C_{l_{\delta DS}}$	0.0426	0.0520	0.0516	0.0426
$C_{L_{DS}}$	1.1604	1.3447	1.2957	1.1583	$C_{n_{\delta DS}}$	0.0447	0.0520	0.0516	0.0447
$C_{D_{DS}}$	0.0137	0.0191	0.0185	0.1446					

Table 46-Trim condition of Saena

H [ft.]	α [rad]	δ_{DS} [rad]	T [lbf.]	$\bar{q}$ $[lbs/ft^2]$
15000 (practice area)	0.0023	0.0056	1953	495.09 (high subsonic)
30000 (cruise I)	0.0234	0.0043	1297	269.61 (high subsonic)
30000 (CAS Dash Out)	-0.0029	0.0067	5922	725.06 (low supersonic)

Saena longitudinal and lateral-directional poles for derivatives in Table 45 are checked in Table 48 and Table 49.

9.4.1 Roll performance

The roll performance of Saena, as a class IV aircraft, is measured using equation (21.17b) in [11] and is calculated by assuming full deflection of roll control surfaces. Max 1g roll rate of Saena and couple of other advanced jet trainers is compared in Table 47. Based on MIL-HDBK-1797, the aircraft should have at least 90 deg/s roll rate which is already met.

Eq. 4

$$P = -\frac{2V}{b}\frac{C_{l_{\delta cs}}}{C_{l_p}}\delta_{cs} = -\frac{2V}{bC_{l_p}}\left(\boldsymbol{C_{l_{\delta DS}}}\delta_{DS} + C_{l_{\delta if}}\delta_{if} + C_{l_{\delta of}}\delta_{of}\right) = 865\ \frac{deg}{s}$$

Table 47-roll rate comparison

Jet Trainers	Saena	M346	KAI T-50	T38C
Max. Roll Rate [deg/s]	865	230	200	720

9.4.2 Nonlinear simulation

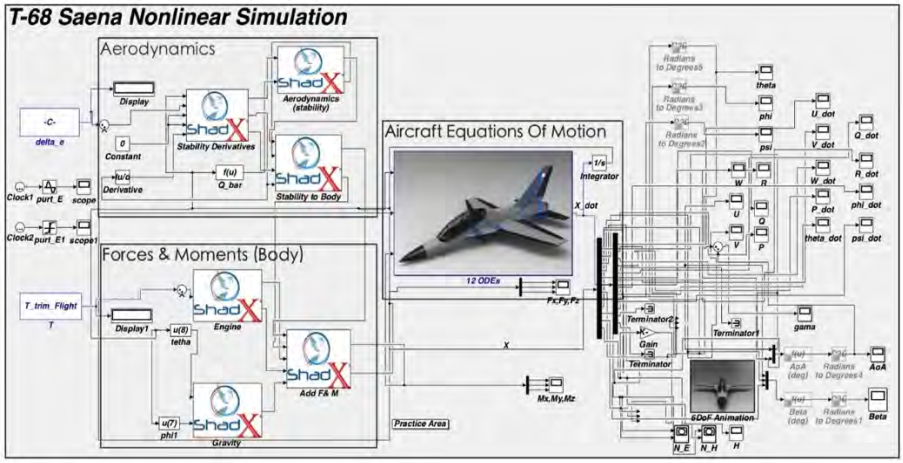

Figure 48-Saena nonlinear simulation-practice area

As the best tool for verification, nonlinear simulation for practice area has been used and presented in Figure 48 As seen in Figure 49 Saena has been trimmed perfectly.

9.4.3 Saena with Variable Stability

This section describes how variable stability has been implemented in Saena. In fact, we show why Saena needed this many control surfaces and its control system operates through combining different control surfaces to achieve its dynamic goals.We start off with a simple scenario during which Saena is expected to

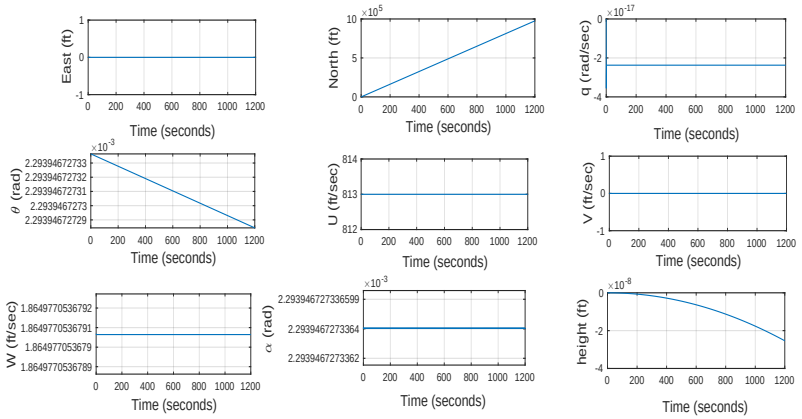

Figure 49-Trim Time History, Practice Area Nonlinear Simulation

demonstrate the F-22 inherent stability. In general, with the help a carefully designed tracker (an Autopilot mode) we turn Saena into a condition where it could perform the desired maneuver with desired handling qualities (HQ). In essence, an algorithm is executed to find suitable gains to be fed into the control system (Figure 51 and Figure 50). Here, five cases have been presented; including their poles and related SAS-Gain sets) which correspond to high subsonic practice maneuvers (Table 48,Table 49,Figure 51 and Figure 50). Other cases have been excluded to observe page limitations. It is, however, important to observe: All poles are chosen in such a way to satisfy level I requirements of MIL-F-8785-C.

- Knowing the fact that higher values of the so called servo break frequency associates itself with higher cost, Saena utilizes the standard off-the-shelf servos for its control system. Obviously, with the help of a well-designed SAS, K_δ is then adjusted in such a way to pass desired design limitations.
- We have made a great effort for all cases, to have discrete gain sets for α_SAS, pitch damper, airspeed holding, pitch attitude holding, β_SAS, bank angle holding, yaw as well as roll damper, within appropriate range of available hardware. We expect future versions of Saena to enjoy some sort of artificial intelligence and is programmed to be adaptive to dynamic maneuvers and is able to recalculate gains during maneuvers.
- The system is selected to be dually redundant to ensure accepted level of safety in all foreseen scenarios.

Table 48-Longitudinal pole places of Saena and targets, Servos a/(s + a); a=5 rad/sec

Level 1 requirement	Set 5	Set 4	Set 3	Set 2	Set 1	F22(inherent)	Saena	Longitudinal poles
$\xi > 0.35$	-0.056 ∓0.6977i	-0.042 ∓0.5985i	-0.03 ∓0.4991i	-0.02 ∓0.3994i	-0.012 ∓0.2997i	Unstable P_1 =2.6468 P_2 =-4.0783 $P_{3\&4}$ =-0.0041 ∓ 0.074i	$\xi = 0.7$	Short period
$\xi > 0.04$	-6∓10.392i	-4∓9.1651i	-4.4∓6.681i	-2.7∓5.358i	-1.4∓3.74i		$\xi = 0.066$	Phugoid

Table 49-Lateral-directional pole places of Saena and targets; servos; a/(s + a); a=20 rad/sec

Lateral-directional poles	Saena	F22 (inherent)	1	2	3	4	5	Level 1 requirement
Roll	$T_R = 1$	-1.2831	-7.28	-5.28	-3.28	-2.28	-4.28	$T_R = 0.114$
Spiral	$T_{2s} = 35$	-0.0222	-0.022	-0.0322	-0.0287	-0.05	-0.0422	$T_{2s} = 12$
Dutch Roll	$\xi = 0.057$ $\omega_n = 4$	-0.0321 ∓0.908i	-0.45 ∓i	-0.6 ∓ 0.9i	-0.75∓0.75i	-0.9∓0.6i	-1 ∓ 0.4i	$\xi > 0.4$ $\omega_n > 0.1$

9.4.4 Saena SAS and Autopilot Basic Features

With Figure 51 and Figure 50, the desired poles locations are selected in such a way that the magnitudes of required gains are practical. It is further emphasized that having a variable stability feature requires careful combination of control surfaces as fight conditions change. We also need to be careful about control surfaces authorities. That is, any individual control surface deflections must be kept less than the required total deflection to prevent control surface saturation. As an example, during high-subsonic maneuvers within practice area, Saena's autopilot software substitutes the gain sets to achieve F-22 dynamic characteristics as close as possible. To achieve all contradicting goals, a control surface allocation has been devised; the detail of which is described in section 9.4.5 .

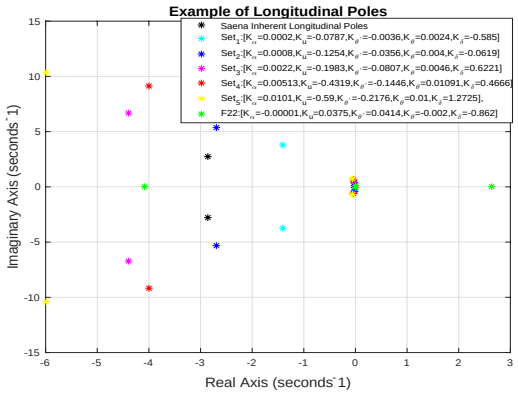

Figure 50-Longitudinal poles and related SAS-Gain sets in high subsonic practice area

9.4.5 Control Surface Allocation System

Saena's control surface allocation system follows certain mathematical steps to achieve combination of $\delta_{directional}$ & $\delta_{lateral}$ and $\delta_{longitudinal}$, wherever needed.

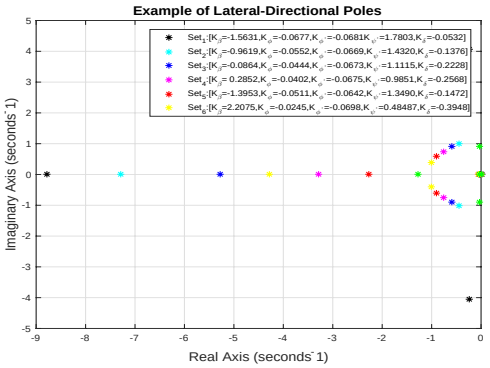

Figure 51-Lateral-directional poles and related SAS-Gain sets in high subsonic practice area

Equation 1

Some pole placement steps have been taken to find SAS-gain sets in 9.4.4. Following describes steps taken to inversely achieve the required control surface deflections (δ_{DS_l}, δ_{DS_r}, δ_{f_l} . , δ_{f_r}, δ_{r_1}, δ_{r_2}) Therefore, for high subsonic regime in Equation 1., which suggests that both δ_{f_l} and δ_{f_r} have the same values but are in the opposite directions. Their corresponding effect is then calculated from $\delta_{f_{l\&r}} = \frac{\delta_{f_l} + \delta_{f_r}}{2}$. We further stress that for low supersonic regime, aileron surfaces will be used instead of flap. For the case of Dutch-roll, relevant rudder control surfaces deflection $\delta_{directional} = \frac{\delta_{r_1} + \delta_{r_2}}{2}$ can be used. Moreover, differential stabilizer deflection $\delta_{longitudinal} = \frac{\delta_{DS_l} + \delta_{DS_r}}{2}$ will be used for longitudinal pole substitution. Obviously, variable stability feature implemented in Saena makes

$$\left.\begin{aligned} \delta_{lateral-directional} &= \frac{\frac{\delta_{DS_l} - \delta_{DS_r}}{2} + \delta_{f_{l\&r}}}{2} \\ \delta_{DS_{l\&r}} &= \frac{\delta_{DS_l} + \delta_{DS_r}}{2} \\ 2(\delta_{DS_l} - \delta_{DS_r}) &= \delta_{f_{l\&r}} \end{aligned}\right\} \xrightarrow{yields}$$

$$\begin{bmatrix} \delta_{DS_l} \\ \delta_{DS_r} \\ \delta_{f_{l\&r}} \end{bmatrix} = \begin{bmatrix} 0.4 & 1 & -0.2 \\ -0.4 & 1 & 0.2 \\ 1.6 & 0 & 0.2 \end{bmatrix} \begin{bmatrix} \delta_{lateral-directional} \\ \delta_{DS_{l\&r}} \\ 0 \end{bmatrix}$$

it a great platform to be used as an in-flight simulator to imitate the dynamic characteristics of a wide range of fighter aircrafts.

10 STRUCTURAL DESIGN

The purpose of this chapter is to show that the aircraft structure would withstand all demonstrated flight conditions. Considering critical loads would let us select proper materials and structural layout design.

10.1 V-N DIAGRAM

First step for structure analyzing is to sketch V-n diagram using Military Standard and RFP design limit load factors, in range of +9 to -3 g's (Figure 52). Figure 52 (a) was stablished in clean configuration at max gross weight at sea level, which is in high loaded condition for structural assumption. It is clear from diagram that max level flight speed for Saena is 1.15 Mach (760 knots) and the dive speed is 1.44 Mach (950 knots) at this condition. RFP required 2133 psf. dynamic pressure (M=1.2 at sea level) tolerance for structure. This requirement is illustrated with a vertical line in Figure 52. The orange area is in the caution region with safety factor of 1.5 as RFP mandated and beyond that is structural fracture zone. According to [9] part V the max upward gust load has been specified for 25ft/s for structural consideration. Figure 52 shows that this gust load does not affect the maneuver diagram; so the two ultimate loads (shown in Figure 52) has been considered in structural load calculations.

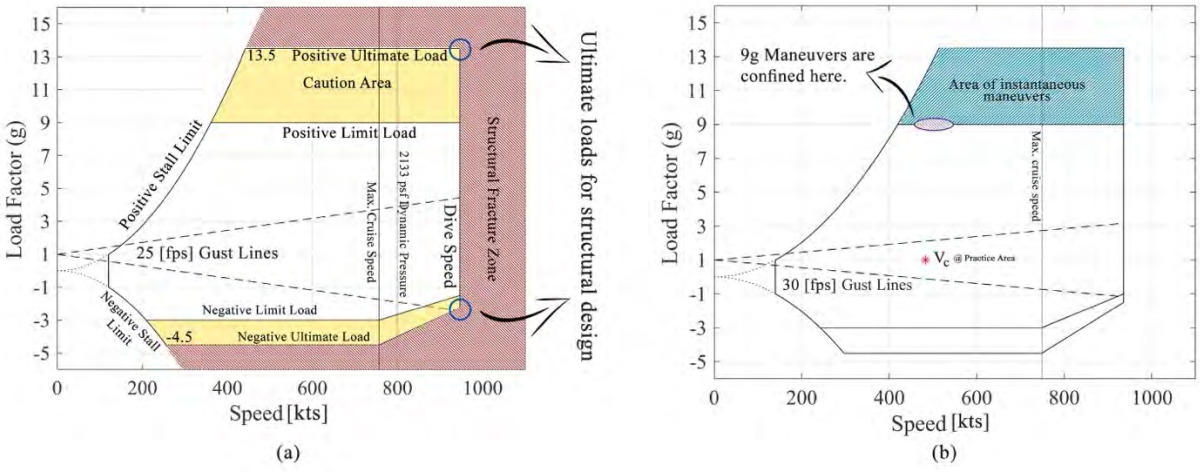

Figure 52: (a) V-n diagram at sea level and MTOW showing structural states. (b) V-n diagram at 15000 ft and combat weight

Figure 52 (b) illustrated the V-n diagram for Saena at sea level and combat weight. The 9 g's maneuvers and cruise speed in practice area is presented in diagram. Figure 52 (b) shows response to 30 ft./s vertical gust in dashed lines as

RFP imposed for in 50 percent fuel which is assumed to be at 15000 ft. altitude in practice area. It is clear that this gust load does not affect the maneuver diagram.

10.2 Material Selection Approach

The material of Saena is selected based on several criteria as strength efficiency (ultimate strength over density), fracture toughness, producibility, and cost. Selected materials and their properties are illustrated in Table 50.

Nonmetallic materials have high strength efficiency due to low density and high strength. However, in compare with metallic materials, nonmetallic materials would increase production and maintenance costs also manufacturing complexity in large scales. In result most parts of Saena would be made of metal while high-loaded parts would be made of nonmetallic materials such as some spars, frames and control surfaces. Among metallic materials, Al alloys have more appreciable strength in present of cracks and used as damage tolerant structure, beside its low density and good strength; so it was used as main material in Saena.

Table 50: Material Properties used in Saena

Material	Density [lb./in^3]	E [10^6 psi]	F_y [ksi]	F_u [ksi]	Fatigue Strength [ksi]	Elongation at Break	Structural Efficiency	Thermal Expansion [µin/in°F]
Al 2024-T81	0.101	10.5	65.3	70.3	18.1 for 5e8 cycle	6%	696.0	13.7
Al 7075-T6	0.102	10.4	73	83	23 for 5e8 cycle	11%	813.7	13.1
Steel 300M	0.283	29.0	230	280	N/A	7%	989.4	6.3
Ti 6A1-4V	0.160	16.5	128	138	74 for 1e7 cycle	14%	862.5	4.78
Al-Li	0.09	11.2	62.4	71.1	N/A	9%	790	11.9
Fiber-glass	0.065	3.6	N/A	80	N/A	3.50%	1230.8	N/A
Graphite Fiber Epoxy	0.056	up to 75.4	up to 384	up to 550	N/A	up to 11%	3035.7	1.2

10.3 Wing Structure

Lift distribution in most critical condition (9g maneuver at 1.44 Mach and sea level) has been calculated with AAA. Figure 54 (a) shows this data along with the effect of wing and fuel weight distributions. The shear force and bending momentum of wing span wise are obtained Figure 54(b,c). It is realized that max shear (4060 lbf) and max bending momentum (260690 lbf.ft) are exerted on wing root. As RFP mandated, a safty factor of 1.5 must be applied to these ultimate loads for further calculations.

A multi-spar wing has been selected because of the low aspect ratio and thin airfoil (figure). Each wing contains 3 main spars, which are oblique in order to transmit tip loads to root better. The other 2 spars are attached to leading edge device. The rear spar is almost parallel to flaperon edge and the distance between rear spar and flaperon is set about 10% of chord for actuator places. There are 13 ribs in each wing and their functions are described in Table 51. Rib space differs through span wise and increases with taking distance from wing root. All Ribs have holes for reduction in weight and transmission of fuel to center fuel tank. A plate cover is used for wing skin. Skin strengthening applies to ribs and spars positions also in wing root joint to tolerate bending moment in high g maneuvers.

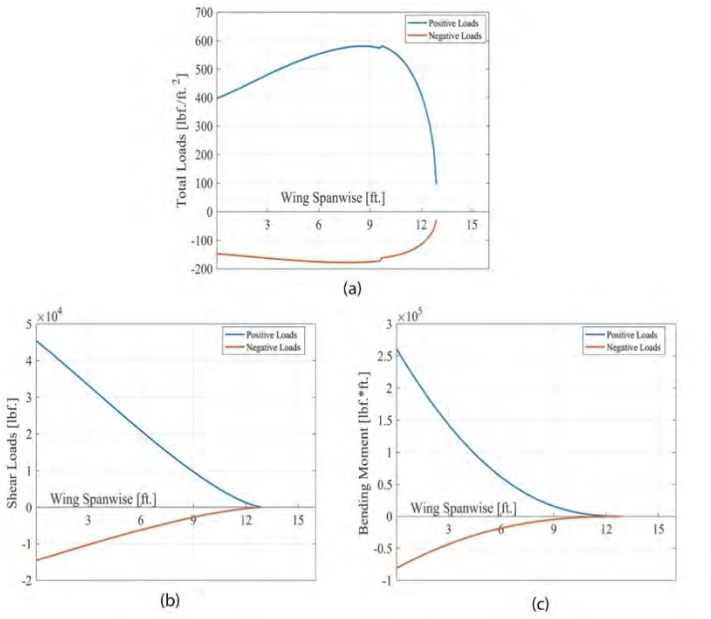

Figure 54-(a) Total loads per area on wing spanwise (b)) Positive and negative Shear loads on wing spanwise (c)) Positive and negative Bending momentum on wing spanwise at sea level and 9 g condition

Used max shear and bending loads of Figure 54, wing component sizes are obtained.(Figure 54) Table 52 represents all wing components materials, thickness and the reason behind their decision process.

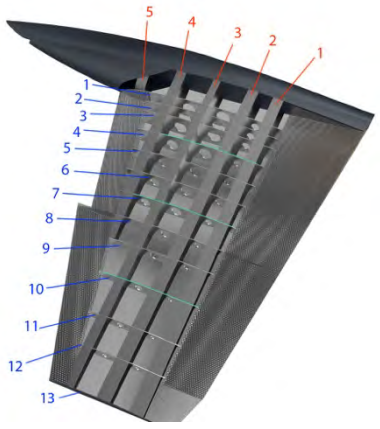

Figure 53-Wing Structure

Table 51: Rib functions

Rib Numbers	Functions
1	Root joint
2,3,4	First fuel tank and control surface support
5,6,7	Second fuel tank and control surface support
8,9,10	Small fuel tank support
11,12	Wing Support
13	Wing tip rib

Table 52: Material selection for wing components

Parts	Materials	Thickness [inch]	Description
Spars 1,2,3	Graphite composite	0.5	High Strength and damage tolerance
Spars 4,5	Al 7075-T6	0.4	
Ribs	Al 7075-T6	0.1	
Upper skin	Al 7075-T6	0.3	Better withstand compression stresses
Lower Skin	Al 2024-T81	0.3	Better withstand long application of tension stresses
Control Surfaces	Graphite composite	N/A	

10.4 EMPENNAGE STRUCTURE

Internal structure of vertical tail is similar to the wing. It has 2 main spars from tip to root and 4 oblique ribs. The spars connected to longeron inside fuselage to transfer loads to airframe.

The horizontal tail is an all-flying tail. It has one main spar which goes through AC point to tolerate and transfer loads to pivot region. Tail core made with full depth honeycomb of graphite epoxy due to high strength and low weight. Flying tail is bonded to the fixed part in airframe by trunnion. As described in section 11.1, speed brake area is 6.8 square feet. Four surfaces of 1 ft*1.7 ft has been considered for speed brakes at the end of fixed parts behind the hinge.

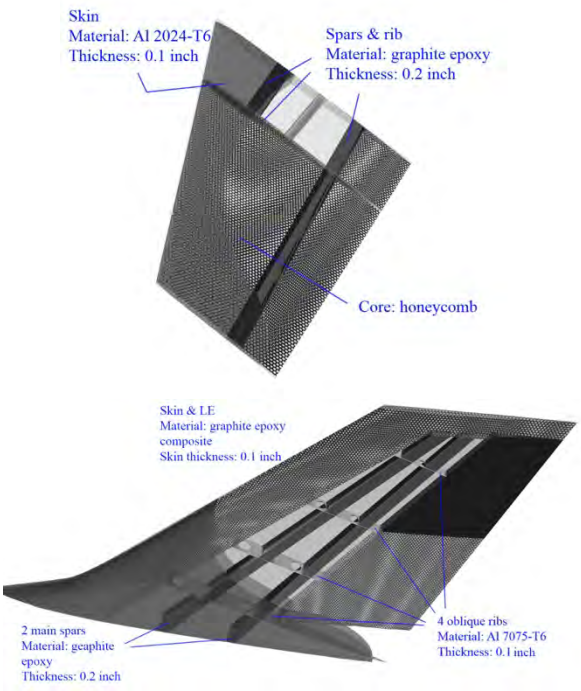

Figure 55-Vertical & Horizontal Tail Structure

10.5 FUSELAGE STRUCTURE

Longeron and frame locations have been determined based on some critical loads during flight and emergency situations, subsystem locations and components attached to airframe.

The airframe includes 6 longerons and 6 main frames. Four of the longerons run from engine mount to cockpit section which are located in wings, horizontal tail and main landing gear attachments. The other two longerons placed on top and bottom of fuselage connection. The top one runs from vertical tail connection toward cockpit, and the bottom one along the fuselage length around receptacle, and air refueling system is strengthened due to impact loads during air refueling. Main frames and their functions are listed in Table 53.

Supporting frames are used in cockpit position, wing connection, and engine mount. Components, their thickness and material selection are listed in Table 54. Main frames are made with graphite composite due to better strength and fuselage skin is made with Al-Li alloy which is lighter, stiffer, and has better fatigue strength.

Table 53: Main frame functions

Main Frame Numbers	Functions
A	Trainer ejection seat and equipment support
B	Instructor ejection seat and equipment support

C	Center fuel tank and Payload drop load and wing spar conjunction supports
D	Landing load and center fuel tank loads and wing spar conjunction supports
E	Engine mount and its equipment and vertical tail spar support
F	Horizontal tail and engine mount support

Table 54: Material Selection for Fuselage Components

Parts	Materials	Thickness [inch]
Main frames	Graphite composite	4
Supporting frames	Al 7075-T6	3
Longerons	Al 7075-T6	0.1
Skin	Al-Li alloy	0.08
Nozzle	Ti 6A1-4V	N/A
radome	Fiber glass	N/A

Figure 6

10.6 Structural Service Life

To meet service life of 30,000 hours, as imposed in RFP, fatigue analysis under critical conditions must be carried out. With assuming that structure joints are the first critical parts susceptible to fail, max stresses of these conditions calculated (Table 55) by number of repeating in one training mission. The worst case one has been assumed 13.5g turn rate in every mission. Based on this assumptions, 30,000 flight hour leads to 220,000 cycles. Primary life cycle which is estimated in advanced is 16,250 hours training operation that causes 120,000 cycles.

[39] is used for calculating cumulative critical loads in Table 55. To find out the number of cycles for every load conditions, estimated of S-N diagram have been created and used. According to MIL-A-8866 scatter factor for USAF trainer is 4.

Table 55: Critical Maneuvers, loads and their numbers

Maneuvers	G loads	Max Stress [ksi]	Numbers in one training mission (n)	Number of cycles to failure (N)
Max Instantaneous turn rate	13.5	~130	1	7×10^5
360 degree turn pulling	9	~80	3	5×10^6
pull-up/push-over maneuvers pulling	9	~88	3	2×10^6
payload delivery in a 180 degree turn	7	~70	1	10×10^6
landing and TO and touch & go	N/A	~60	4	20×10^6

Eq. 5

$$Number\ of\ cycles = \frac{\sum n}{scatter\ factor \times \sum {}^{n}/_{N}}$$

From Eq. 5, number of cycles which our aircraft can tolerate was calculated. Based on this method and the max stresses, Saena can sustain 6.52×10^5 cycles which is more than required. This number of cycles leads to 40,000 hours service life for long lasting platform concept.


Wing Fuel Tank
Canopy
Intake
Engine
Center Fuel Tank
Ladder
Radar
Nose Landing Gear Bay
Main Landing Gear
Nose Landing Gear

10.7 MANUFACTURING

Manufacturing process goal of Saena is cost reduction. For supporting this concept, most components would be supplied in U.S in order to eliminate transporting cost. To decrease labor force costs, some assemblies must be done in low-cost countries.

With advancement in 3D print technology, more and more components could be made with this method which causes in weight, time, and cost reduction (in comparison with CNC which removes materials). In addition, more complex shapes may be made with this technique. In comparison with normal production of metals which increasing in strength causes reduction in toughness, with 3D printing both strength and toughness would be improved.

Manufacturing from raw materials, integration, assembly, and quality control would be accomplished in U.S. Dominant material used in aircraft is metallic materials, which is easier and low-cost to manufacture in comparison with composite materials.

11 DESIGN VERIFICATION

11.1 PERFORMANCE

In this section, the final design has been reviewed and verified based on the performance measures of merit. In each verification step following data has been used; Drag Polar (section 7.3), stability derivatives (section 9), and max available installed thrust (section 6). Verification has been carried out mainly engaging [40] and [13]

11.1.1 Stall Speeds

The stall speeds for takeoff, landing, and cruise at 15k and 30k ft. segments of the BFM mission are determined using [40]. Only power-on stall speeds are reported in Table 56.

Table 56-Power On Stall Speeds for Different Flight Conditions

Flight Phase	Weight (lb.)	Stall Speed (kts)
Takeoff	12651	105
Landing	8845	83
Practice Area, 15k ft.	11080	145
Practice Area, 15k ft.	W_{Combat} = 11308	147
Cruise, 30k ft.	12263	220

11.1.2 Required Runway Length

Use of speed brakes or drag chutes is common in the existing APTA. Saena also benefits from speed brakes. Mainly to reduce the landing distance to 6000 ft. also to have a better control characteristic in formation flight trainings due to the rapid airspeed control. Furthermore, use of speed brakes help Saena become more agile during maneuvers; attaining positional advantage. Speed brakes area has been estimated using the correlation according to [41]:

Eq. 6

$$S_A = 0.08853 + 0.00008156W$$

Eq. 6 results in an area of 6.80 ft^2 for speed brake/brakes. Assuming no changes in surface effectiveness, two pairs of speed brakes are installed on each side of the tail far enough from the wing and control surfaces so that the pressure field does not affect wing pressure field. Each speed brake has an area of 1.7 ft^2. The total weight of the speed brakes with their high-speed actuators has been estimated at 20 lbs.; hence their effect on the CG location and weight and balance is negligible. but negative effects on the pitch equilibrium is inevitable (due to the distance from the CG) and must be accounted for properly.

The eq. 4.85 of [9] Part VIused to calculate the drag coefficient of deployed speed brakes, which resulted in a drag coefficient of 0.0193. Use of speed brakes in landing phase with an assumed deflection of 60-degrees for each plate, has resulted in an average deceleration in ground run value of 0.50 and 193 drag counts increase in CD_0. The landing distance could then be further reduced as much as 10.5%, which equals to 480 ft. shorter runway.

As expected, a shorter takeoff distance than the requirement is available because of the high value of T/W that was resulted from choosing the engine. The landing field length requirement has already been met in the optimization process and because of the W/S value of the final design.

Figure 56 shows the dimensions and max deflection of the speed brakes. Further analysis of the effectiveness of the speed brakes and their effects on the handling qualities must be performed in wind tunnel testing so as to determine their exact location.

The results of initial sizing and optimization plus the final verified values (in case of deployed/retracted speed brakes) are presented in table2, assuming different values for

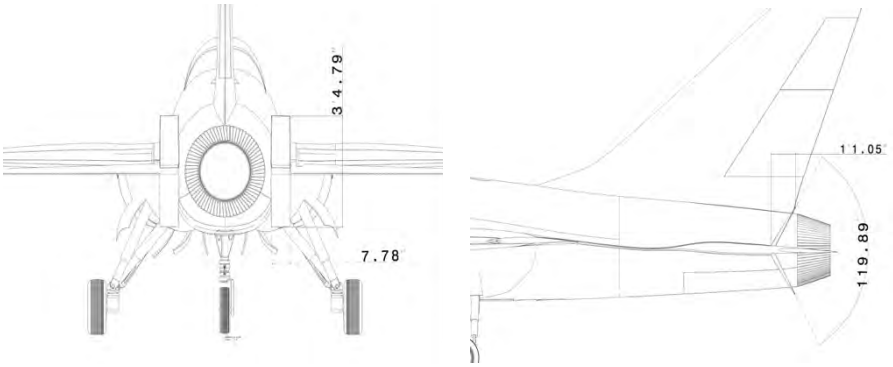

Figure 56-Dimensions of The Speed Brakes

μ_g, $C_{Lmax,\ TO}$ = 1.6 and $C_{Lmax,\ LA}$ = 1.9. With the use of speed brakes, Saena is able to take off and land on a 5610 ft. runway. The airports discussed in section 1.3 can accommodate Saena.

Table 57-Verified takeoff (brakes off) and landing (brakes on) distances

Distances	Optimized Value (ft.)	Verified Value (SB deployed) (ft.)	Verified Value (ft.)
Takeoff Distance (dry concrete)	1950	1150	1150
Takeoff Distance (icy concrete)	1940	1145	1145
Landing Distance (dry concrete)	2780	2790	2790
Landing Distance (icy concrete)	4450	4460	4860
Required Runway Length	6400	5610	6010

11.1.3 Max Level Speed

As can be seen in figure 5, the max achievable speed at 30000 ft. in cruise 1 (BFM mission) and weight of 12263 lb at the start of the cruise is 756 knots (Mach 1.283). At 36000 ft. and combat weight (11308 lb), the max achievable speed is 748 kts (Mach 1.303). The drag polar used for this verification is presented in Table 58.

Table 58-Drag Polar for Max Level Speed

Flight Condition	Drag Polar
Clean, Mach 1.3	$0.0357 + 0.223C_L^2$

In comparison with other advanced jet trainers, Saena has an acceptable max cruise speed. In fact, it is in parity only with T-38 in this matter and is superior to others, with the exception of KAI T-50 and Hongdu L-15 which play a light combat aircraft role. A brief comparison is summarized in Table 59that shows the relative advantage of Saena over other jet trainers.

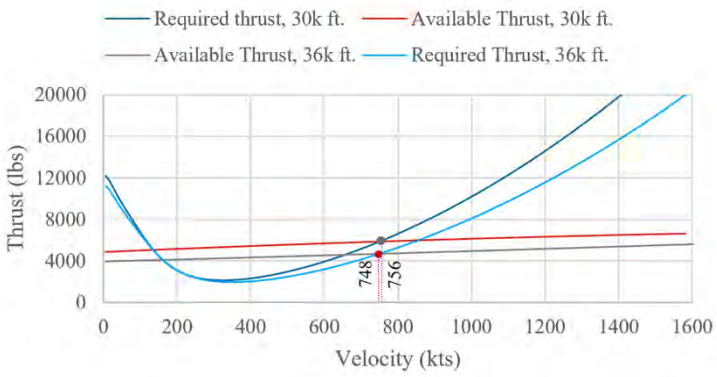

Figure 57-Thrust vs. Speed

Table 59-Max Level Speed Comparison

Jet Trainers	Max. Level Mach
Saena	1.3
M346	1.2
Hongdu L-15	1.4
T-38C	1.3
KAI T-50	1.5

11.1.4 Max Rate of Climb

Using equation 3.38 in [9] Part I, the relation below was generated to calculate the climb path angle corresponding to the best climb performance (max R/C) sizing:

Eq. 7

$$\sin\gamma = 0.997 \times T/W$$

note that a value of (L/D)max = 12.8 was used to arrive at the above relation. With the installed thrust at sea level and the weight at the start of climb, the equation above resulted in a 55-degree flight path angle. Figure 59 & Figure 58show that the max rate of climb achievable for Saena is 24868 and 36930 fpm for dry and wet thrust conditions at sea-level, respectively. The corresponding climb speeds would be 497 and 511 knots. Best climb speed for a jet usually falls in the range of 300 to 500 kts based on [13],hence Saena is within the statistical range.

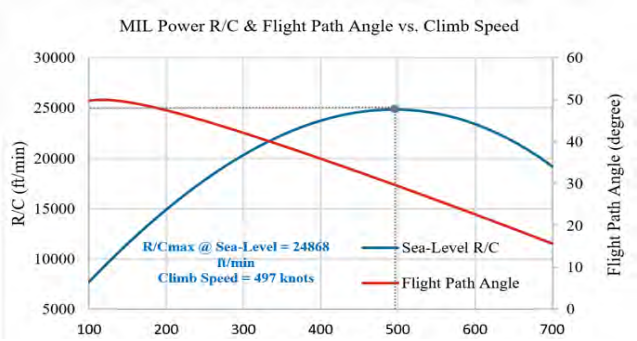

Figure 58-MIL Power R/C& Flight Path Angle vs. Climb Speed

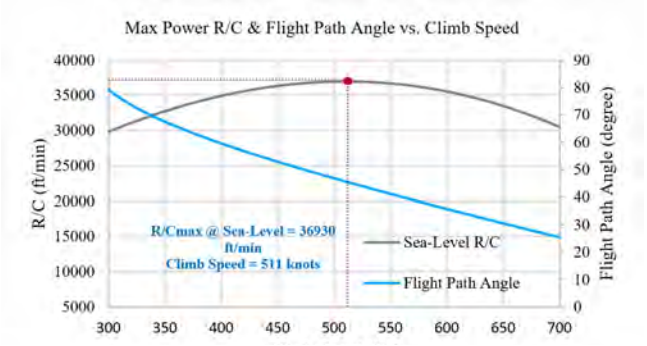

Figure 59- Max Power R/C& Flight Path Angle vs. Climb Speed

Acceleration factor (change in forward speed due to an increase in altitude) in these calculations has been taken to be 0.01 s^{-1}.

With the help of equation 3.35 [Roskam's Part I], the climb speed corresponding to the max R/C has been calculated to be 243.78 kts .at RFP mission climb weight at sea level. Based on [Raymer], this velocity may be on the order of twice the velocity for min power if the effects of thrust are accounted for, so the values above (max R/Cs) are verified with a calculation error of only 1.9% and 4.8%.

Climb performance of Saena has been compared with existing advanced jet trainers in table... Based on table…, Saena has a higher than average max rate of climb at sea level; about 15000 ft./min higher than the others with the exception of Hongdu L-15, Guizhou JL-9 and KAI T-50 which have oddly high values of max. R/C due to them being light combat aircrafts or modifications of fighter jets. Saena is of course exhibiting a high-performance behavior in climb performance.

Table 60-Comparison in Max R/C

Jet Trainers	Max. R/C [fpm]
Saena	37000
T-38C	33600
M-346	22000
Yak-130	10000
Hongdu L-15	40000

11.1.5 Glide Performance

In an engine shutdown scenario, Saena has an acceptable glide performance, which is calculated at combat weight (11308 lb) and is presented in Table 61 [9] is used for these calculations.

Table 61-Glide Performance of Saena

Flight Condition	Velocity (kts)	Max. R/D (fpm)	Max. Time of Glide (min)	Max. Range of Glide (nm)	Drag Polar
Practice Area, 15k ft.	482	4940	9	31	$0.0174 + 0.0915C_L^2$
Cruise, 30k ft.	461	6360	14	62	$0.0175 + 0.0915C_L^2$

11.1.6 Aerodynamic Efficiency Analysis

Figure 60provides useful information on aerodynamic efficiency of the design, as requested by the RFP. Lift-to-drag ratio peaks at Mach 0.59 and 36000 ft., reaching its max value of 12.8.

Around Mach 0.81, (L/D)max begins to decrease due to the onset of high speed drag rise up to Mach 1.04 and continues to do so with a lower reduction rate. The supersonic value is 4.7 at Mach 1.6, going towards a constant value at higher Mach numbers. A comparison is done between existing jet trainers, using [9]method for estimating zero-lift drag coefficient and [42]. The results suggest that Saena would show a relatively higher aerodynamic efficiency.(Table 62)

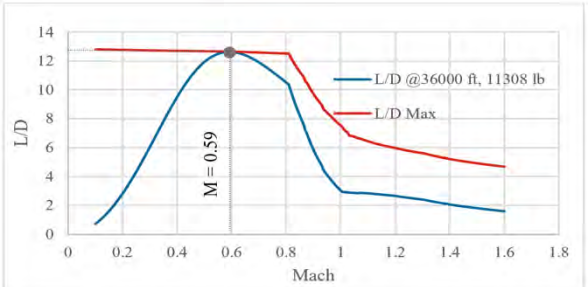

Figure 60-L/D and (L/D)max Variation with Mach

Table 62-Comparison in Aerodynamic Efficiency

Jet Trainers	CD0 at Mach = 0	(L/D)max
Saena	0.0167	12.8
T-38C	0.0207	11.3
M-346	0.0188	12
Yak-130	0.0196	12

Also the LRC mission's optimized Mach number, is calculated to be 0.75 using the $C_L^{0.5}/C_D$ vs. Mach diagram, shown in Figure 61. It has a 5.1% error with the value of Mach 0.79 calculated for weight sizing.

11.1.7 Maneuvering Performance

In this section, verification of the 9g maneuvers requirement is presented and turning performance capabilities of Saena is discussed. Operational envelopes are assessed under different loading conditions, so as to verify Saena as a leading platform to fulfil its objective of offering 5th gen. fighter pilot training.

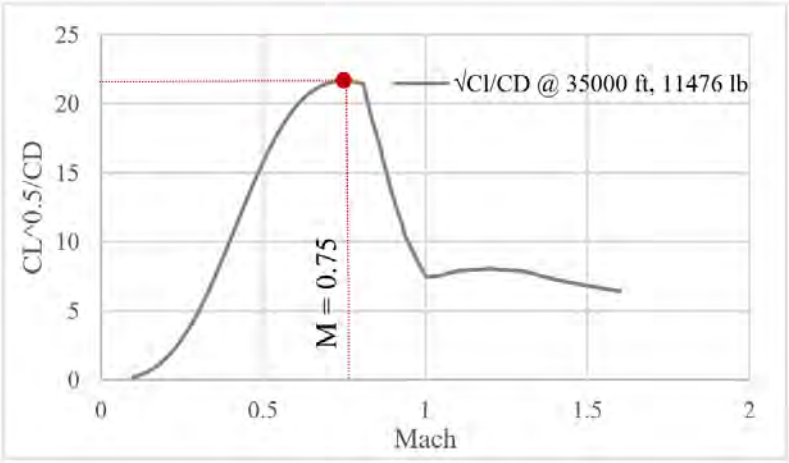

Figure 61-LRC Optimum Speed Verification

A thorough comparison in matters of max. specific excess power and max. sustained and instantaneous turn rates is done later, between Saena and its rivals.

11.1.8 High-g Maneuvers Verification

If the aircraft is allowed to slow down or lose altitude, which is the case in an instantaneous turn (negative specific excess power), the load factor is limited only by the max combat lift coefficient or the structural strength of the aircraft [Raymer]. Combat $C_{L_{Max}}$ has been taken as 1, based on the suggested range of 1-1.5 [Raymer's] and the fact that the aircraft has leading & trailing edge flap systems which could be used during maneuvers. It is noted that this value is lower than $C_{L_{Max,Clean}}$, due to high-speed effects. As Saena is designed to withstand 13.5gs, the combat $C_{L_{Max}}$ of 1 will be the only limitation, as maneuvering lift coefficient must always be less than the $C_{L_{Max}}$ for instantaneous maneuvers.

As Saena is able to withstand 13.5gs, the Combat $C_{L_{Max}}$ of 1 would be the only limitation, as maneuvering lift coefficient must always be less than the $C_{L_{Max}}$ for instantaneous maneuvers.

The verification analysis was done for both RFP and CAS missions, but only RFP mission results are presented here. The weight of the aircraft at the start of practice area in CAS mission is only 200 lb. higher than the same segment in RFP mission, so after consuming this extra fuel, the same results will occur for same maneuvers. All the maneuvers are executed with A/B on, with the exception of payload-drop maneuver. Table 63summarizes the performance parameters of each RFP maneuver. Trainee must choose the suitable throttle setting according to the trainings so as not to exceed his/her g-limit during maneuvers.

Mach Drag Divergence Mach (0.87) was not reached in any of the executed maneuvers (except for instantaneous turn rate demonstration maneuvers; Mach = 0.9) and all maneuver speeds were higher than stall speeds at 15000 ft. under different loading conditions. Stall speeds are presented in Table 64 & Table 66.

Table 63-Summary of Each BFM Maneuver Giving the Important Performance Parameters

Mission Segment	TReq. (lbs)	VAvg. (kts)	Time to Complete (s)	Bank Angle (deg)	Radius (ft)	Turn/Pitch Rate (rad/s)	CL, M	Fuel Consumed (lbs)	WManeuver (lbs)	Load Factor *
9g 360-degree turn	10367	505	18	83.9	2403	0.35	0.85	35	11000	9.31
9g pull-up	10364	494.2	10	0	2606	0.32	0.87	33	10965	9.34

9g 360-degree turn	10365	496.6	17.5	83.9	2349	0.36	0.86	35	10932	9.39
9g pull-up	10364	494.7	10	0	2609	0.32	0.87	33	10897	9.43
9g 360-degree turn	10365	495.9	17.5	83.9	2329	0.36	0.87	35	10864	9.47
6g 180-degree turn	5759	485.9	13	80.6	3461	0.24	0.59	15	10829	6.15
Total			86					186		

Table 64-Stall speeds during high-g maneuvers, BFM mission

Altitude (ft)	Average Loading	Stall Speed Range (kts)
15000	9.38g	440-444
15000	6.15g	357

*It is well noted that weight limitations must be considered in order to execute high-g maneuvers. Verified loadings are in the allowable range of 5% error (based on [Roskam]) in performance analysis, which is 0.45g's.

There exists an iteration between fuel consumption, maneuver weight and performance specifications of each maneuver. Fuel consumed is reported for a 10-second maneuver in each segment.

As can be inferred from Table 63, At the worst aircraft weight scenario, which is the start of the practice area, Saena has been able to execute a sequence of high-g maneuvers.

Table 65Summary of each RFP Instantaneous maneuver giving the important performance parameters

Instantaneous Maneuvers	Corner Speed	Max Turn/Pitch Rate (rad/s)	$C_{LMax,C}$	$W_{Maneuver}$ (lb)	Max Load Factor*
360-degree turn	558.9	0.46	1	11000	13.48
Pull-up	558	0.43	1	10965	13.49

*Instantaneous turn rate (lift-limited turn) demonstration maneuver is done at corner speed; classical dogfight training.

Performance at combat weight is also reported in Table 68. There is no sequence in maneuvers done at combat weight, so each maneuver will be evaluated at combat weight as the weight at the start of the maneuver. Table 3 gives the stall speeds under different loadings occurred in these maneuvers. Figure… shows a schematic of two 9g 360-degree turn and pull-up/push-over maneuvers and their specifications.

Table 66- Stall speeds during high-g maneuvers, combat weight

Altitude (ft)	Average Loading	Stall Speed (kts)
15000	9.12g	444
15000	5.98g	359

Table 67-Instantaneous capabilities demonstration maneuvers

Instantaneous Maneuvers	Corner Speed	Max Turn/Pitch Rate (rad/s)	$C_{L_{Max}}$	W_{Combat} (lb)	Max Load Factor*
360 degree turn	566.7	0.45	1	11308	13.45
Pull-up	566.9	0.42	1	11308	13.48

Table 68-Summary of each BFM maneuver at combat weight (50% internal fuel) giving the important performance parameters

Mission Segment	TReq. (lbs)	VAvg. (kts)	Time to Complete (s)	Bank Angle (deg)	Radius (ft)	Turn/Pitch Rate (rad/s)	CL,M	WCombat (lbs)	Load Factor*
9g 360-degree turn	10366	499	18.5	83.7	2447	0.34	0.86	11308	9.12
9g pull-up	10366	499	10	0	2717	0.31	0.86	11308	9.12
6g 180-degree turn	5794	497.3	13.5	80.4	3729	0.23	0.57	11308	5.98
Total			42						

The aircraft is capable of instantaneous maneuvers, pulling up to 13.5g's, as suggested by Table 67 The decision on $C_{L_{Max,Clean}}$ value of 1.1 is also verified, as it is high enough with an acceptable margin to allow for adequate combat lift coefficients needed to execute the maneuvers. Figure 63 shows the variation of g-loading with flight speed.

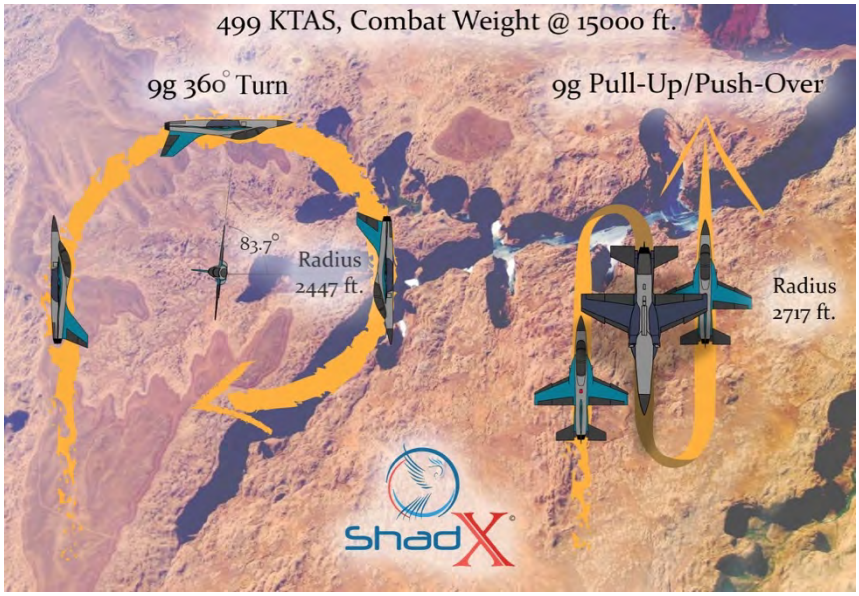

Figure 62-9g Maneuvers at 15000 ft. and Combat Weight

As can be seen in Figure 63 Higher instantaneous g-loadings (higher than 13.5g) are structurally-limited and not thrust-limited. The structure failure zone is colored in red. It is noted that the available thrust does not impose a limitation on instantaneous maneuvers capabilities, hence g-loadings in figure… can be achieved.

Drag Polar used for these assessments are found in [drag determination section]. Control surfaces deflections needed to keep the 9g turn & pull-up maneuvers at combat weight are calculated and presented in Table 69&Table 70, so as to verify the feasibility of the maneuvers.

Figure 63--Max Instantaneous Load Factor vs. Velocity

In order to assess the controllability of the aircraft, the angle of attack and CS deflections for two maneuvers in practice area flight condition with combat weight (50% internal fuel) has been calculated using equation 22.23 of [Nicolai]. To verify the results, the trim equations, presented in [Roskam] has been used and the increase in δ_{CS} (CS deflection) for the 9g pull-up maneuver has been computed. The results are presented in Table 69&Table 70.

Eq. 8

$$\delta_{Trim} + \mathbf{\Delta}\delta_{CS} = \delta_{Pull-up}$$

Table 69Steady Symmetrical 9g pull-up trim data and related CS deflections

V [ft./sec]	W [lbs.]	R [ft.]	$\delta_{Pull-up}$ [rad]	AOA [rad]	$\Delta\delta_{CS}$ [rad]	$\delta_{Trim} + \Delta\delta_{CS}$ [rad]
842.14	11308	2717	-0.0189	0.1662	-0.0267	-0.02

The needed aft tail deflection has been verified then, with 5.5% difference.

Table 70 Steady 9g 360-degree turn trim data and related CS deflections

V [ft./sec]	W [lbs.]	φ [rad]	δ_{Turn} [rad]	AOA[rad)]	β [rad]	δ_r [rad]	δ_a [rad]
842.14	11308	1.4608	-0.0191	0.164	0.0001	-0.0012	0.0006

As mentioned in [9] part , flight in a steady level turn takes place at a higher angle of attack and requires a larger (negatively) differential stabilizer deflection angle, in comparison with steady state straight line flight, as has been the case in this calculation.

11.1.9 Operational Envelope and Energy Maneuverability Assessment

Using an off-the-shelf engine, a requirement mandated by the RFP, is a critical task that usually results in an excess thrust, as it has been the case for Saena. Obviously, as designers, we must think using such extra power to

enhance maneuvering capabilities. The goal is to have a more competitive aircraft compared to the suggested one by the RFP. For Saena, the goal is to achieve higher sustained and instantaneous turn rates, improved roll rates, better climb performance (max. R/C, time to climb, ceiling), and in general expansion in the requested operational envelope. Such approach could help reach a high-performance and agile trainer; which supersedes existing jet trainers, such as M346, Yak-130 and T-38C. As an example, Saena exhibits a much better turn rate over its competitors, at least theoretically. Preliminary calculations suggest that such superiority could amount to 11.5 deg/sec; which is highly significant in the field. We expect a significant portion of such superiority remains throughout the Saena development process. The calculation of max achievable turn rate has been done according to [Raymer's] equation 5.19 and 5.20. Saena exhibits better high-g capabilities, due to its higher thrust loading and sturdy structure. Table 71 presents max turn rates for mentioned jet trainers along with their design limit load factor. A thorough analysis on turning performance will be carried out later, in this section.

Eq. 9

$$\frac{W}{S} = \frac{qC_{L_{Max}}}{n}$$

Table 71- Max. turn rate and limit load factor of advanced jet trainers at 15k ft.

Jet Trainers	Max. Turn Rate [deg/s]
Saena	25.8
M346	13.0
Yak-130	14.5
T-38C	15.5[2]

[2] This data was extracted from numerous pilots reports which may not be a reliable source.

A thorough analysis on turn performance will be carried out later, in this section Due to thrust pinch occurrence near M = 1, area ruling was of great importance to be applied to the design. The design benefits from a high takeoff T/W, so after the geometry was area ruled, the marginal excess thrust problem in transonic region was solved and the operational envelopes were plotted in figures 1 to 5. These figures prove that Saena is capable of passing through this region and reaching Mach 1.3 at 36000 ft.

Figure 64 shows the flight envelope of Saena, containing the constant specific excess power lines in normal maneuvering conditions. As Figure 64 suggests, we have been able to keep Saena sturdy enough, so its structure would not cause a severe barrier on max achievable speed even during dive from different altitudes (Fig. x V-n diagrams). Moreover, the calculations suggest that max achievable Mach number at sea-level is 1.15; which apparently is 4.5% lower than the structural limit requested by the RFP. It is noted that aircraft structure has been designed to withstand dynamic pressure at Mach 1.44; which corresponds to diving scenarios (section 10).

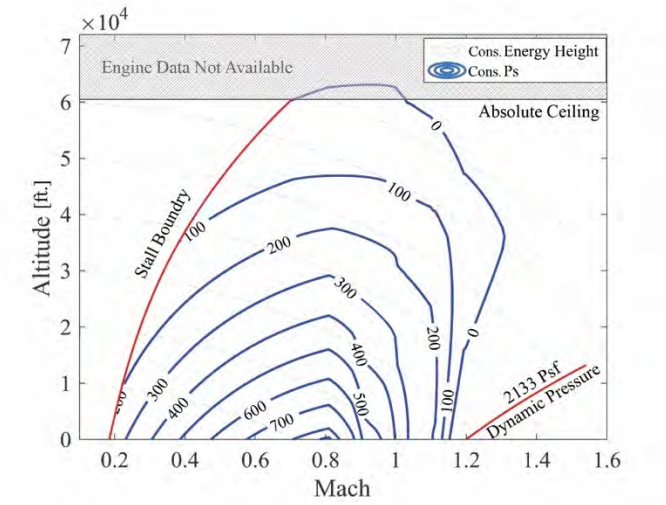

Figure 64-1g Max. thrust specific excess power envelope, takeoff weight (50-ft. obstacle, 12440 lb)

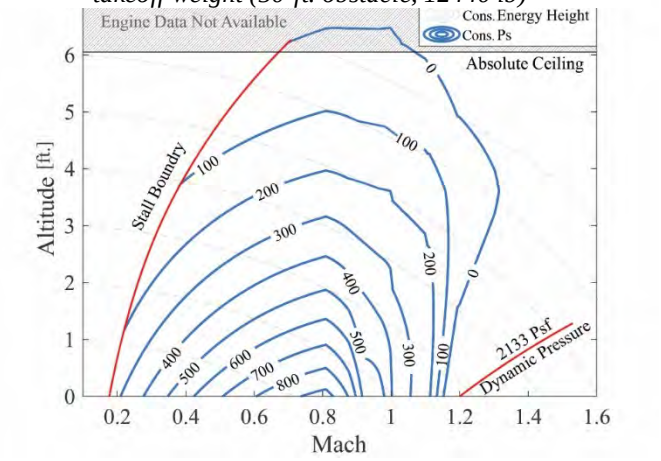

Figure 65-1g Max. thrust specific excess power envelope, combat weight

Needless to mention that Saena would reach the supersonic speed with its afterburners. The flight envelopes for 1g and 5g loading with max thrust are plotted in Figure 65 and **Error! Reference source not found.**, respectively. The h-v diagram for military thrust is presented in Figure 67.

The constant Ps lines in figure 43 and 45 verify the design point selected earlier; Saena has 840 and 485 ft/s specific excess power in max and military power condition at sea level (climb weight), respectively. It possesses Ps value of 900 ft/s at combat weight (sea level, max. power). These values correspond to Mach 0.77 and 0.75 respectively, which are the climb speeds for max achievable rate of climb at sea level [section max rate of climb]. Under 5g loading, Ps

values up to 800 ft/s are also achievable. Table...compares sM-346 and Saena in the matter of acceleration/climb capabilities

Table 72-43Max specific excess power for different jet trainers

Jet Trainers	Max. Ps @ sea level [ft/s]
Saena	900
M346	800[3]

Figure 67 shows the min time to climb to the absolute ceiling, which has been calculated using [AAA]. The climb lines are tangent to both P_s lines and constant energy lines, beginning at takeoff M = 0.2 and accelerating to M = 0.5 at sea level to achieve the max rate of climb, then climbing to 53000 ft., which would take slightly less than 2 minutes.

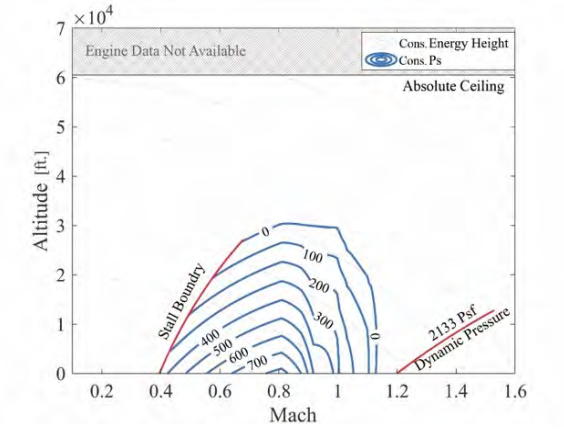

Figure 66-5g Max. thrust specific excess power envelope, combat weight

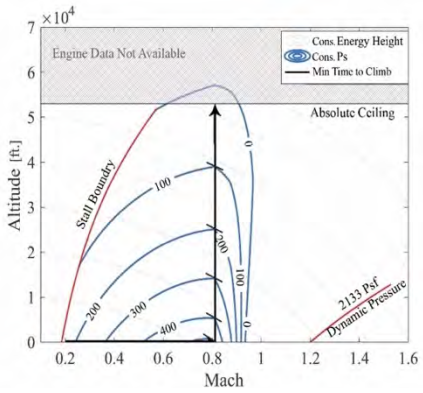

Figure 67-3Climb analysis, 1g MIL thrust specific excess power envelope, climb weight (50-ft. obstacle, 12440 lb.)

Figure 69 compares the two operational envelopes, which is Saena and F-22. The figure helps highlight the training effectiveness of Saena for an F-22 fleet. F-35A data has not been available for comparison, nonetheless, we expect Saena to perform satisfactorily for a F-35 fleet; as Saena employs a Variable Stability and Augmentation System (VSAS).

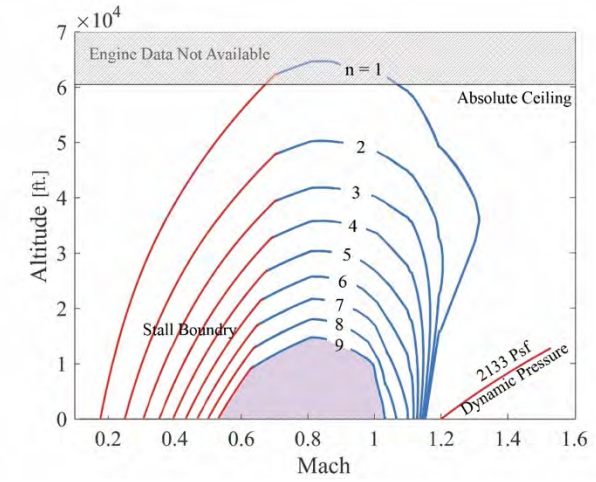

Figure 68-Max. thrust sustained load factor envelope, combat weight; the shaded area shows the region of 9g maneuvering capability

[3] Data was extracted from online sources and may not have high reliability [www.ainonline.com/aviation-news/defense/2007-11-07/m-346-gets-lighter-faster-more-agile]

With reference to the RFP, it is well-noted that APTA wishes to fill the current training gaps by covering the region where it could get a step closer to the training targets, F-22 and F-35, while maintaining its role as a lead-in fighter trainer and not a fighter itself. We firmly believe that Saena could perform such a role as it is able to maintain a 9.0g turn with any velocity between Mach 0.55 and 1.1 close to sea-level (Figure 68).

With the help of [Nicolai's Appendices], we have been able to conservatively estimate F-22 capabilities, and it so appears that Saena could be able to perform the role of a pre-operational trainer at high subsonic, in addition to transonic and low supersonic speeds (Figure 69Note that F-22 has a relatively superior performance at supersonic speeds, a region it has been designed to be operated in.

The cruise Mach with max. power, dash Mach and drop Mach with MIL power are within the operational envelope of Saena, as shown by Figure 69, suggesting that the design requirements are met.

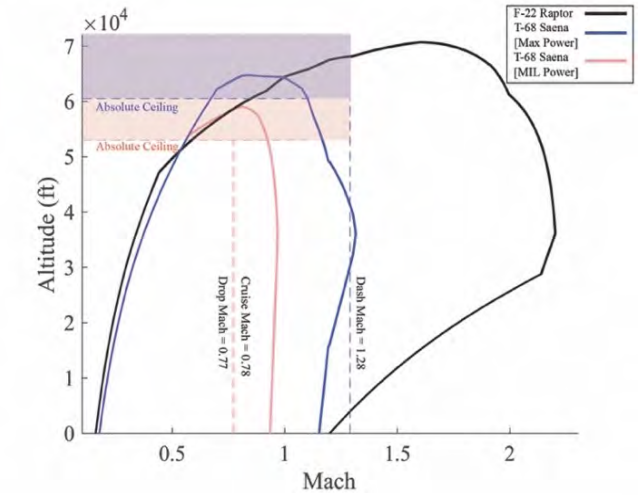

Figure 69-1g Ps=0 Operational envelope of F-22, T-38 and Saena, combat weight

Energy maneuverability diagrams are shown in **Error! Reference source not found.**. Saena is comparatively better to the existing rivals; when it comes to the sustained turn rates. The goal for Saena is to have high turn rates at Mach numbers within 0.5 to 1. That is, sustained turn rates are in agreement with F-22

capabilities for that region. As seen in Figure 74 and Table 73, Saena has an average of 45% higher sustained turn rates over F-22 at altitudes of 8 to 25k ft., within aforementioned Mach range.

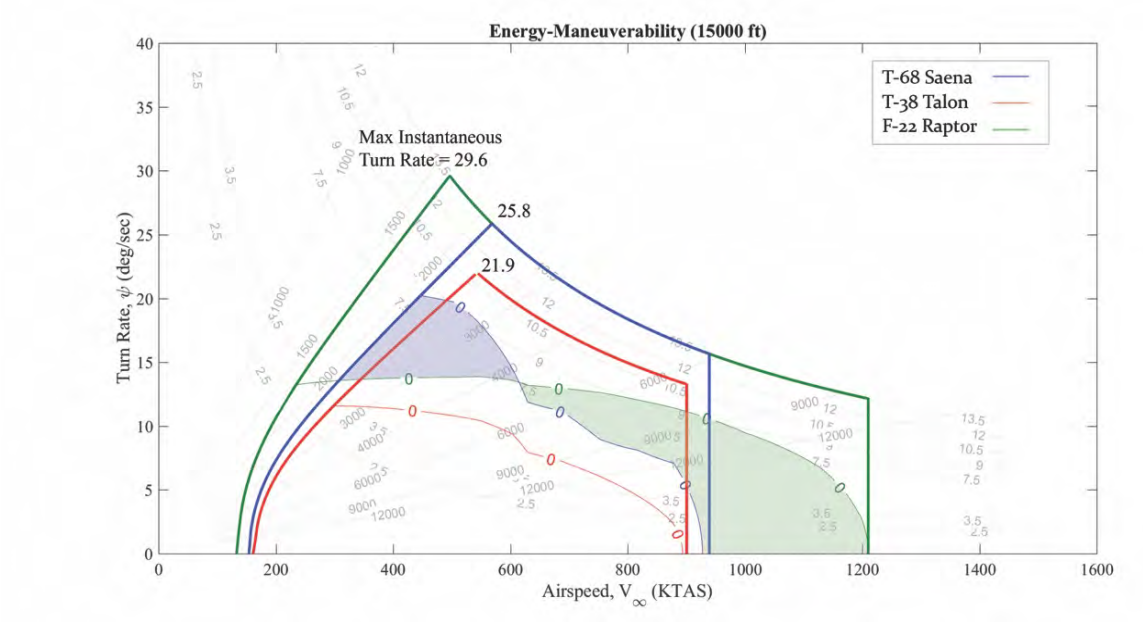

Figure 70-Energy maneuverability diagram, 15000 ft., combat weight. The regions of relative superiority are colored

The E-M diagram created for T-38 shows a max instantaneous turn rate of 21.9, which is still inferior to the Saena. Figure 70 shows the capability of Saena to fill the existing training gap between an F-22 and T38.

Table 73- Max. sustained turn rate of Saena and F-22

Aircraft	Max. Sustained Turn Rate [deg/s]
Saena	20.3
F-22	14

Meanwhile, Saena exhibits a relatively lower max instantaneous turn rates at low speeds. This is due to the thrust vectoring capabilities of F-22 and its low stall speed; which results in a lower corner speed. Currently, there is no sign of an off-the-shelf engine with thrust vectoring capabilities. However, we have enough provisions built-in Saena to enhance its engine, in case such options become available.

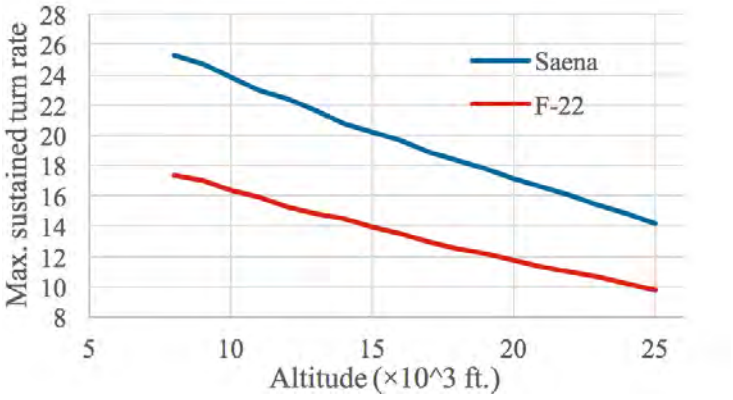

Figure 71-Max. Sustained Turn Rate vs. Altitude for F-22 and Saena

With Figure 70 and Figure 71, Saena exhibits the potential to have a max instantaneous turn rate of 25.8 deg/s @ 15k ft. This is 12.8% lower than its target value; which might not be satisfactory (F-22 has a max. turn-rate of about 30 deg/s). Different approaches to re-shaping the aircraft's configuration while considering the overall cost requirements have not led to meaningful results. To respect the RFP mandate, we have thoroughly studied the effect of altitude on the turn rates; such investigation includes altitudes between 8 and 25k ft. The aim has been to get closer to the target turn rate (Figure 72). As Figure 72 suggests, we could effectively satisfy the requirements at higher altitudes such as 20k ft. That is, we suggest training area be used in wider range of altitudes from 8 to 25k ft.

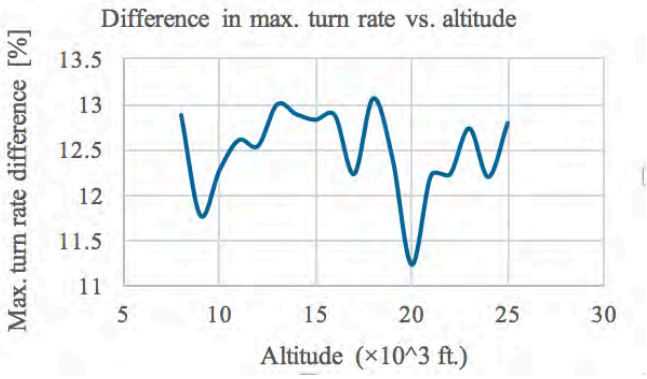

Figure 72-Max. turn rate difference between F-22 and Saena

11.2 AERODYNAMICS

In order to verify the theoretical values in design aerodynamics, a CFD analysis of the wing planform is carried out using ANSYS Fluent software. A full scale model of the wing is used with a 15 layered boundary layer mesh with a growth rate of 1.2 as shown in Figure 73. Additionally, adaptive meshing is set with the setting listed in Table 74.

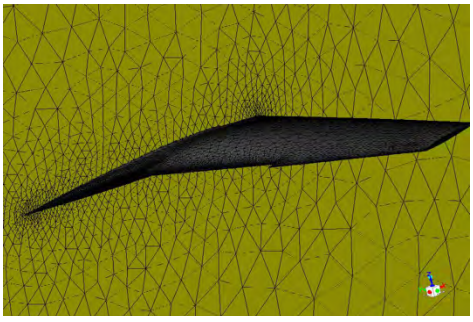

Figure 73-half Wing mesh (ANSYS

Table 74 - CFD parameters

	Subsonic	Supersonic
Parameter	Value	Value
No. Mesh Element	1,486,782	313,000
Domain size	150x120x75	120x120x75
Turbulent model	Realizable k- ε	Realizable, k- ε
No. Iterations	50,000	8,000

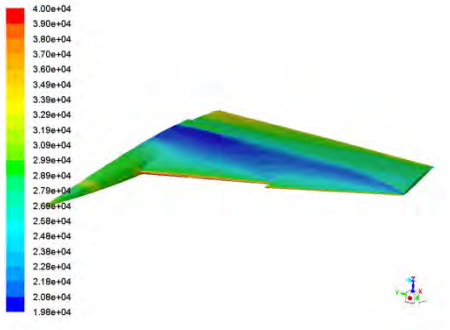

Figure 74-Pressure Distribution in M=0.8

The flight conditions of cruise at M=0.78 at 15000 ft and 0.8 & 1.3 at 30000 ft above SLS are used for the analysis. The results of the analysis converge after the indicated number of iterations. The C_L and C_D values of the design and CFD analysis are compared in Table 75. Pressure distribution on the wing surface is shown in Figure 73. Finally, the difference between the two approaches are reported in Table 75. The results show a 13% difference in subsonic and 19% in supersonic between the determined and computed values. The subsonic analysis shows a formation of shock on the surface of the wing, which shows that the wing critical Mach is below 0.78, while the designed critical Mach was 0.85. This 8% difference calls for a modification to the wing. A proposed modification is reduction in thickness of the wing. In supersonic speeds the shock formation in front and behind the wing is expected and the overall pressure pattern is reasonable. The high difference in supersonic region, might be the result of inaccurate theoretical methods.

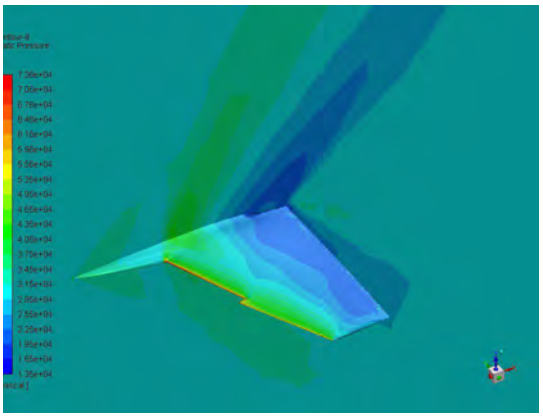

Figure 75-Pressure Distribution in M=1.28

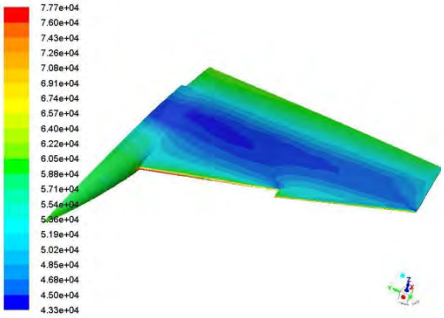

Figure 76-Pressure Distribution in M=0.78

Table 75- CFD Results

	Subsonic M-0.78		Subsonic M = 0.8		Supersonic	
Parameter	C_L	C_D	C_L	C_D	C_L	C_D
Theoretical	0.21	0.024	0.24	0.0073	0.07	0.07
CFD	0.182	0.0286	0.2727	0.0061	0.0835	0.0734
Error	10.5 %	19.16%	13.6%	12.9%	19.3%	4.8%

12 MARKET & LIFECYCLE COST

12.1 MARKET

Market study of military aircraft has more constraints and considerations than commercial aircraft such as more Limited costumers and political considerations.

12.1.1 Existing Market

Although RFP declared that main costumer of Saena is USAF. Potential demand of Saena which would be a replacement for T-38, has been studied in USA and the countries operate T-38:

- US Air Force: About 430, T-38 (65% of them are fully available) are being used in USAF bases in advanced pilot training programs. [43] [44] There are about 12000 pilots in USAF which 2500 of them are fighter pilots.

Although, 250 fighter pilots join USAF annually. There are 1000 less pilots than needed. The main reason is early retirement of pilots due to low salaries and disaffection. In 2016, 250 fighter pilots were trained, which should be increased to 400 to meet the need. [44]. Assuming that the trainees' flight hours and mission time of Saena would be same as current T-38 fleet, total predicted number of required Saena for USAF would be 450. Max number of USAF orders also would be 473 [2].

- NASA has 32, T-38 for scientific analysis like supersonic experiments and training astronauts for high g-force [45]
- German Air force: Germany has 30, T-38 and their target fighters are Eurofighter and Typhoon.
- Turkish Air force: Turkish Air force has 33, T-38 and their target fighter is F-16. They also use F-5 for training [46]

12.1.2 Market Expansion

F-22 and F-35 are the training targets of Saena so it is possible to expand the target market to other countries which use F-22 or F-35. According to a Congress bill, F-22 must not get exported. However, in near future F-35 is going to be delivered to some countries like UK, Italy, Netherlands, Australia, and Canada. [47] So, the number of required trainers could be estimated. (Table 76)

Table 76- Estimated Number of Saena Requirement for Each Country

Country	Current	Expansion	Total
US : USAF	450	0	450
US : NASA	30	0	30
Turkey	30	0	30
Germany	30	0	30
Canada	0	15	15
Netherlands	0	15	15
Denmark	0	10	10
Norway	0	10	10
Total	540	50	590

12.2 LIFE CYCLE

Timing of different phases in Saena life cycle has been studied respect to time and cost limitation and needs. According to Figure 1 manufacturing phase begins right after RDTE phase, in 2022 with a rate of 3 aircraft per month. First Delivery of Saena would be in 2023, and by 2030 all T-38s would be retired, disposed, and replaced with Saena [2] . To achieve this goal, the production rate would increase to 5 aircraft in a month in just 2 years. [47]. F-35 delivery would be finished by 2038. The fifth generation fighters would be in service up until 2060 [48]. Therefore, Saena has

been designed to be in service for 35 years. Also, there would be some modifications to extend the lifetime, in case of need. Finally, there would be five years of disposal.

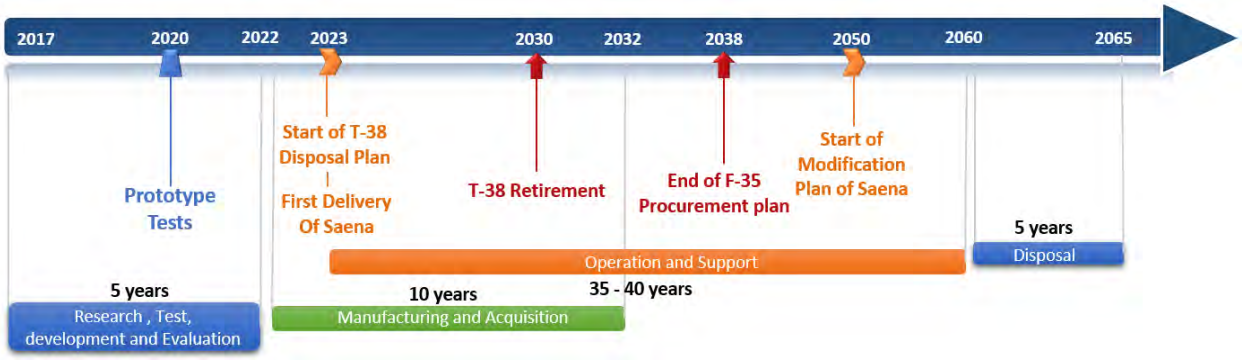

Figure 77- Life Cycle Plan Timeline

Table 77- Delivery Plan Date and Quantities

Fiscal Year	FY22	FY23	FY24	FY25	FY26	FY27	FY28	FY29	FY30	FY31	FY32	Total
Monthly Rate	3	4	5	5	5	5	5	5	5	4	3	-
USAF Delivery	28	37	46	46	46	46	46	46	46	37	26	450
Other Costumers	8	11	14	14	14	14	14	14	14	11	12	140
Total Manufactured	36	48	60	60	60	60	60	60	60	48	38	590

Modification plan: There are 3 levels of modifications that would be applied to the aircraft in lifetime:

- Airframe and structural modifications: referring to (section 10.6) lifetime of airframe and structure would be more than 30,000 hours that would be enough up until 2060. If nothing unusual happens in manufacturing process airframe would not need any modification or reinforcement.
- Engine Modifications: Although, Engine MTBO is about 6000 hours so with three overhaul it would cover entire lifecycle of the aircraft. It would be replaced. If, operation cost increases due to fuel consumption.
- Avionics. It may require to upgrade the Avionics Systems due to demand changes or requirement of new avionic platforms in future. To make this process easier, modular avionics method used in aircraft.

12.3 COST MODEL

In Cost Estimation Model selection, several cost models have been studied. Roskam cost model [9] would be the base of this cost estimation calculations because of more detailed breakdown of all cost components in comparison to other cost models such as DAPCA-IV [49] which estimates the costs based on previous database of aircraft. DAPCA-IV final results are also presented. Validations of cost models also has been studied in. All prices in this section has been reported in 2018 US dollars with assuming a stable economic condition.

12.3.1 Cost Model Sensitivity Analysis

To meet the RFP mandate, and reduce the operational and manufacturing cost, Sensitivity of cost model to design parameters had been studied. Most of decisions and optimizations in design process have been made based on the cost Table 1represents the results of this sensitivity analysis.

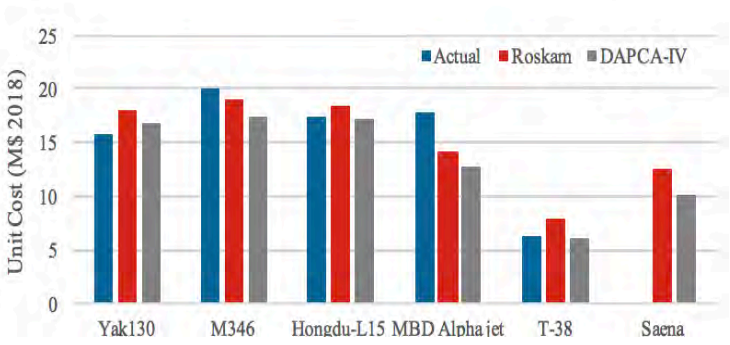

Figure 78-Cost Models Validation

Cost minimizing has been the first priority in decision-making process:

- Fuel amount has been optimized in weight sizing for missions (3.1.2)
- Aspect Ratio has been optimized in performance sizing for min weight and cost (3.2)
- Idea of whether to Rubberizing the engine or not has been justified by cost (6)

Table 78-Sensitivity Analysis

Parameter	Current Value	Change	Unit	Effect on unit cost
Takeoff weight	13350	+280	lb.	+ 100 K$
Max never exceed speed(SLS)	950	+16	knots	+ 100 K$
Total Number built	590	+18	Aircraft	- 100 K$
Engine and avionics Price	3750	+85	K$/Aircraft	+ 100 K$
Profit fraction	10	+1	%	+ 100 K$
Manufacturing Labor Rates	20	+11	$/hour	+ 100 K$
Difficulty Factor	1.4	+0.04	-	+ 100 K$
Material Factor	2	+0.05	-	+ 100 K$

12.3.2 RDTE cost

In this section the NRE costs have been estimated including Research, Development, Test, and Evaluation. The total cost of RDTE has been estimated to be 755 M$ figure 2 represents the breakdown of the RDTE cost. The costs are in Million dollars. Judgmental Factors which have noticeable effect on cost are listed in Table 5. Considering the advanced technologies used in the design, the difficulty factor which has an important effect on cost has been determined to be 1.4. Such as Intelligent Embedded Training System (ETS). Saena also utilizes semi-complex high lift leading system plus a LERX device.

Table 79- Total Used Material Breakdown

Material	F_mat	Percentage
Al 20-24	1.1	15%
Al 70-75	1	20%
Al-Li	2.2	20%
Composite	2	20%

steel	3	2%
Titanium	2	5%
Carbon	2.5	18%
Total	2	100 %

Table 80- Judgmental Factors

Factor	Domain	Determined value
Difficulty of Program	1 to 2	1.4
CAD Capability	0.8 to 1.2	0.8

12.3.3 Manufacturing cost

- Airframe Engineering includes Designing, Integrating, Lab works, systems, and subsystems.
- No costs invested in designing a new engine and just decided to use off-the-shelf with a 3 M$ price per engine (6)
- All labors and engineering rates also have been excerpted from ref [50]

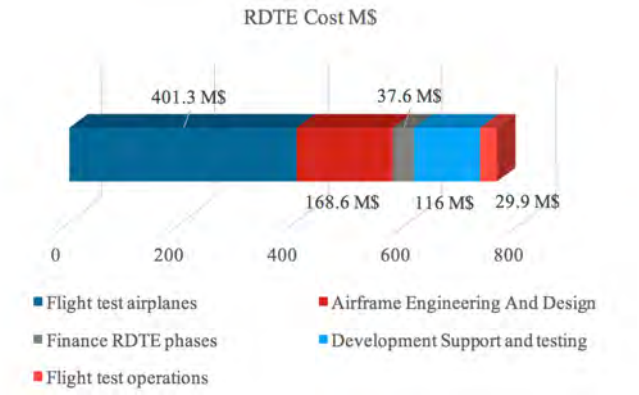

Figure 79-RDTE Cost

- To reduce the cost of aircraft, Government Furnished Equipment has been used in This aircraft, RFP has mentioned cost for most parts of the avionics system such as ICNIA, MFDs, and HUD etc. Which results in 750 K$ for avionics per aircraft.
- Manufacturing Material: includes the raw material, hardware, and purchased parts required for the fabrication except engines and avionics.
- NRE expenses in production phase, which primarily consists of planning for production, is included in Finance Manufacturing phase.

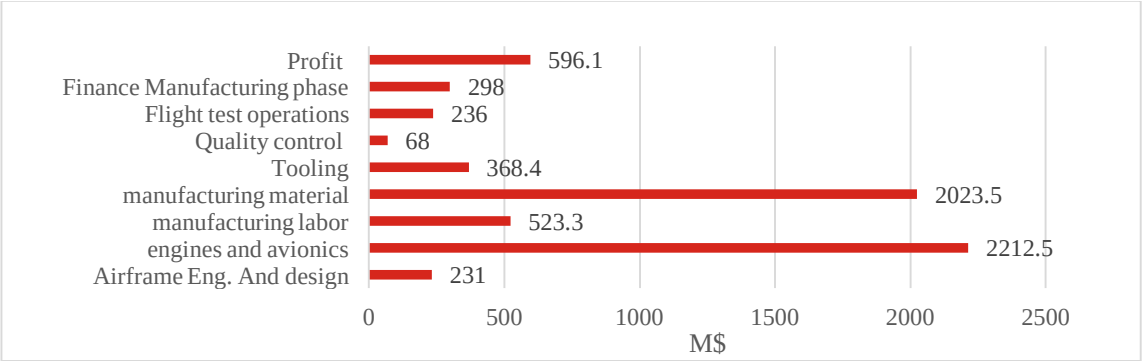

Figure 80 Manufacturing Cost

With a 10% profit margin, 5% financing cost, and producing 590 aircraft totally with the average rate of 5 aircraft per month, the unit cost of aircraft would be 12.39 M$, via Roskam and 10.14 M$ via the DAPCA-IV method. Increasing production number would cause an exponential decrease in unit cost due to learning curve. **Error! Reference source not found.** represents the difference in aircraft unit cost estimated by 2 cost models in learning curve.

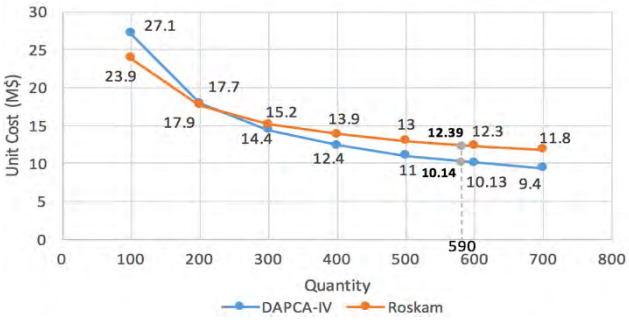

Figure 81-Unit Cost vs. Quantity

Breakeven point analysis shows selling 331 aircraft is the point that costs and revenue become equal:

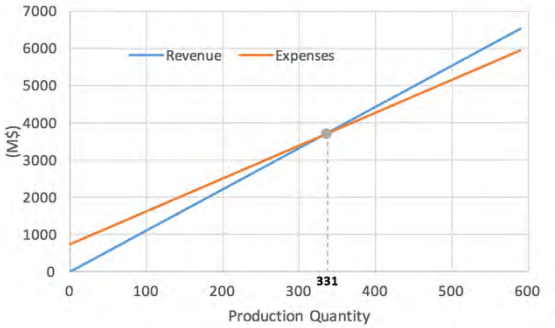

Figure 82-Breakeven Point Analysis

a) Existing Parts; Landing Gear

The effects of using an already designed landing gear for a similar aircraft on cost have been studied. Table 81 represents the results of using F-16 landing gear in. Although, it reduces a fraction of RDTE cost. It causes an increase in manufacturing cost due to extra weight so the idea was rejected:

Table 81- Effect of Using an Existing Landing gear on Cost

Factor	Weight (lbs.)	Reduction in RDTE Cost (M$)
Saena Landing Gear	755	-
F-16 Landing Gear	1500	14.6

b) Labor Cost

Sub-contracting with underdeveloped countries would reduce manufacturing cost about 617 M$ and unit cost 1.2 M$ due to low cost of labor.

c) Ground Based Training System

Each GBTS unit approximately costs 170 to 200 M$ and USAF max GBTS orders may be 46 [2].So Total acquisition cost of Aircraft and GBTS cost would be 13.5 B$ with respect to 16.3 B$ mentioned in [2].

12.3.4 Operating Cost

Main part of operating cost:

- Cost of fuel, oil, and lubricant : Fuel JP-8, 2.15 $ per gallon [51]
- Direct Cost of personnel: Including cost of Aircrew (Instructor and trainee) and maintenance

personnel. Annual salary Considered 100000 $ for Instructor and 70000 $ for Trainee.

- Indirect cost of personnel: cost of all squadron level personnel which are not directly involved in flight or maintenance.
- Cost of Consumable materials: consumable materials used in conjunction with military airplane maintenance functions.
- Cost of Spares: like Pumps, Inverters, Wheels, Gear parts, Actuators, Batteries, Interior parts etc.
- Cost of Depot
- Cost of miscellaneous Items: requirement for technical data, training data, support equipment.

Assuming two training missions per day, each lasting 1.5 hours and about 215 days of pilot training in a year, the overall annual operating hours of each Saena is around 650 hours and is comparable to the range of 600 to 1000 hrs suggested by [9] Cost of Operating would estimate 5440$ per flight hour.

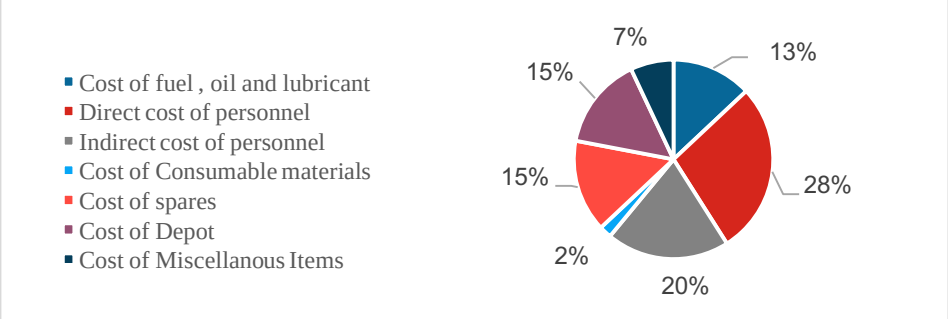

Figure 83: Operating Cost Breakdown

12.3.5 Maintenance Cost

In this section, availability, reliability, and maintainability of Saena has been analyzed and discussed. Also the interaction between these concepts for Saena has been represented.

12.3.6 Maintainability of Saena

Maintainability of an aircraft is related to the cost and time of the maintenance process, which is a part of life cycle cost [52]. The goal is to reduce the maintenance cost, time to repair, and increasing the availability of aircraft. For this purpose, used methods are represented as below:

12.3.6.1 Airframe Maintenance

For preventative maintenance of the Saena, Condition Based Maintenance (CBM) method is proposed. With implementing this method, sensors on the structure of aircraft will be utilized to assess the health and monitor the condition of aircraft [53] Furthermore, CBM can provide warning of many mechanical problems to minimize

unexpected failure and risks of components damage. On the other hand, CBM will reduce the expense of depository also maintenance costs. [53] Reducing inspection time by 44 percent [54]. CBM method will increase the reliability of aircraft and reduces the maintenance cost of an aircraft. All computers and systems across the fuselage and cockpit displays are considered modular. Hence, ground crew will be able to access easily and quickly to maintain the aircraft with min ground support equipment. Also, wing access doors are considered below the wing and fuselage access doors drop down for easy maintenance of fuel systems.

12.3.6.2 Using VMT for maintainers training

Virtual maintenance training is a program that nowadays is used for train maintainers and improve product maintainability in the design process. Virtual maintenance is a technology which uses IT and virtual reality to implement the maintenance process and realize interactive operating simulation through digital mock-ups and virtual humans [55]. Benefits of this system are summarized in Table 82. MMT/FH will be dropped [11]. Furthermore, maintainers would do their training tasks in a safe environment without any damage or risk [56].

Table 82-Effect of Implementing VMT

	operational Benefits	explain	Results
1	Improve maintainer training efficiency	Training maintenance tasks for low observable parts of aircraft in virtual environment	Save turn-around time 10% and improve awareness about task
2	Availability of virtual system	Maintainers can train task in times without real system	Reduce costs and increase maintainer throughput
3	Lower need for real equipment for training	Providing real equipment need high initial budget	Reduces costs

12.3.6.3 Availability Analysis of Saena

As CBM has been implemented to Saena, selected engine and modularity which has been considered in decision-making process during the design, availability of Saena has been analyzed. According to equation in Fig.1.2 [57], the operational availability of Saena would increase because of decreasing the MMT which has been mentioned in section (Maintainability). Also, with the selected engine which has the more MTBO (2000 hrs. more than F404) availability has been increased. With the selected modular engine, ejection seat, and locating the subsystems at the side of the fuselage, the maintenance time would decrease and maintainability improve. As a result, it would increase the availability of Saena which increases reliability.

12.3.7 Maintenance Cost

To improve Saena aircraft maintainability and reducing operating cost, Integrated Modular Avionics (IMA) method has been proposed to use for cockpit. With using this method, weight of avionics and maintenance cost has

been reduced. Also, avionics and cockpit could be easily modified in future modifications. Using CBM with structural health monitoring system would reduce maintenance cost to 25%.

12.3.8 Disposal cost

For the case Saena aircraft fleet service life is predicted to be up until 2060. So, after this time some problems may acquire such as increasing in Operation and Maintenance cost, difficulty in production or depository, inability of upgrading the systems of aircraft due to old technology after 35 years. At this state disposal phase would begin. First, Saena should be stored for probability of next application .Some of aircraft components could be reused like Engines, Landing gears, some parts of airframe, and avionics. Doors and wings could be used in other aircraft or for other uses. [58] Commonality of cockpit with F22 and F35 makes the possibility of cockpit and interiors to get used for ground trainings and simulation in case of early retirement. Another idea would be converting to unmanned target in future training programs. For the Components of aircraft which are not reusable, depending on Recyclability (some materials may not be able to recycle due to cost or environmental considerations) enters in various stages of recycling. Recycling materials like Aluminum, Titanium, composites and other alloys is the last level of disposal. The total cost of disposal phase estimated to be 664$ million by Roskam method.

12.3.9 Compatibility of Saena with USAF Budget Limitations

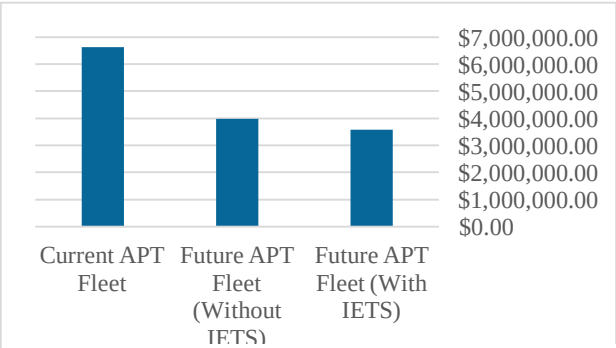

Figure 85- Operational Cost of Training Per Pilot

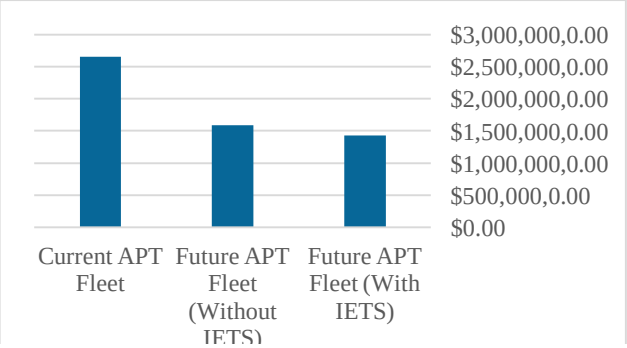

Figure 85- Comparison of Current & Future APTA Fleet Per Year

ShadX validates that Saena is the best response for USAF budget limitation. The operational cost of training during lifecycle also the cost per pilot have been represented. Saena would operate for 25 years in the APT program. ETS would drop the operating cost dramatically due to lower need to another aircraft for ACM and Formation flights. Therefore, operating cost of Saena would be 3.75 B$ which is half the operating cost for T-38 F-16 combination per year. According to number of pilots who would be trained with Saena, in average the cost of pilot training in APT level would be 3.58$ million per pilot. So, ETS would decrease the operating cost of training per pilot by 400,000$.

12.4 SUMMARY

There is always a Tradeoff between operating and acquisition cost of an aircraft, but applied cost reduction methods has been reduced cost in both acquisition and operation phase (with main focus on acquisition). That made Saena an affordable aircraft with better performance in comprehension to other competitors.

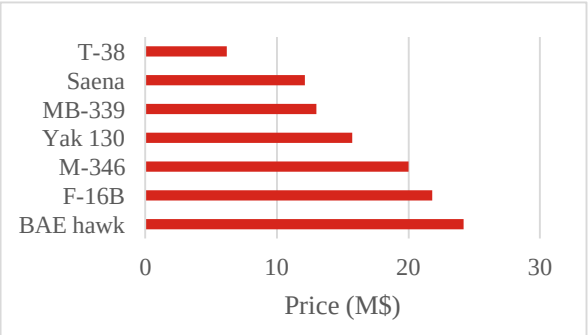

Figure 87- Unit cost Comparison

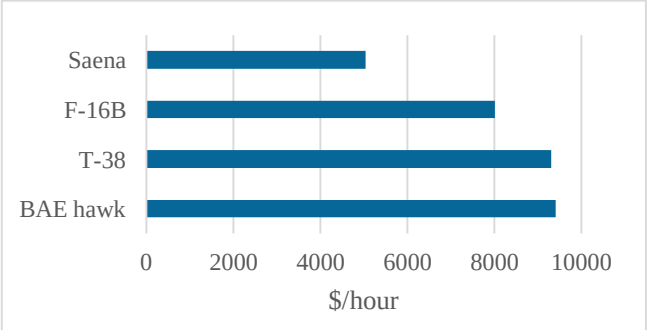

Figure 86- Operating Cost Comparison

Table 83- Cost Summary

Cost	Value	Unit
Production Number	590	Aircraft
RDTE Cost (NRE)	753	M$
Manufacturing Cost	5961	M$
Profit	596	M$
Acquisition Cost	6558	M$
Unit Cost	12.39	M$/Aircraft
Per Unit Flyaway Cost	11.1	M$/Aircraft
Unit cost per Weight	2153	$/lb.
Operating Cost	52156	M$
Operating Cost per Hour	5440	$/hour
Disposal Cost	664	M$

13 CRITICAL DESIGN REVIEW

13.1 TECHNOLOGICAL RISKS

ShadX decided to have a clean-sheet design instead of modification and implemented technologies to Saena (embedded training, AI, and SHM), TRL of these technologies and risk of EIS of Saena has been evaluated. Also, affordability of aircraft has been evaluated in section Market & Lifecycle Cost

As using M-88 off-the-shelf engine for Saena, the engine has been used in Raffaele fighter. So the engine has TRL of 9. The technology of health monitoring is now implemented in many civil and military aircraft and also VMT technology is now used by USAF for training of F-16 fighter maintainers. So, technologies were implemented for maintenance of Saena have TRL of 9, too.

Based on UTC aerospace company report [59], selected ejection seat is conducted to validate the performance of seat and reliability, which means the seat is developed and system prototype is demonstrated in the operational environment. So the seat has TRL of 7 and mechanism of automatic multi-positioning of the seat that considered has TRL of 9 because of its use in 5^{th} generation fighters.

Intelligent Embedded Training System (ETS) implemented for Saena, has been developed by companies and institutes like NLR, Leonardo, KAI, Elbit aerospace, and etc. Also, this system is implemented in T-100 and T-50A trainer's prototypes. So this system has TRL $>$ 7.

The technologies used for Saena have TRL $>$ 7. As mentioned in section ### (stability & control), Variable Handling Quality Control system is implemented to Saena and this system is used at Yak-130 AJT. So this system has TRL of 9. The hardware which has been used for data analysis of the pilot action suggestion (the intelligent instructor), has been developed in different industries and sciences like image processing. This technology has TRL equal to 7 and even more because the implemented intelligent instructor has no control on aircraft.

Based on table###, the technologies used for Saena have TRL $>$ 7 Meaning that Saena has low-risk of production pause so it would be ready for EIS.

Table 84 TRL Risk Ratings ([60])

	TRL 1-5	TRL 6	TRL 7-9
Low			✖
Moderate		✖	
High	✖		

13.2 Conclusion

Saena is an advanced trainer aircraft that has been designed in a response to the 2018 AIAA design competition RFP. As it is evident by now, Saena has been carefully designed to be a cost-efficient Purpose-Built training aircraft of the future that with the help of its unique Variable Stability Augmentations System (VSAS) is expected to effectively replace T-38 fleet. Saena takes advantage of smart proven technologies to reduce its life cycle cost (LCC) to efficiently meet possible USAF budget limitations. Considering, EIS of 2023, T-68 fleet depository reduction, ShadX Saena would be a great alternative to fill in with less operational cost, better safety features and more effective training. Implementation of ETS and low operating cost, would save as much 30.5 billion dollars per pilot in a 25 year

cycle; which is quite noticeable based on future uncertainties involved. Table 1 summarizes the advantages of Saena over T-38.

Table 85 Benefits of Future APT Fleet in comparison with Current APT flee

Measures of Merit	Saena	T-38
Limit Load Factor	+9/-3 g	+8/-3 g
Aerial Refueling	✓	✖
T/W (maneuverability)	1.26	0.65
W/S	60	69.5
Cockpit Commonality	✓	✖
Operating Cost ($/hour)	5440	9300
Unit Price (million $)	12.3	6.17
Operational Cost of Training (per pilot)	3.58 million $	6.63 million $
Max Level Speed	1.3	1.3

Fighter Pilot Training Will Never Be Better...

Benefiting from advanced intelligent technologies, Saena trains pilots in a more effective and affordable manner, while maintaining high level of safety.

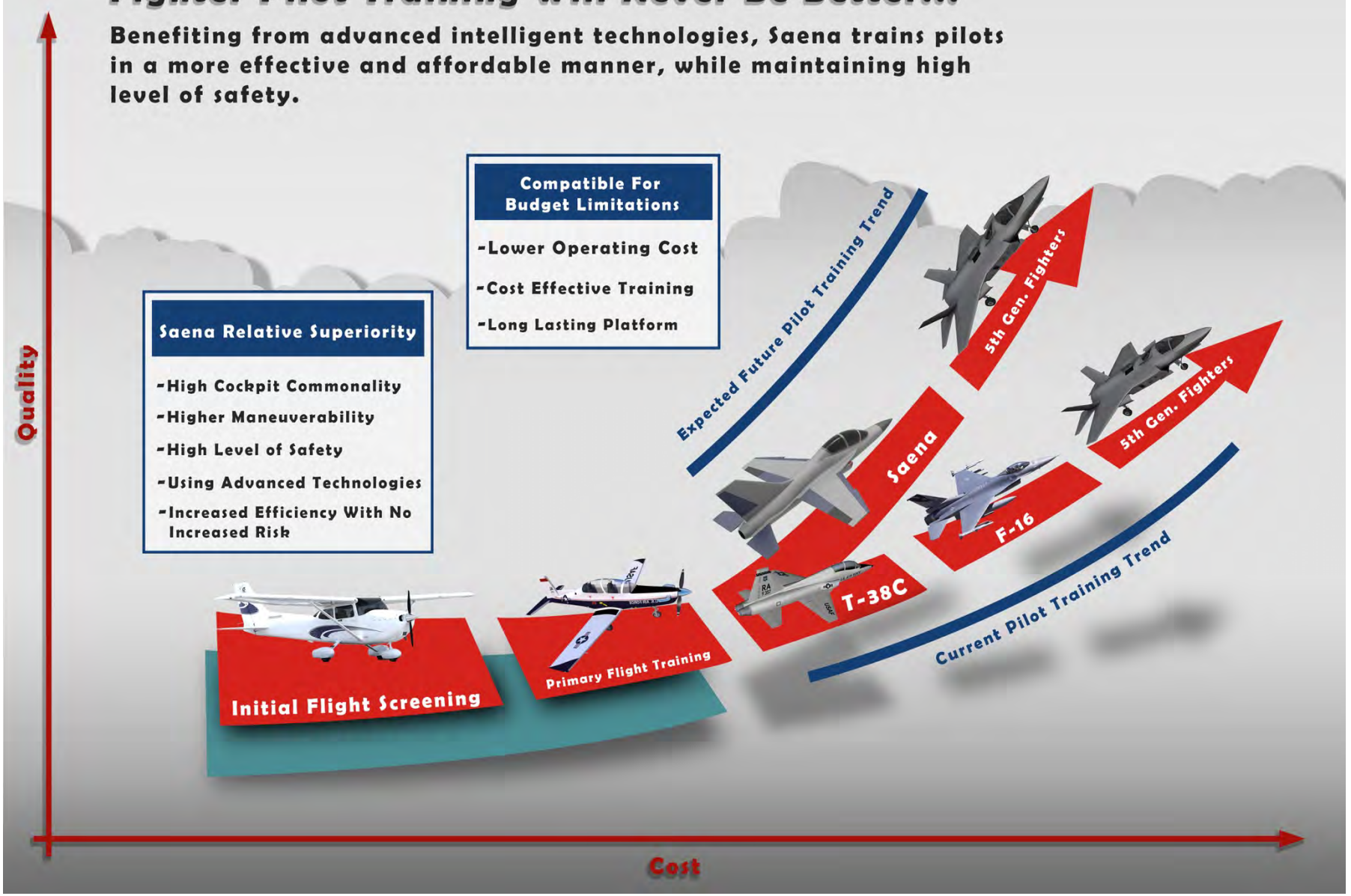

1] Request for Proposal - Advanced Pilot Training Aircraft, 2018: Amerocan Institute of Aeronautics and Astronautics.

2] Gertler, Advanced Pilot Training (T-X) Program, 2017.

3] System Specification for the Advanced Pilot Training Program, 2016.

4] Millitary Flying Training , Office National Audit.

5] Jekinson, 2003.

6] J. Gertler, *Advanced Pilot Training (T-X) Program*, Congressional Research Service, 2017.

7] Request for Proposal - Advanced Pilot Training Aircraft.

8] Supersonic and Transonic Aircraft Problems, E.Reichert.

9] Airplane Design, J.Roskam.

10] Aircraft Engine Design, Matingly.

11] Fundumentals of Aircraft and Airship Design, M.Nicolai.

12] Aircraft Performance, Spakovszky, Z. S..

13] Aircraft Design ,Raymer.

14] Korean Air Force Tactics, Techniques & Procedures 3-3, Volume 5, Basic Employment Manual F-16C, 2005..

15] Estimating the Oswald Factor from Basic Aircraft Geometrical Parameters, M. Nita, D. Scholz, 2012].

16] N. 2. T-38 Flight Manual.

17] Selecting Wing Loading and Thrust to weight ratio for Military Jet Trainers, K. Ibrahim.

18] Aircraft Design Projects, Jenkinson.

19] Large Air Tanker for Wildfire Attack Proposal, ShadX, 2016.

20] Procedures and Design Data for the Formulation of Aircraft Configurations, Sieron.

21] KAI, Global Defense Industry.

22] https://www.globalsecurity.org/military/systems/aircraft/f-22-cockpit.htm.

23] 1988 Anthropometric Survey of U.S. Personnel , Gordon.

24] A. G. R. I. T. C. Evolution of Aircraft Flight Control System and Fly-By-Light Control System.

25] Electro-Hydrostatic Actuation ,Elbig, Dr. Achim.

26] The Property Comparison of Electromechanical and Electro-hydraulic Flight Control Actuators, F.Adamcik, J.Labun, J. Pila.

27] N. 2. Embedded Training For Lead-in Fighter Training.

28] ainonline.com Pocock, Chris.

29] aviation.stackexchange.com.

30] T-X Conops.

31] Aircraft Engine Design David Pratt. Heiser, Mattingly.

32] Design for Air Combat,Whitford, Ray.

33] Aero-Engines Intake: A Review and Case Study,Ahmad-El-Sayed, Mohamed S.Emeara.

34] Aircraft propulsion, Farokhi, Saeed.

35] Effect of Atmospheric Altitude on Drag of Wing At Subsonic And Supersonic Speeds, Abdulkareem SH. Mahdi Al-Obaidi.

36] Flight Dynamics and Automatic Flight , J.Roskam , 2001.

37] Aircraft Dynamics: From Modeling to Simulation , Napolitano, Marcello R..

38] http://www.dept.aoe.vt.edu/~mason/Mason_f/F22S05.pdf.

39] Palmgren-Miner method in Airframe Structural Design , Nui.

40] J. a. W. A. A. A. A. 2. L. D. 2. c. s. Roskam.

41] K. “. D. f. B.-L. C. o. A. J. T. A. A. a. M. C. A. J. o. A. S. O. I. V. N. M. 1. Ibrahim.

42] N. W. f. t. T.-3. A. C. P. E. o. t. T.-3. A. w. a. N. W. Design.

43] Pilot Training for the Future , EVERSTINE, BRIAN W..

44] PILOT SHORTAGE, BACK WITH A VENGEANCE , AIR FORCE Magazine , Skowronski, Will.

45] FAA REGISTRY , http://registry.faa.gov/aircraftinquiry/AcftRef_Results.aspx?Mfrtxt=&Modeltxt=T38&PageNo=1.

46] Aircraft in the Inventory , Turkish Airforce , https://www.hvkk.tsk.tr/en-us/Turkish_Air_Force/Todays_Air_Force/Aircraft_in_the_Inventory.

47] ESTIMATED JSF AIR VEHICLE PROCUREMENT QUANTITIES , https://web.archive.org/web/20090327082340if_/http://www.jsf.mil/downloads/documents/ANNEX%20A%20Revision_April%202007.pdf.

48] How the Air Force Could Fly the F-22 Raptor Until 2060 , Mizokami, Kyle.

49] Aircraft Airframe Cost Estimating Relationships: All Mission Types , R. W. Hess, H. P. Romanoff.

50] BUREAU OF LABOR STATISTICS , https://www.bls.gov , 2018.

51] Standard Prices , Agency, Defense Logistics , http://www.dla.mil/Energy/Business/StandardPrices.aspx.

52] Design for Maintainability,primciples,modularity and rules , Taylor, Andrew.

53] Overview of condition based maintenance , Banks, Jeff.

54] Introduction to Structural Health monitoring , BALAGEAS, Daniel.

55] The Application Research on the Virtual Maintenance in Aircraft DesignThe Application Research on the Virtual Maintenance in Aircraft Design , Shu LI, Yi LIU Jia LIU, Niandong WANG.

56] http://www.streetdirectory.com/travel_guide/135294/technology/operational_benefits_of_virtual_maintenance_training_systems.

57] Introduction to Operational Availability , Street, Mill.

58] Toward a Strategic Approach to End-of-Life Aircraft Recycling Projects A Research Agenda in Transdisciplinary Context , Samira Keivanpour, Daoud Ait-Kadi, Christian Mascle.

59] ACES 5 Advanced Concept Ejection Seat.

60] SOLICITATION PROVISIONS IN FULL TEXT EVALUATION FACTORS FOR AWARD.

61] Locheedmartin.com.